

# Solar-Terrestrial Centre of Excellence

## Annual Report 2017



## **STCE**

Solar-Terrestrial Centre of Excellence

<http://stce.be/>

Ringlaan 3

B-1180 Brussels

Tel.: +32 2 373 0211

Fax: + 32 2 374 9822

*Front page: The 6-meter solar radio telescope at the Humain Radioastronomy Station. Fitted with two antenna and three receivers, it provides important radio observations between 45 and 1500 MHz used for solar research and space weather forecasting.*

## Table of Contents

A word from the STCE coordinator.....	4
Structure of the STCE .....	5
Monitoring Space Weather: Solar-Terrestrial Highlights in 2017 .....	8
Public Outreach meets Science .....	12
ESWW14.....	12
The 2017 STCE Annual Meeting.....	13
SWIC 2017 .....	14
Fundamental Research .....	16
Detection of quasi-periodic pulsations in solar EUV time series.....	16
How Alfvén waves transport energy in the solar corona and the solar wind .....	17
Signatures of a not so typical solar eruption.....	19
The 4 November 2015 event .....	20
Local midnight ionospheric and plasmaspheric anomaly over West Antarctic .....	22
Homogenisation of GPS integrated water vapour time series.....	24
Instrumentation and experiments .....	28
Extreme Ultraviolet Imager (EUI) ready for launch! .....	28
The HOP334 solar observation campaign and the "lucky imaging" technique .....	29
SOLAR-ISS, a new solar reference spectrum.....	31
Applications, Modeling and Services.....	34
SSA Space Weather Coordination Centre – User Support.....	34
The reddish sun phenomenon on 16-17 October 2017.....	35
Ionospheric models used for calibration of GNSS timing stations.....	36
Real-time monitoring of travelling ionospheric disturbances.....	38
The ever-changing plasmasphere.....	40
Publications .....	43
Peer reviewed articles.....	43
Presentations and posters at conferences .....	46
Public Outreach: Talks and publications for the general public .....	59
List of abbreviations .....	61

## A word from the STCE coordinator



During the afternoon of November 4, 2015, the Sun produced a medium sized solar flare that was accompanied by a surprisingly strong radio disturbance. These intense radio bursts, which were also observed by the Human Radioastronomy Station, affected radar frequencies causing significant problems in the Swedish air traffic control.

This space weather event directly impacted aviation technology, and strengthened my conviction that the work we do matters in

our society and our daily life. It also makes it clear that we still have a lot to learn about the engine that drives all of space weather: the Sun.

One way we are going to do this is by developing and exploiting our brand-new scientific instrument EUI which is now being integrated into the Solar Orbiter spacecraft.

Also, the accurate measurement of the solar spectral irradiance (SSI) is fundamental to solar physics, terrestrial atmospheric chemistry and Earth climate studies.

Finally, I want to highlight an international observation campaign that was intended to squeeze the last drop out of SUMER, an instrument on board the 21 years old (!) space weather satellite SOHO. With the novel “lucky imaging” software, we got an amazing view of the solar surface.

I invite you to read about the above and other achievements of the STCE in the following pages. Happy reading!

Ronald Van der Linden  
General Coordinator of the Solar-Terrestrial Centre of Excellence  
Director General of the Royal Observatory of Belgium

## Structure of the STCE

The Solar-Terrestrial Centre of Excellence is a project of scientific collaboration that focuses on the Sun, through interplanetary space, up to the Earth and its atmosphere.

The solid base of the STCE is the expertise that exists in the 3 Federal Scientific Institutes of the Brussels Space Pole: the Royal Observatory of Belgium, the Royal Meteorological Institute and the Royal Belgian Institute for Space Aeronomy. The STCE supports fundamental solar, terrestrial and atmospheric physics research, is involved in earth-based observations and space missions, offers a broad variety of services (mainly linked to space weather and space climate) and operates a fully established space weather application centre. The scientists act at different levels within the frame of local, national and international collaborations of scientific and industrial partners.

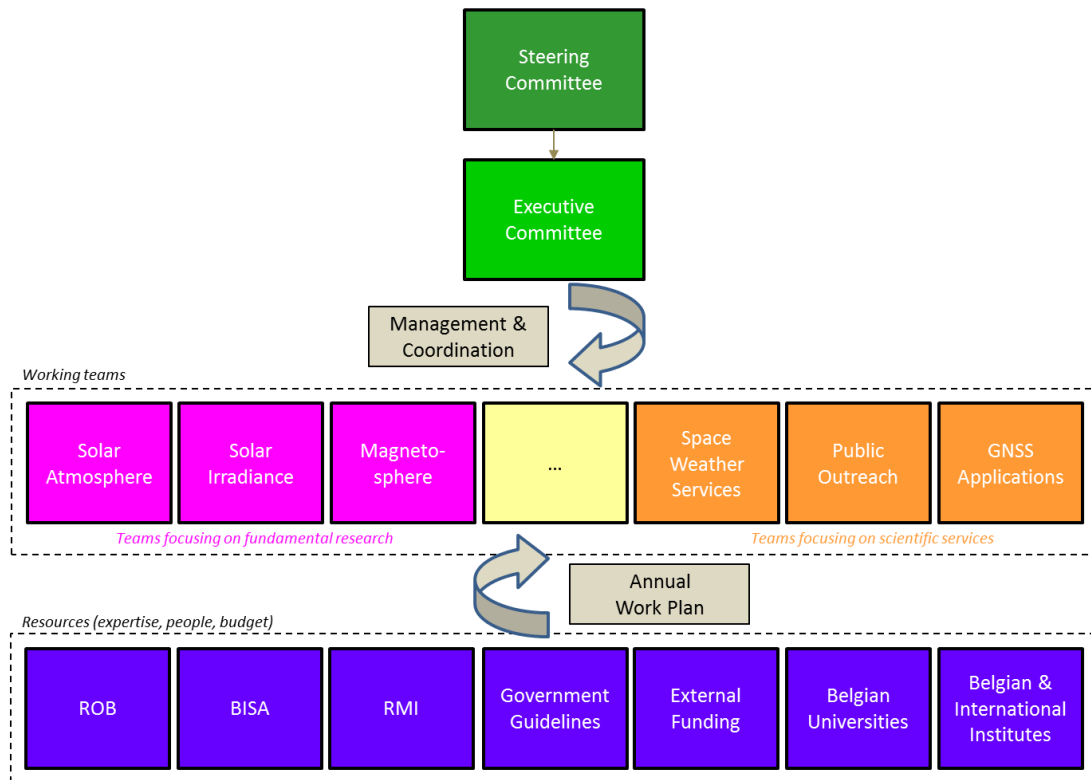


Figure 1: The STCE management structure

The STCE's strengths are based on sharing know-how, manpower, and infrastructure.

In order to optimize the coordination between the various working groups and institutions, as well as the available resources such as ICT, personnel and budget, a management structure for the STCE was put into place, consisting of a steering committee and an executive committee.

The **steering committee** takes all the final decisions on critical matters with regard to the STCE. It assures the integration of the STCE into the 3 institutions and the execution of the strategic plans. It is composed of:

- BELSPO Director General “Research Programmes and Applications”

*Dr. Frank Monteny (BELSPO)*

- Director General of each of the 3 institutions at the Space Pole

*Dr. Ronald Van der Linden (ROB)*

*Dr. Daniel Gellens (RMI)*

*Dr. Martine De Mazière (BISA)*

The **executive committee** assures the global coordination between the working groups and the correct use of the budgetary means for the various projects. It also identifies new opportunities and is the advisory body to the Steering Committee. It is composed of:

- STCE Coordinator

*Dr. Ronald Van der Linden*

- Representatives of the research teams in the 3 institutes

*Dr. David Berghmans (ROB)*

*Dr. Carine Bruyninx (ROB)*

*Dr. Johan De Keyser (BISA)*

*Dr. Norma Crosby (BISA)*

*Dr. Stanimir Stankov (RMI)*

*Dr. Steven Dewitte (RMI)*

*Dr. Hugo De Backer (RMI)*

A promotional movie giving a flavor of the STCE’s tasks, interactions and various research programmes can be found via the [STCE](#) website (in [English](#), and subtitled in [French](#) and [Dutch](#)).



*Figure 2: The honey bees were given a new home in the ROB garden. In times of ever reducing budgets, these zealous, numerous and especially cheap workforces are very welcome! Now we just have to teach them how to do solar research and space weather forecasting...*

## Monitoring Space Weather: Solar-Terrestrial Highlights in 2017

The official annual sunspot number (SN) for 2017, as determined by the WDC-SILSO (World Data Centre - Sunspot Index and Long-term Solar Observations), was 21.7. This is a further decrease compared to 2016, when it was 39.8. The highest daily sunspot number (119) was recorded on 5 September. However, there were also 96 spotless days (see SILSO's [Spotless Days](#) page), with stretches of about 2 weeks on 6-20 March, 9-20 October, and 1-13 November.

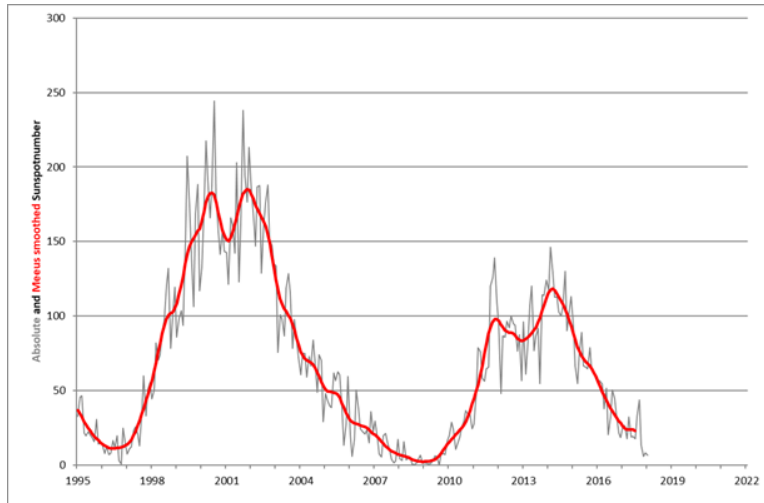


*Figure 3: The evolution of the monthly and monthly smoothed SN (1995-2017). Pending the smoothing formula used, SC24 reached its maximum of 116.4 in April 2014 (SILSO formula), or 118.2 in March 2014 (Meeus formula).*

In 2017, the Sun produced 39 M-class and 4 X-class flares. These solar eruptions came in 3 bursts of moderate to high activity.

Early April, the sudden emergence of opposite polarity magnetic flux in sunspot group [NOAA 2644](#) made this active region produce 7 M-class flares in less than 3 days, ending a drought of this type of events that started on 29 November 2016. The two strongest events were an M5.7 flare on 2 April and an M5.8 flare on 3 April.

The radio burst associated with the latter flare (M5.8) was also captured by the solar radio telescopes in [Humain](#). It was the first Type II radio burst observed by ARCAS (Augmented Resolution Callisto Spectrometer) since it became operational late October 2016. As the active region was close to the Sun's west limb, the associated coronal mass ejection (CME) was not directed to Earth.

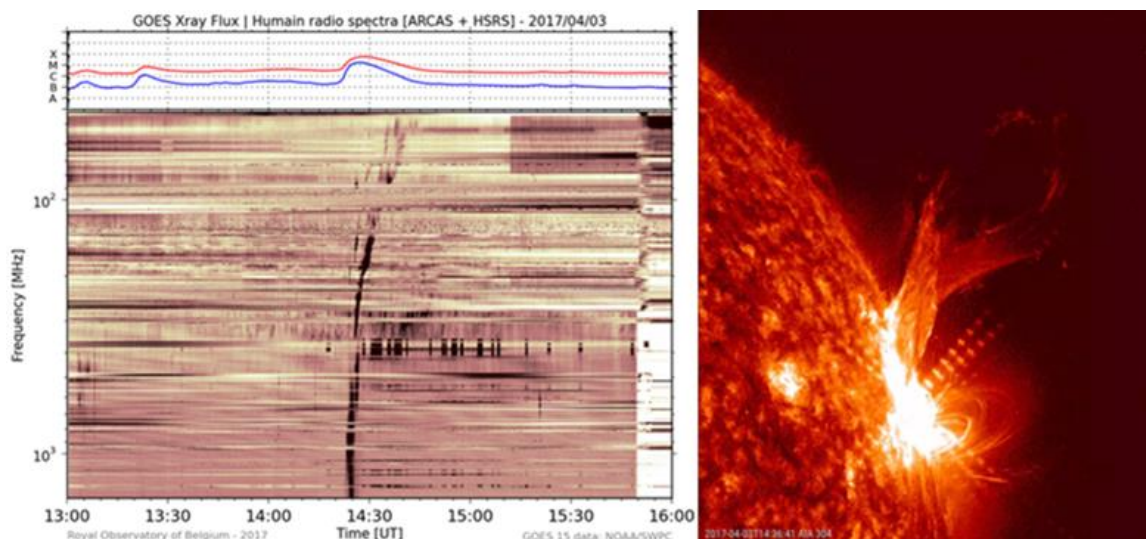


*Figure 4: The M5.8 flare on 3 April as viewed in extreme ultraviolet (EUV) by [SDO/AIA](#) (right) and the radio-spectrogram (left) as recorded by the Humain radio telescopes.*

[NOAA 2665](#) was the third largest sunspot group of the year, transiting the solar disk from 5 till 17 July. It was a compact region and had a surface area 4 times that of Earth, making it an easy naked-eye target (using eclipse glasses of course!). It produced spectacular long duration events on 14, 17 and 20 July, with the one on [Bastille Day](#) being the strongest: an M2.4 flare lasting for more than 2 hours. There was also a minor proton event associated with it, the first since 2 January 2016. The related CME arrived early on 16 July and resulted in a moderate geomagnetic storm ( $K_p = 6$ ,  $Dst = -72$  nT). The passing CME temporarily reduced the cosmic rays arriving at Earth, and a Forbush decrease of 7% was recorded by neutron monitors on Earth ([Oulu NM](#)).

On 23 July, it produced [another strong event](#) on the farside of the Sun, as observed with the EUVI instrument on board [STEREO-A](#). The intensity of the flare was estimated to be in the M3.0 to X1.2 range, with the strong coronal dimming, the obvious coronal wave, and the series of bright post-flare coronal loops ("arcade") testifying for the strength of this eruption. STEREO-A instruments also recorded a substantial increase in the proton flux.

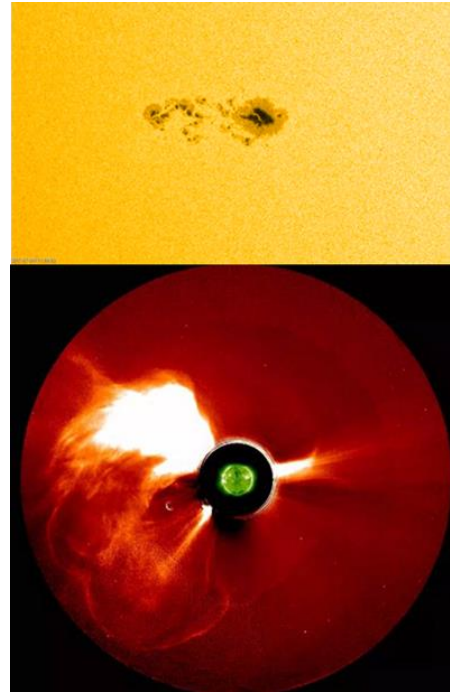


*Figure 5: NOAA 2665 imaged in white light by SDO/HMI (top), and the 23 July event on the Sun's farside as imaged by the STEREO-A instruments.*

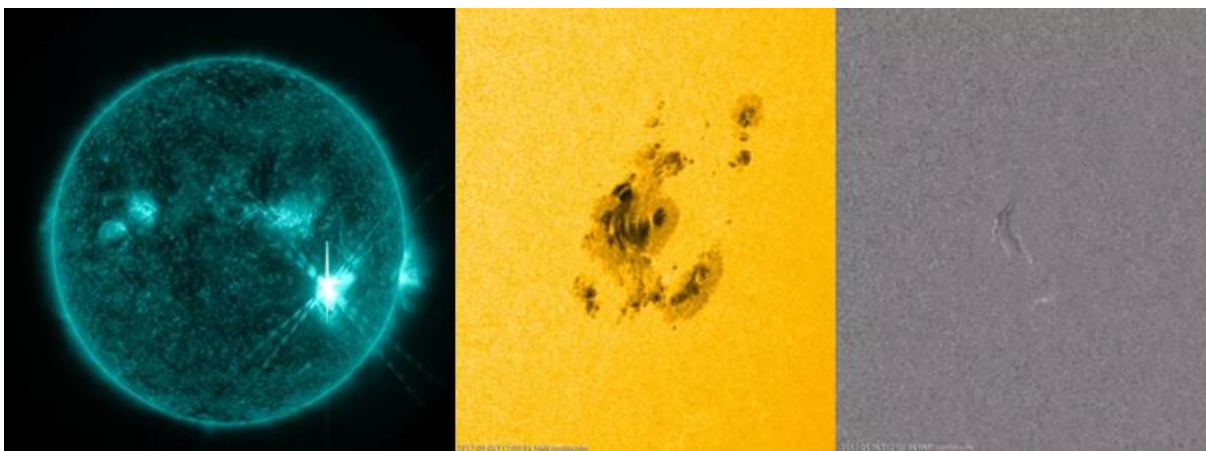


*Figure 6: Left: An EUV image of the X9 flare (SDO/AIA 131). Middle: A close-up of NOAA 2673 in white light (SDO/HMI) during the X9 flare. Right: A white-light difference image (one image subtracted from the previous), showing faint emission and indicating that this was a white-light flare (WLF) as seen by SDO.*

In 2017, the vast majority of all M-class flares (26 out of 39) as well as all X-class flares were produced in just one week, from 4 till 10 September, and by just one region: NOAA 2673. This sunspot region started its quick development on 3 September, and together with another large (but inactive) sunspot region NOAA 2674, drove the sunspot number (119 on 5 September) and total sunspot area to the highest

levels of the year. NOAA 2673 would become the largest sunspot group of 2017, and was visible to the naked eye (using protecting eclipse glasses).

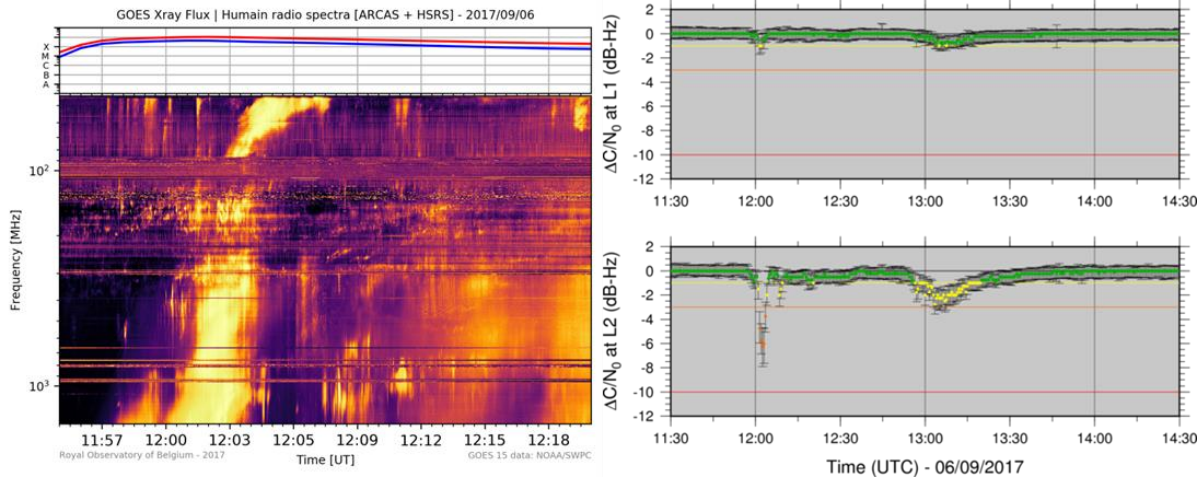


Figure 7: The radio burst associated with the X9 flare on 6 September as observed by the Humain solar radio station (left). GPS frequencies were affected for several minutes. This was also observed by ROB/GNSS (right) as a signal fade of especially the L2 GPS signal.

Then, on 6 September, the region produced an X9.3 flare, the strongest observed during SC24 and the first X9 flare since 5 December 2006. It was also observed in white light (just as e.g. the Carrington flare in 1859) by the HMI instrument on board the SDO satellite. The associated solar radio burst degraded GPS communications for about an hour, and its effects were observed by ROB/GNSS. The associated CME had a plane of the sky speed of around 1200 km/s and disturbed the earth environment starting on 7 September. Peak wind speeds and Bz were at resp. 840 km/s and -32 nT, the highest values of the entire year.

The resulting geomagnetic storm reached severe storming levels (the only time in 2017), with the preliminary Dst at -124 nT. The passing CME also reduced the cosmic rays arriving at Earth, and a Forbush decrease of 9% was recorded by neutron monitors on Earth (Oulu NM) on 8 September. The succession of strong flares hampered HF communications during relieve and warning efforts in the Caribbean in the wake of hurricane Irma.

NOAA 2673 had just rounded the west limb when it produced the second strongest x-ray flare of SC24. The X8.2

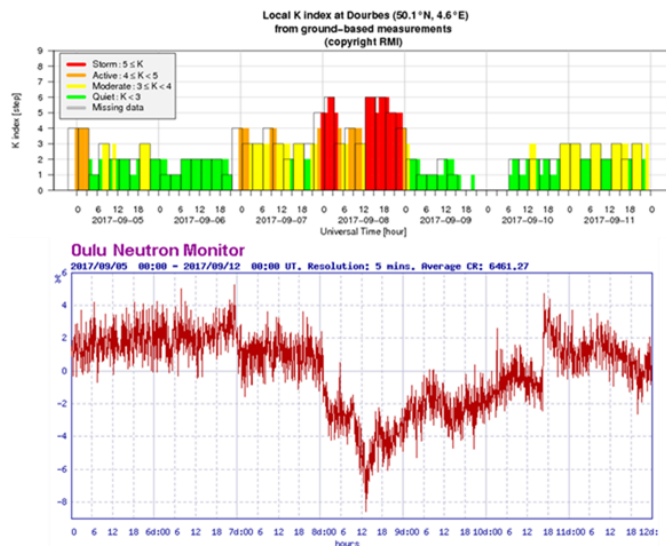


Figure 8: The CME associated with the X9 flare caused a moderate (Dourbes, top chart) to severe (Kp) geomagnetic storm on 8 September. Neutron monitors such as in Oulu (Finland) recorded a decrease in the neutron flux of about 9% compared to normal background levels (bottom chart). During the recovery phase, the GLE of 10 September can be seen as a sudden increase of about 4-5% in the neutron flux.

flare was associated with impressive and long-lasting [post-eruption coronal loops](#) towering over the solar limb, making its outlook very similar to the [19 July 2012](#) event. A strong proton event (1490 pfu) was recorded, being the strongest since 22 May 2013. The event increased the flux of solar cosmic rays, creating a secondary particle shower in the Earth's atmosphere which was subsequently detected by neutron monitors on ground as a [Ground Level Enhancement](#) (GLE). This was only the second GLE in SC24, after the 17 May 2012 GLE. It was also only the 72<sup>nd</sup> event since neutron measurements started in the early 1940s. The Oulu neutron monitor recorded an increase of about 5% over the background neutron flux, compared to 15% in 2012. The associated CME had a projected speed of well over 2000

km/s, and managed to deliver a glancing blow to the earth environment. In the remnants of decaying NOAA 2673, a long and persistent filament would develop and remain present for the next 3 months.

So far this ongoing solar cycle, no extremely severe geomagnetic storm has been observed (Kp = 9). In 2017, aside the severe geomagnetic storm on 8 September (estimated Kp), there were only two other strong geomagnetic storms in 2017. The disturbance on 28 May was due to a CME associated with a filament eruption near disk centre late on 22 May. The preliminary Dst reached -125 nT, the most intense of the year. Kp reached also 7 on 28 September, as Earth was under the influence of a high-speed stream (HSS) from the extension of the positive polarity coronal hole (CH) at the Sun's north pole.

A recurrent trans-equatorial coronal hole, extending from the Sun's south pole, reached its largest area early March, with an area equivalent to nearly 600 times the surface area of the Earth. It was the largest coronal hole of the year, and the associated wind stream produced moderate geomagnetic storming (Kp = 6; Dst = -74 nT) during its late March transit. The coronal hole fell apart and dissolved over the subsequent months. The presence of the coronal holes and their associated wind stream regularly resulted in minor to moderate geomagnetic storming throughout the year. Often, geostationary satellites recorded very high fluxes of energetic electrons (energies  $\geq 2$  MeV), which are an important source of electrostatic charging effects inside satellites.

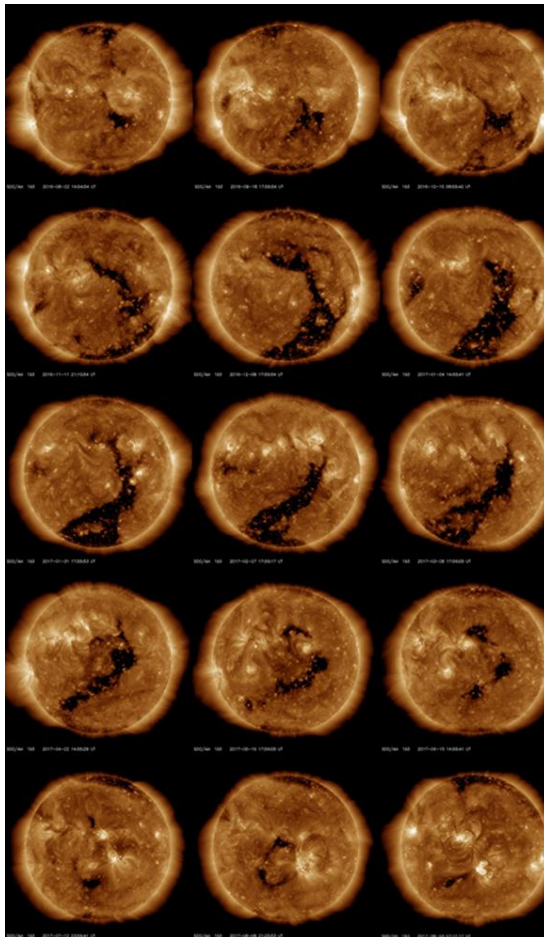


*Figure 9: Evolution in EUV of a negative polarity coronal hole that developed during the latter half of 2016, reached its maximum size during spring of 2017, and then gradually dissolved over the subsequent months. The upper left image was taken on 22 August 2016, and all subsequent images are 1 solar rotation apart. The last image at the bottom right dates from 4 September 2017.*

## Public Outreach meets Science

### ESWW14

The European Space Weather Week (ESWW) is one of the main international conferences when it comes to space weather. For many years now, the Solar-Terrestrial Centre of Excellence (STCE) has a privileged position in the space weather community because of its role in the organisation and coordination of this conference. As such, the STCE remains the driving force behind the dynamics of the ESWW and puts the interaction and the exchange of knowledge between the various space weather stakeholders on the foreground.



*Figure 10: Researchers from the SSA Space Weather Coordination Centre (SSCC) making their final preparations for the Fair on Wednesday afternoon. (Picture by Olivier Boulvin)*

For the third year in a row, the [ESWW](#) took place in the Casino Kursaal of Oostende. From 27 November till 1 December 2017, the participants could attend [15 sessions](#) and [20 topical discussion meetings](#). Each day started with a [keynote lecture](#) introducing the main themes of that day's sessions.

This year's ESWW was co-organised with the [9ECS](#) (CubeSat) symposium. A CubeSat is a type of miniaturized satellite for space research that is made up of multiples of 10x10x10 cm cubic units. CubeSats weigh about a kilogram per unit, and often commercial off-the-shelf (COTS) components are used for their electronics and structure. As a result, the main theme of this year's ESWW [Tutorial](#) was "CubeSats". It consisted of a couple of lectures, some hands-on, and a panel discussion.



*Figure 11: Olivier Boulvin took this picture during the ESWW14 conference dinner. The molding depicts a famous person; can you guess who this is? Koen Stegen master-minded this amusing activity, and conceived also the "Create-your-own-CubeSat" hands-on during the Tutorial.*

On Monday evening, the [medal award ceremony](#) preceded the welcome reception. The ESWW14 continued the good experience of a [daily space weather briefing](#) (immediately after the keynote lectures), with each time two space weather offices making a presentation. A total of six space weather offices were involved, with the MetOffice and the SIDC making two presentations each.

On Tuesday evening, there was a very successful

[music happening](#) in the Casino's Lounge bar, and on Wednesday, there was the traditional [space weather fair](#) with "Beer tasting". ESWW14 continued also the practice that a company could [sponsor](#) the ESWW for an entire week. The conference dinner took place at the soccer stadium of KV Oostende. It was followed by a molding contest (mold the answers of 3 relatively easy questions).



*Figure 12: To honor the important contributions from Kristian Birkeland, a planeterrella demonstration was given by Jean Liliensten (on the right) during the ESWW. Jean is the father of this significantly improved version of Birkeland's "Terrella". Since its conception about a decade ago, tens of these aurora simulators have been built and can be found in institutes and museums worldwide.*

During the 2017 edition of the ESWW, the important contributions from the Norwegian physicist Kristian Birkeland were emphasized. Birkeland was the first scientist to explain that the Sun was the source of the northern lights and founded much of today's modern space research. Birkeland's theories about the northern lights and electrical currents in the atmosphere were eventually confirmed in the 1960's when satellites became available. As a tribute to one of the greatest scientists in space research, one of the three ESWW medals bears his name. There was also a keynote lecture on Tuesday, and a planeterrella ("aurora simulator") demonstration on Wednesday.

### *The 2017 STCE Annual Meeting*

This year's STCE annual meeting, a relaxed gathering of all STCE members, took place on 8 June and was as usual organised by Petra Vanlommel (including the preliminaries to the various workshops).

A full Meridian room first enjoyed a double lecture on the international SOHO/SUMER observation campaign, followed by a talk on the completed EUI telescope. Emil and Laurent highlighted an international observation campaign that was intended to squeeze the last drop out of SUMER, an instrument on board the 21 years old (!) space weather satellite SOHO. The STCE contributed to this campaign. With the 'lucky imaging' trick applied to our ground based telescopes ([USET](#): Uccle Solar Equatorial table), we got an amazing view of the solar surface. And Cis brought us the hot-of-the-press news that the Extreme



*Figure 13: The "Dark-and-Dusty" tour had several stops such as at the RMI (left) for an explanation of the ozone soundings preparation, and at the seismology department (top right). The annual meeting ended with a tasty lunch in the RMI canteen (bottom right).*

Ultraviolet Imager (EUI) was ready to be mounted on the Solar Orbiter satellite! A more in-depth discussion of both topics can be found in the chapter on “Instrumentation and experiments”.

The main part of the meeting consisted of the visit of important but not-so-well-known measurement tools in the basement of the various institutes on the Space Pole. For this "Dark-and-Dusty" tour, the participants were split into several small groups of about 10-15 persons. Each group was accompanied by a guide who knew his/her way around the Pole. The visit of each point took about 15 minutes (with 5 minutes for getting to the next point), making this a quite dynamical and very interactive walk. An overview of the various stops can be found [here](#).

### SWIC 2017

The STCE continues to prove itself as a valuable partner when it comes to space weather services. Over the last few years, the Dutch military and the Royal Netherlands Meteorological Institute (KNMI) have developed a strong interest in space weather and the effects it can have on their technologies. To set up the services they have in mind, they need of course space weather expertise which they found at the STCE.



*Figure 14: (top left) The ROB/Meridian Room was the location of the SWIC 2017. - (top right) Assisting the weekly SIDC space weather briefing. - (bottom left) Emil and Bram revealing a few secrets of the tools used by the SIDC space weather forecasters. - (bottom right) Participants at work during a practical session on the URSIgrams interpretation.*

Hence, in collaboration with the Dutch military and the KNMI, the Cell Communication of the STCE co-developed a “Space Weather Introductory Course” (SWIC). The SWIC is not a space weather forecasting course, rather it aims at getting the participants acquainted with the space weather jargon so that they can correctly interpret the daily bulletins (such as the [URSIgrams](#)) and alerts (such as the [PRESTO alerts](#)), and can translate this in relevant space weather effects for their own technologies.

The SWIC took place during 8-9 and 22-23 May in the Meridian room of the ROB. It was attended by operators from the Dutch military, the KNMI, the Belgian military, and a few new SIDC space weather forecasters and other interested persons. A [SWIC event webpage](#) was created with the planning and presentations.

The first two days covered a general introduction, the drivers of space weather, the magnetosphere and the ionosphere. The last two lectures were given by experts from BISA and ROB/GNSS. In between these lectures, there were also some more relaxing visits, showing the tools and instruments that the SIDC space weather forecasters use. Participants also attended the SIDC space weather briefing on Monday.

The second part was more practical with space weather effects on the specific instruments and technologies from the Dutch military, a lecture on ground- and space-based sensors, and practical exercises on reading and interpreting the URSIgrams. All 16 participants had to pass an exam (open-book multiple-choice quiz) and got a certificate.

This first edition of the SWIC was very well received. Plans for [SWIC2018](#) were immediately made, as the other members of the KNMI and Dutch military need to be brought to the same level of space weather expertise.



*Figure 15: Curiosity did not kill the cat! - The Sun fascinates all, and so it is no surprise that the general public wants to know more about our star and how its activity can affect our community and our technology. As a result, STCE collaborators regularly convey their passion for solar-terrestrial research in public observatories, schools, clubs, societies, and at public outreach science events. The picture above shows such an event ([‘Talk cosmic to me’](#)) with the cartoon on the left reflecting a human interpretation of solar activity (“crowded Sun”) as presented during that [talk](#). No animals or participants were harmed while giving these presentations.*

## Fundamental Research

### Detection of quasi-periodic pulsations in solar EUV time series

Quasi-periodic pulsations (QPPs) are oscillations that have been detected in the integrated solar or stellar emission during flares. QPPs were first detected in the late sixties and were, for several decades, only observed in the hard X-rays (HXR) and radio wavelength ranges - see e.g. [Parks and Winckler](#) (1969 – they produced Figure 16), or [Kane et al.](#) (1983).

However, a new generation of space instruments has allowed extending the detection of QPPs to other parts of the solar spectrum. In particular, the Large Yield Radiometer (LYRA – [Dominique et al.](#) (2013)) on board the PROject for On-Board Autonomy 2 (PROBA2), an instrument of which the Royal Observatory of Belgium has the PI-ship, reported QPPs in the soft X-rays (SXR) and extreme ultraviolet (EUV) emission of the million-degree solar corona.

As this instrument observes the full Sun “as-a-star” instead of focusing on a specific region of interest, and does that on a quasi-uninterrupted way, it recorded most of the flares that happened during the

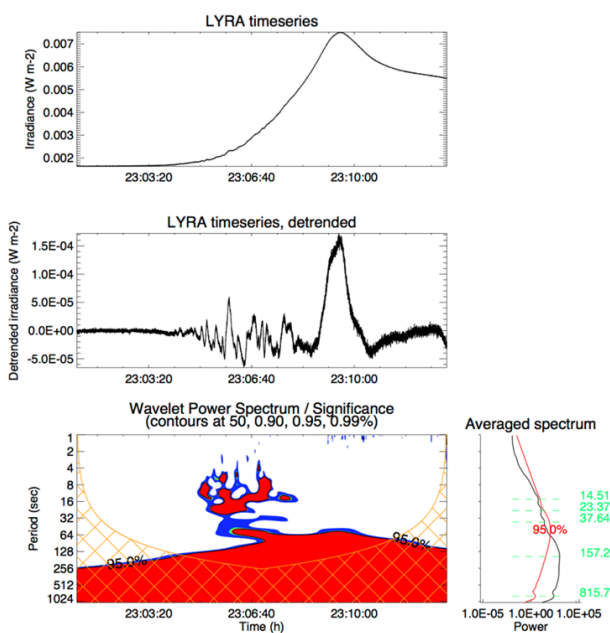


Figure 17: Detection of QPPs with several periods from the LYRA pre-processed time series.

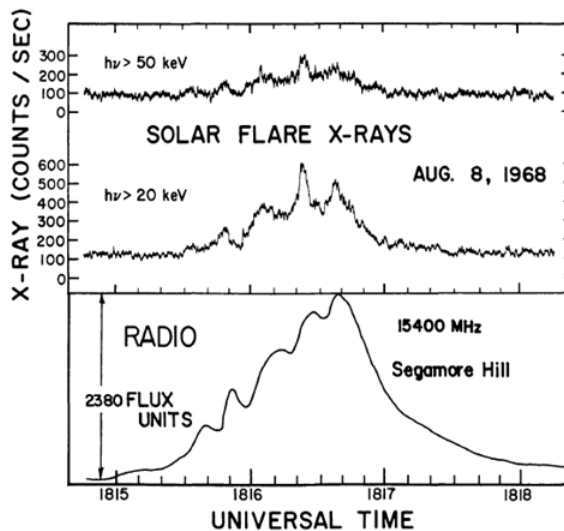
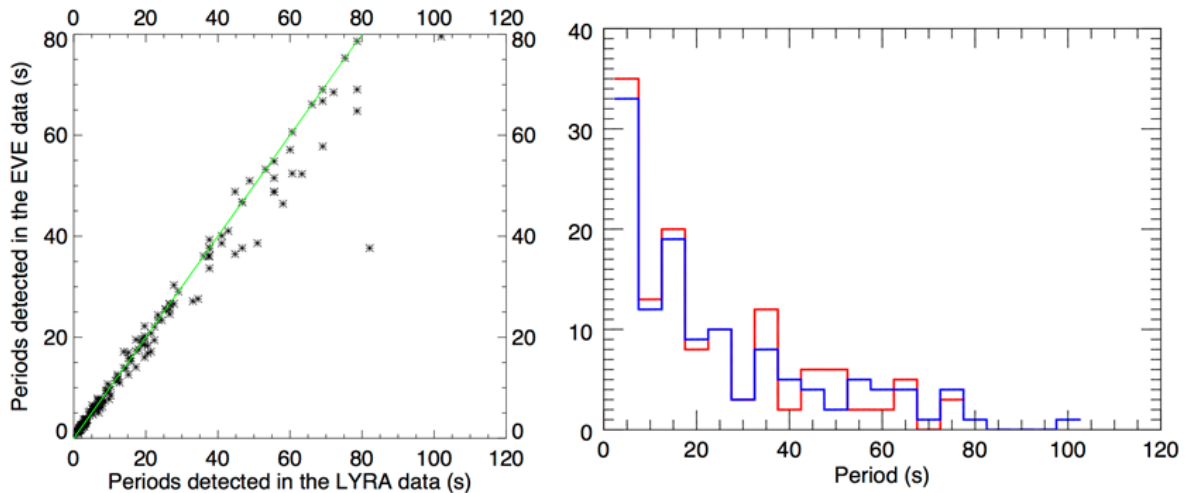


Figure 16: First detection of QPPs by Parks and Winckler in 1969.

24th solar cycle and offered the possibility to perform a statistical survey of the QPP phenomenon. Such surveys, which were not possible with the sporadic observations from the old generation of instruments, might help us to better understand the origin of QPPs, and further, the flaring process itself.

Unfortunately, the amplitude of QPPs in the SXR and EUV spectral ranges is much smaller than in the HXR and radio ranges. Therefore, it is often needed to pre-process the time series so as to amplify the oscillation amplitude to allow their detection. Such pre-processing techniques, known as “detrending”, have been regularly used in this context, but they come with a risk: they can result in spurious QPP detections and invalidate the conclusions of the statistical survey.

[Dominique et al. \(2018\)](#) proposed a set of criteria to help identifying real QPP detections from pre-processed time series and to discard artefacts. They also applied these criteria to 90 flares stronger than M5.0 that had been observed by SDO/EVE/ESP ([Woods et al. \(2012\)](#)) and PROBA2/LYRA to search for QPPs with periods between 1 and 100s. They confirmed that most of the flares exhibit such QPPs, but they found no dependence on the flare longitude or the flare class.



*Figure 18: (left) Correlation of the periods detected in the EVE and LYRA data for 90 flares of the solar cycle 24 of class above M5. – (right) Histogram of all periods detected in these flares that were observed by LYRA (blue) and EVE (red).*

### *How Alfvén waves transport energy in the solar corona and the solar wind*

At present, there is still no generally accepted explanation for the very high temperature of the corona, the millions of degrees hot solar atmosphere. Hence, the question on how energy is transported from the solar photosphere (“solar surface”) to the tenuous plasma (charged particles) in the corona and converted there to heat remains open. The most promising explanation is that this energy transport occurs in the form of waves.

In situ spacecraft observations have convincingly demonstrated that the wave energy in the solar wind is dominated by the magnetohydrodynamic (MHD) Alfvén mode. Alfvén waves generated at the solar coronal base propagate outward through the solar corona and interplanetary space, and thus they can transport this energy to the corona and farther into the solar wind. The amount of energy appears sufficient to drive the plasma heating and particle acceleration observed in the solar corona and solar wind. However, the difficulty is that MHD Alfvén waves interact only weakly with plasma particles, so while the energy can be transported to the corona, it is still not clear how it can heat the particles there. Therefore, the search is still open.

Energy transport from large- to small-scale plasma perturbations (the so-called plasma turbulence energy cascade), as well as nonlinear scalar decay of Alfvén waves, have been discussed recently as feasible alternatives to direct Alfvén wave-plasma interactions. In these processes, waves with similar scales (similar wavelengths) interact efficiently and generate a local spectral transport of the wave

energy from large to small scales – and providing energy to the solar wind particles at small (kinetic) scales is, effectively, increasing their temperature.

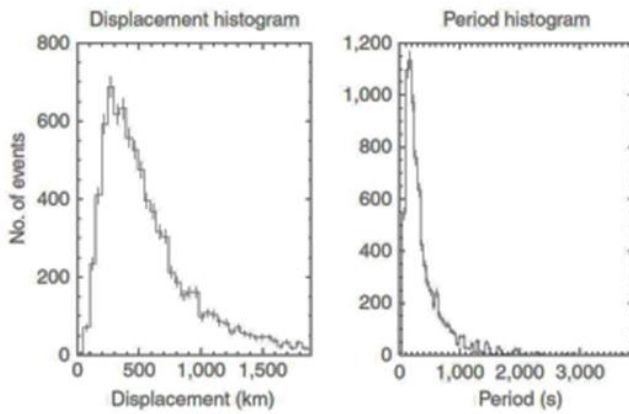


*Figure 19: Characteristics of Alfvén waves observed by SDO on open magnetic field lines above the Sun’s poles. The wave motion is measured directly by comparing the positions of thin flux tubes in successive images. The fine-scale motion of such flux tubes is characterised by an average displacement-amplitude of 590 km and a period of 470 s. (From Morton et al., 2015)*

In collaboration with Purple Mountain Observatory of CAS (Chinese Academy of Sciences; Nanjing, China), we have discovered a new decay type for MHD Alfvén waves – vector decay. Such a decay mechanism describes how plasma waves at a given scale can interact with each other to transform into other waves at smaller scales. Every wave participating in this decay propagates out of the plane in which the two other waves propagate. For the majority of Alfvén waves observed in the solar wind, the vector decay appears to be faster than the aforementioned familiar scalar decay where all waves propagate in the same plane. In addition, the vector decay makes the spectral transport non-local, in the sense that

the wave energy is directly transported to small (kinetic) scales, skipping intermediate scales. At small (kinetic) scales the waves dissipate efficiently, thus heating the plasma. This direct transport from large to very small (kinetic) scales is called “tunneling”.

This process is illustrated in Figure 20, where the horizontal axis shows the wavelength of the initial MHD Alfvén waves,  $\lambda_0/\rho_i$ , and the vertical axis shows the wavelength of the produced Alfvén waves,  $\lambda_1/\rho_i$ ; all wavelengths are expressed here in units of the ion gyroradius  $\rho_i$ , a characteristic small kinetic scale of a magnetized plasma. The colour represents the decay rate, that is, how fast a wave at a given scale is transformed into smaller waves. The decay rate is the inverse of the decay time and is expressed here in units of the ion gyroperiod. The dashed arrows illustrate how the wave energy tunnels from MHD to kinetic scales close to the ion gyroradius. The resulting waves have short wavelengths,  $\lambda_1 \sim \rho_i$ , and interact strongly with particles, thus heating the plasma.

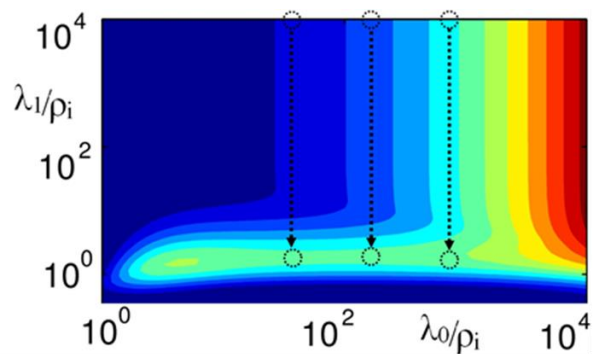


*Figure 20: Transport of Alfvén wave energy from MHD wavelengths  $\lambda_0 \sim (10^2-10^3)\rho_i$  to kinetic wavelengths  $\lambda_1 \sim \rho_i$  ( $\rho_i$  is the ion gyroradius) where the waves become strongly dissipative (see text for detailed explanation). (Adapted from Zhao et al., 2018)*

So, in summary, we have found a mechanism that helps to fill in the gap in our understanding of how the plasma in the solar corona and the solar wind is heated to millions of degrees Kelvin.

### *Signatures of a not so typical solar eruption*

On 14 August 2010, a wide-angled coronal mass ejection (CME) was observed. This solar eruption originated from a destabilized filament (a bundle of twisted magnetic field lines that holds solar plasma) which connected two active regions. The unwinding of this filament gave the eruption an untwisting motion that drew the attention of many observers. The different stages of the eruption are shown in Figure 21.

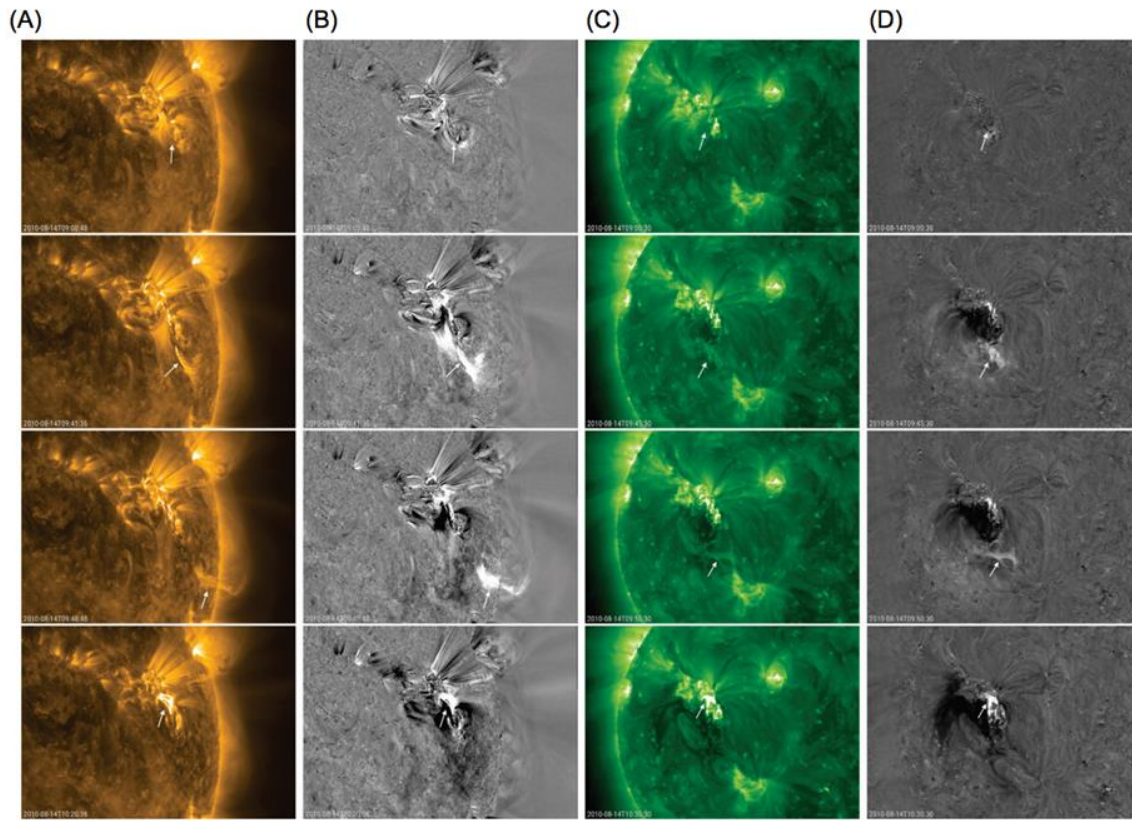


*Figure 21: SDO/AIA 171 plain and base difference images (columns A, B) of the eruption on 14 August 2010, combined with STEREO-A EUVI 195 Å images (plain and base difference; columns C, D) taken at approximately the same time. These images show (from top to bottom and indicated by the white arrows): the rising filament, its unwinding motion as it is hurled into space, and the post-eruptive loops.*

In addition to the erupting filament and the associated CME, several other low-coronal signatures that typically indicate the occurrence of a solar eruption were associated with this event. Solar observers, acting on information obtained from both satellites and ground-based stations, also reported a solar flare, radio bursts, an EUV darkening, and a minor proton event (the first of solar cycle 24). Some clips of this event can be found in the STCE [movie](#) on the finest solar eruptions in 2010.

With a velocity above 900 km/s, the speed of this CME can be considered as fast, certainly when compared to the intensity of the accompanying solar flare, which was quite weak (C4.4, where ‘C’ stands for a common flare). This is not what one would expect based on the current solar eruption models, which often link fast CMEs to strong solar flares.

To find out why this case was so different, we analyzed the initiation and the trajectory of the associated CME using three-dimensional reconstruction techniques. The resulting diagram of the height of the CME flux rope as it rises up in time is shown in Figure 22. For this plot, measurements were made on images taken by different EUV telescopes as well as coronagraphs. Note especially how the unique large field-of-view of the SWAP EUV telescope on board the PROBA2 ESA spacecraft is able to fill the observational gap between the other EUV telescopes and the coronagraphs. SWAP's observations were especially useful to measure the strong acceleration that the CME flux rope underwent at this height during the eruption.

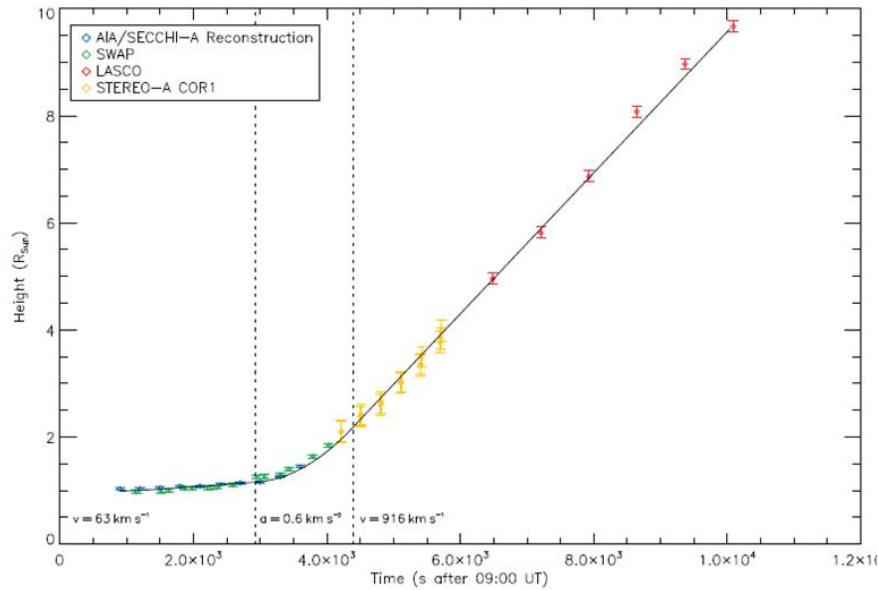


**Figure 22: Height-time diagram for the CME on 14 August 2010, combining measurements made using observations by different EUV imagers and coronagraphs.**

Our detailed analysis of the 14 August CME strongly suggests that this eruption was triggered by an ideal MHD instability, which was responsible for most of the acceleration of the CME. As a result, the eruption was not associated with significant magnetic reconnection, which explains the occurrence of only a weak flare in association with a very powerful CME.

Had this solar eruption occurred just a few days earlier, it could have been a significant event for space weather as the CME would have been directed towards the Earth. The risk of underestimating the strength of this eruption based solely on the C4.4 flare illustrates the need to include all eruption signatures in an event analysis in order to obtain a complete picture of the solar eruption and correctly assess its possible space weather impact.

The results of this study were written up in a paper that was published in the Journal of Space Weather and Space Climate ([D’Huys et al., 2017](#)).

### *The 4 November 2015 event*

Solar flares and other eruptive events are often accompanied by bursts of radio emission produced by energetic electrons. The spectral signature of these bursts provides solar physicists an insight into the scenario of the eruptive event that is taking place. The underlying physics giving rise to the radio emission, makes the intensity of these bursts essentially unrelated to the energy of the associated electrons. This means for example that tiny eruptive events, not detectable in EUV or soft X-ray, can

easily be observed in radio. On the other extreme, if strong flares are often associated with radio bursts, the intensity of the latter doesn't correlate with the strength of the flare.

This wide range of burst magnitudes requires tools that are extremely sensitive. As a result, solar radio astronomers, like all radio astronomers, are very wary in protecting their observations from interferences produced by other users of the radio spectrum. On some occasions however, "Mother Nature" is the one that interferes with radio technologies. On 4 November 2015, around 14:30UT, several Air Traffic Radar stations in western European countries (Sweden, Norway, Belgium and possibly others) suffered from disturbances for a short period of time (several periods spread over about an hour). The extent of the disruption varied from country to country. A team of astronomers and aeronautical experts from different institutes including ROB has investigated what happened on that day and has submitted the results to the [Journal of Space Weather and Space Climate](#).

Shortly before the disturbances started, the Sun produced a flare in an active region close to the central meridian. The flare, which occurred around 13:50UT, was ranked as an M-class event, which is relatively strong but by no means exceptional. Forty minutes later, radio observatories in Belgium, France and Switzerland registered what is called a type IV burst, which is the signature of energetic electrons trapped in post flare loops (new magnetic arcades forming in the aftermath of a flare). What made this radio event peculiar was its exceptional magnitude in a frequency range between ~1000 and 1200 MHz. By cross-calibrating their observations in Humain (Belgium), Nançay (France) and Bleien (Switzerland) scientists could estimate the magnitude of the radio burst to be between 100.000 and 150.000 solar flux units (sfu) in this narrow frequency range. This represents up to 2000 times the typical intensity of the radio quiet Sun. As shown in Figure 23, there were two periods of intense radio emission within half an hour.

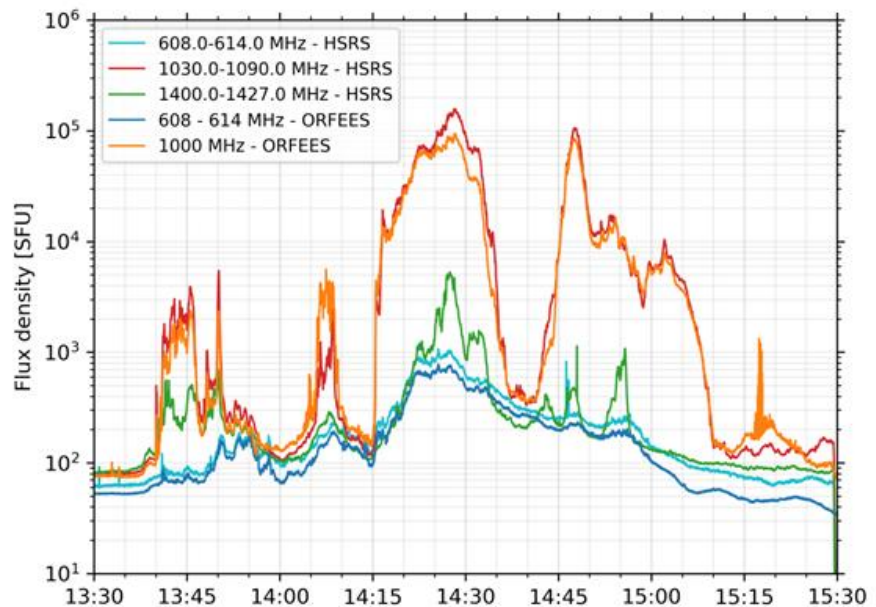


*Figure 23: Light curves of the radio burst as seen by the HSRS (Humain, Belgium) and ORFEES (Nançay, France) instruments. The orange and red curves correspond to frequencies very close to the ones where Secondary Surveillance Radars operate. The other light curves near 600 and 1400 MHz show that this radio burst was especially strong in a narrow frequency range between 1000 and 1200 MHz.*

Air Traffic Radar stations that were affected are the ones operating Secondary Surveillance radars which send coded queries to the plane avionics to collect information about the aircraft. They operate in two frequency bands at 1030 and 1090 MHz which are close to the frequency peak of the radio burst that occurred on that day. Disturbances were seen as ghost echoes lining up with the direction of the Sun.

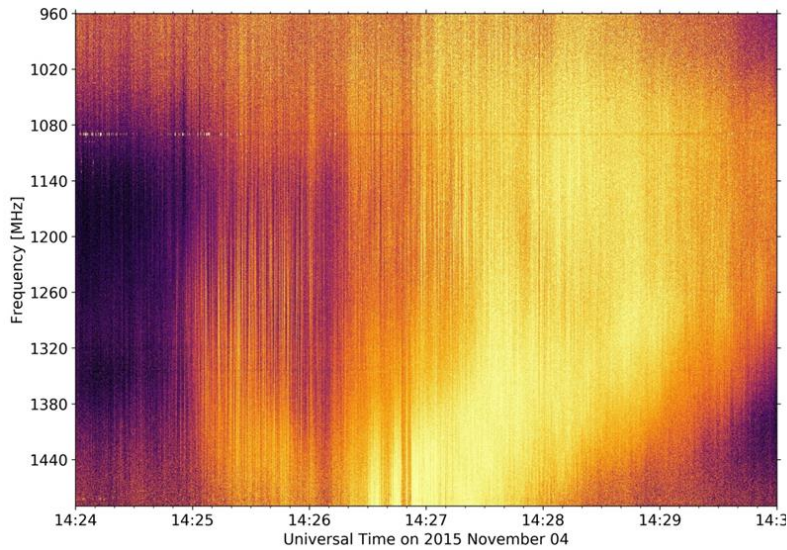


*Figure 24: Dynamic spectrum of the radio burst near the peak of the event as recorded by the HSR instrument in Humain. One can see the very fine spectral (vertical) structures that the burst is made of, which are called pulsations. The fine horizontal line near 1080 MHz corresponds actually to one of the 2 bands used in Secondary Surveillance Radar applications.*

Explaining why the burst was so intense is not easy. Observations showed that near the peak of the burst, numerous, fine and intense radio structures were observed over a more classical background of emission (see Figure 24). Such intense bursts can occur approximately every two years over the duration of a typical solar cycle, and this one was the strongest since March 2012. However, the frequency band at which the peak will occur remains highly variable and might not fall within the band of radars. In the same study, the team also reported problems with radio devices used during landing by an aircraft in Greenland. Other services like

GNSS (GPS or Galileo) are also known to be sensitive to solar radio burst effects. Besides its radio astronomy facility in [Humain](#), ROB also monitors in near real-time the influence of solar radio bursts (SRB) on [GNSS](#).

### *Local midnight ionospheric and plasmaspheric anomaly over West Antarctic*

The polar regions are Earth's windows to outer space. As such, the Belgian polar base Princess Elisabeth Antarctica (PEA), located in Utsteinen, North-East Antarctica, provides a unique opportunity for scientific research that cannot be performed at mid- and low-latitude regions. Moreover, the polar ionosphere-plasmasphere system (see Figure 25), especially over Antarctica, is not well understood as compared to other regions due to a lack of experimental observations. Hence, one of the present challenges of the

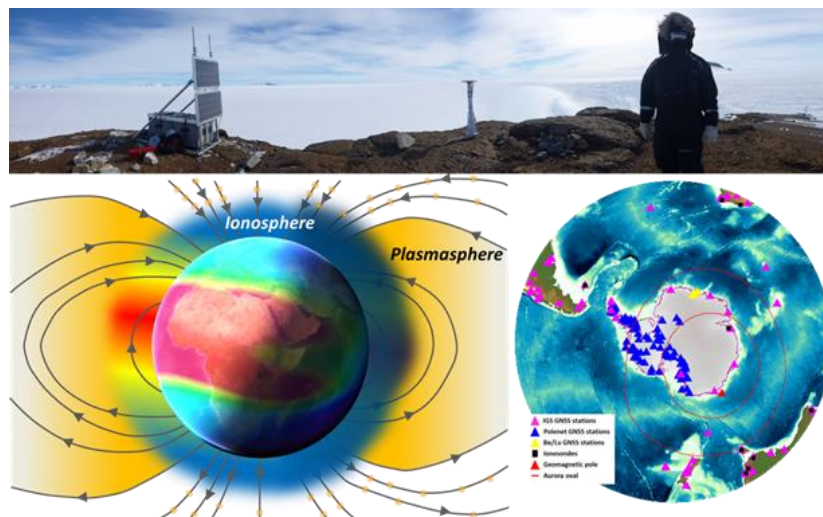


*Figure 25: Top: example of a GNSS station installed at 60 km from the Princess Elisabeth Antarctica Polar Base. Bottom left: Diagram representing the magnetosphere-plasmasphere-ionosphere system. Bottom right: GNSS data used to characterise the plasmasphere-ionosphere system.*

space weather community is to better characterise the climatological behaviour of the polar ionosphere and plasmasphere separately in response to variations in the solar activity at high latitudes. This is a first step to improve ionospheric models supporting on-site measurements (e.g. single frequency GNSS receivers).

During 2017, the STCE ionospheric team reprocessed the GNSS (Global Navigation Satellite System) data available since 1999 up to now for stations situated at latitudes below  $-50^\circ$  latitude using the ROB-IONO software. We used the data from POLENET/IGS (POLAR Earth observing NETWORK / International GNSS Service) networks and stations installed around PEA polar base. The output of this processing ( $\sim 18$  years of data) was then used to develop a model to predict the Total Electron Content (TEC, with  $1 \text{ TECu} = 10^{16} \text{ e}^- \cdot \text{m}^{-2}$ ) using the F10.7 solar index as input. The resulting model allows to estimate the TEC at a given location and specific time in Coordinated Universal Time (UTC), Solar Local Time (SLT) and Magnetic

Local Time (MLT) for southern latitudes from  $60^\circ$  to  $90^\circ$ .

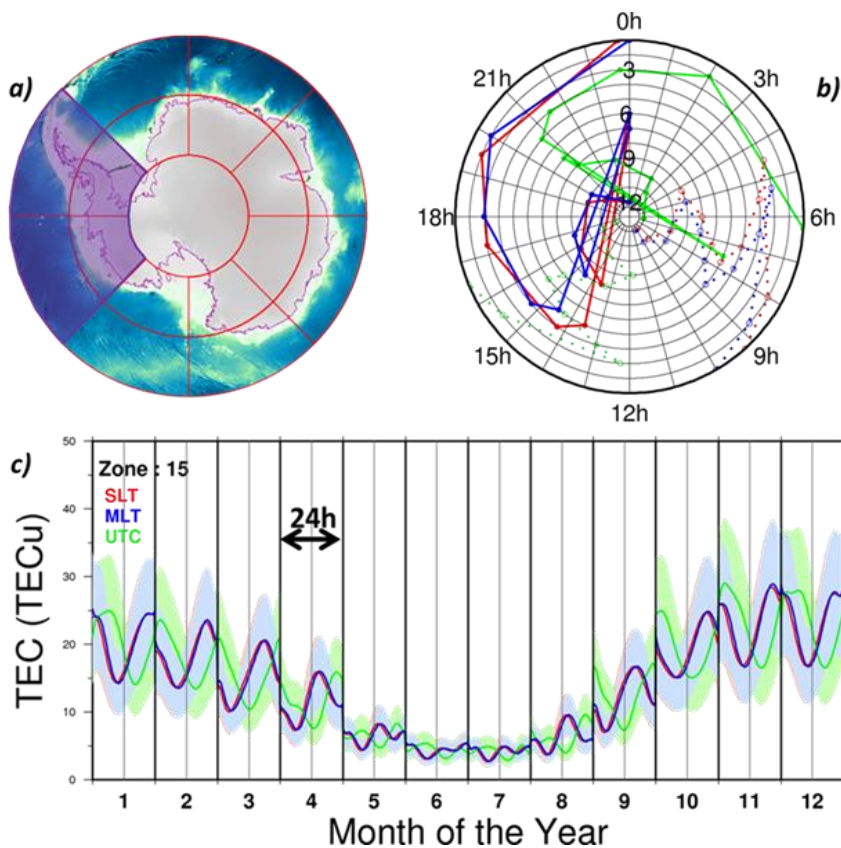


**Figure 26:** Illustration of the climatological pattern of TEC above Antarctica (local midnight summer anomaly). a) In violet, the zones where the midnight ionospheric and plasmaspheric anomaly (WSA) is observed. b) Time of occurrence of maximum (bold lines) and minimum TEC (dashed lines). Internal circles correspond to month of the year with December at the centre of the picture. c) Monthly climatological behaviour of the TEC for an identified pattern and different time definitions: SLT (red), UTC (green) and MLT (blue). The coloured lines are the daily TEC (vertical grey line is noon in given time definition) for medium solar activity level ( $F10.7P = 120 \text{ sfu}$ ). The spread of the colours stands for low and high solar activity ( $F10.7P = 80$  and  $160 \text{ sfu}$  respectively).

One of the main results obtained this year concerned the modelling of the Weddell Sea Anomaly (WSA) known as a summer ionosphere-plasmasphere anomaly, and characterised by a nighttime TEC larger than the daytime TEC in the region near the Weddell Sea (see Figures 26 b) and c)). This is really an anomaly because at other latitudes the TEC increases with day time due to the photo-ionisation of the ionosphere by the sunlight. One of the explanations of this anomaly is the important difference in distance between the magnetic and geographic poles, which at the moment (2017) is significantly larger in the southern hemisphere (about 3000 km) than in the northern hemisphere (about 500 km). This

should imply additional electron fluxes from the aurora zone along the magnetic field lines. Another possible origin is the presence of important neutral winds in the higher atmosphere in this region



## Mutual benefits between atmospheric research and radio based science over polar regions



Figure 27: Official picture of the STCE-SCAR (Scientific Committee of Antarctic Research) scientific workshop organised at ROB on 4 December 2017. The program can be found on the event [webpage](#).

implying more neutral components and consequently more photo-ionisation. Our future work should aim at separating the plasmaspheric contribution from the ionospheric one to better understand the coupling between these two layers and hence improve our understanding of the Weddell Sea Anomaly.

These results have been discussed in the frame of the STCE - SCAR (Scientific Committee of Antarctic Research) workshop called “Mutual benefits between atmospheric research and radio based science over polar regions” at the Royal Observatory of Belgium on 4 December 2017 (Figure 27).

### *Homogenisation of GPS integrated water vapour time series*

As water vapour is an important greenhouse gas and is responsible for the strongest positive feedback effect, estimating the long-term trends in the atmospheric water vapour is important for climate monitoring. Recent studies (e.g. [Van Malderen et al., 2014](#)) have demonstrated the capability of Global Positioning System (GPS) to retrieve the amount of atmospheric Integrated Water Vapour (IWV) for climate studies. However, the sudden offsets introduced in the IWV time series due to changes in the GPS instrumentation can change the resulting trends significantly, hence changing the interpretation in terms of climate. In order to obtain realistic and reliable climate signals a homogenisation of these IWV time series is necessary.

Within the COST Action ES1206 “Advanced Global Navigation Satellite Systems (GNSS) tropospheric products for monitoring severe weather events and climate” (GNSS4SWEC, 2013-2017), a

homogenisation activity was set up under the lead of Eric Pottiaux (ROB) and Roeland Van Malderen (RMI) , targeting the following objectives:

- select one or two long-term GNSS-based IWV datasets;
- apply different homogenisation algorithms on these reference datasets, and build up a list of commonly identified inhomogeneities based on statistical detection and metadata information;
- come up with a homogenised version of the reference datasets that can be re-used to study climate trends and time variability by the entire community.

As a first GNSS-based IWV dataset, we decided to focus on the existing tropospheric product given by the first data reprocessing of the International GNSS Service (IGS) network, named hereafter IGS repro 1. From this homogeneous (one single strategy) reprocessing of the IGS network observations, we selected a set of 120 GPS stations distributed worldwide providing continuous observations from 1995 until the end of 2010. As the distribution of the sites over large areas of the world is rather sparse (see Figure 28), the correlations between the IWV time series of our sample sites are rather poor in most areas. As a consequence, the use of neighbouring sites as reference series to remove similar climatic features and to reduce the complexity of the noise characteristics is problematic. Therefore, for a particular GNSS station, we chose to use the European Centre for Medium-Range Weather Forecasts (ECMWF) numerical weather prediction model reanalysis ERA-interim (or ERAI; [Dee et al., 2011](#)) IWV time series output as the reference.

Consequently, for each site, we calculated the IWV difference time series between the IGS repro 1 and ERA-interim IWV datasets and tested various homogenisation algorithms on the ERAI-IGS repro 1 differences. As a poor agreement was found between the detected offsets by different tools and the available metadata information on instrumental changes in the GPS equipment, we decided to first generate synthetic time series of IWV differences on which the different homogenisation tools could be blindly applied and benchmarked. We introduced known offsets in the synthetic time series, but did not

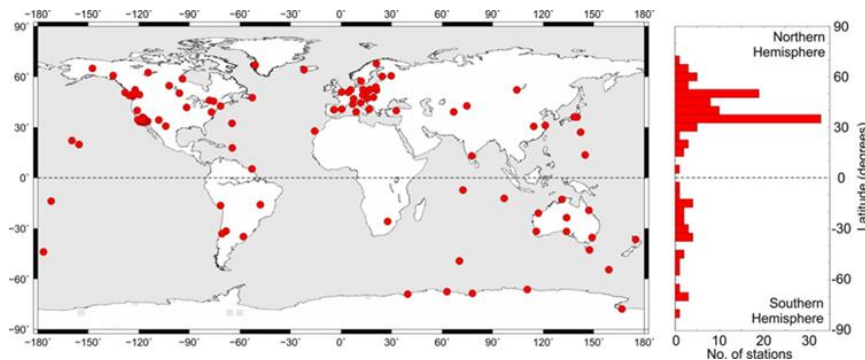


*Figure 28: (Left): Location of the selected 120 GPS stations from the IGS repro 1 with data available from 1995 until the end of 2010. (Right): Number of GPS stations from our selection located in specific latitude bands.*

reveal this information to the homogenisation tool operators to enable the blind testing.

To assess the performance of the synthetic datasets, different homogenisation tools that ran both on the daily and monthly aggregated synthetic time series, participated in our benchmarking activity. Amongst the participants were also colleagues from a

past COST Action ES0601 “Advances in Homogenisation Methods of Climate Series: An Integrated Approach (HOME)”. In this contribution, we will assess the performances of each homogenisation tool on the identification of the epochs of the inserted offsets in the synthetic time series. Therefore, we calculated for every homogenisation tool the statistical scores: the true positives (TP, “hits”), true negatives (TN: no breaks inserted, no break found), false positives (FP, “false alarms”), and false negatives (FN, “misses”).

To visualise the performances of the different tools in terms of those different statistical scores, we adapted the ternary graph (“triangle plot”) from [Gazeaux et al. \(2013\)](#), shown in Figure 29. It depicts the ratios of the statistical detection scores (TP+TN, FP, and FN) by their position in an equilateral triangle, highlighting the trade-off between those. A perfect solution would appear on the bottom right corner of the triangle (see blue lines in the figure). From a glance at this figure, it can be directly noted that the involved homogenisation tools do not perform very well for this dataset: especially the number of false positives is too high. Fortunately, the probabilities of true detection are also high. Some methods nearly detect all the inserted offsets, but at the cost of a high number of false alarms, while other methods are more conservative in detecting offsets, resulting in low scores for both true detection and false alarms. It should however be noted that a good performance of the tools is achieved for the majority of the participating methods on the less complicated synthetic datasets that we generated, especially due to a lower amount of false positives. We can conclude that the performance decreases for almost all the tools when adding gaps and a trend in the benchmark time series; adding autoregressive noise of the first order seems to have less impact.

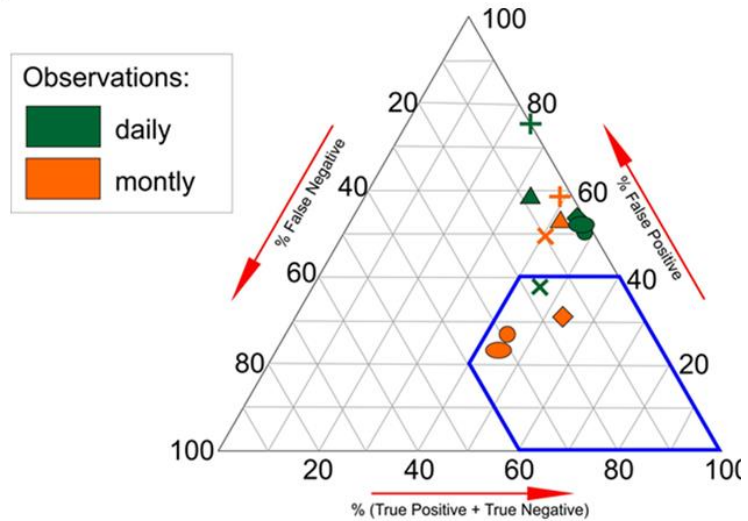


*Figure 29: Ternary graph (“triangle plot”) representing the ratio between three performance measures of the breakpoint detection solutions (TP+TN, FP, and FN). The performance increases with decreasing numbers of false positives and false negatives and increasing numbers of true positives and true negatives, so that a perfect solution is located in the lower right corner, marked by the blue area. The different solutions, here for the fully complicated synthetic dataset, are marked with the symbols and colours outline if the method was run on daily or monthly values.*

In conclusion, we found that the performances of the homogenisation algorithms in identifying the epochs of the inserted offsets especially decreases when adding trends and gaps to the synthetic datasets, due to a larger number of false alarms. On the other hand, the hit rates of most tools are rather good, even when applied on daily values instead of on monthly values.

Owing to the fact that metadata on instrumental changes are available for the GNSS stations, we primarily focused on the identification of the epochs of offsets until now. At the end, we would like to combine the outcome of statistical offset detection with these metadata. However, we will also assess the performances of the different tools by comparing the corrected time series given by different tools with the original time series.

A second round of blind homogenisation using a newly generated synthetic dataset of IWV values is being undertaken at the moment. Based on the performances of the statistical homogenisation tools on these synthetic datasets, we will develop a methodology for combining the results of good performing homogenisation tools with metadata information. This methodology and those tools will then be applied on the IGS repro 1 dataset of retrieved GPS IWV time series, resulting in a homogenised dataset, which will be validated by other sources of IWV time series and finally made available to the community for assessing the time variability of IWV and for validation of climate model IWV outputs.



*Figure 30: The annual **CHARM** meeting (Contemporary physical challenges in Heliospheric and AstRophysical Models) took place on 10 March in the Meridian Room of the ROB. With **topics** such as Kelvin-Helmholtz instabilities, resistive MHD equations, and mesh-free Hamiltonians, this meeting was definitely not for the faint-of-heart!*

## Instrumentation and experiments

### *Extreme Ultraviolet Imager (EUI) ready for launch!*

On 9 June 2017, the solar telescope EUI was delivered to Airbus UK. Integration of EUI onto the Solar Orbiter satellite was completed at Airbus on 5 September. In view of the readiness of EUI for launch and the prospect of its exciting journey ahead, the Royal Observatory of Belgium (ROB) and the Centre Spatial de Liège (CSL) organised a joint press conference in Liège on 2 June (see also the [press release](#)).

EUI was built (during more than 10 years) by an international consortium under the leadership of a dedicated team at the Centre Spatial de Liège. After launch, the instrument will be operated by the ROB. All this is possible thanks to the generous support from BELSPO through ESA/PRODEX.



*Figure 31: Members of the EUI team (ROB & CSL) pose in front of the instrument at the occasion of the press conference on 2 June.*

In sci-fi movies, spacecraft travel to the stars. With the "Solar Orbiter" spacecraft, mankind will make a small step towards the stars and travel first to its own star: the Sun. Obviously, Solar Orbiter will need special protection, the so-called heat shield, to withstand the scorching heat when travelling inward beyond the closest planet, Mercury. Solar Orbiter will not only observe the Sun from closer than ever, its orbit will also allow us to see the backside and the poles, which are hard to observe from the Earth's perspective.



*Figure 32: The Solar Orbiter spacecraft will observe the Sun from a distance 3 times closer than the Earth.*

Solar Orbiter is an ESA-led mission with strong NASA participation. Launch is planned in 2020, and will initiate a few rounds of planetary snooker. Two close encounters with Venus will alter the spacecraft's orbit, sending it to an intimate rendez-vous with Earth, which will bring it close to Venus once again. After a last gravitational slingshot from Venus, the desired orbit will be reached. Science operations will run from 2023 until 2026, and the mission may be extended afterwards till 2029.

On board Solar Orbiter, ten instruments will investigate the Sun and the local environment of the spacecraft. In-situ instruments will monitor the solar wind, magnetic fields and energetic

particles in the vicinity of the spacecraft, while remote-sensing instruments will take a fast succession of high resolution pictures from the Sun in several wavelengths. The resulting combination of instruments, combined with the unique orbit, distinguishes Solar Orbiter from all previous and current missions, enabling science which can be achieved in no other way. Solar Orbiter can therefore be seen as a next step in our exploration of the Sun and the Solar System.

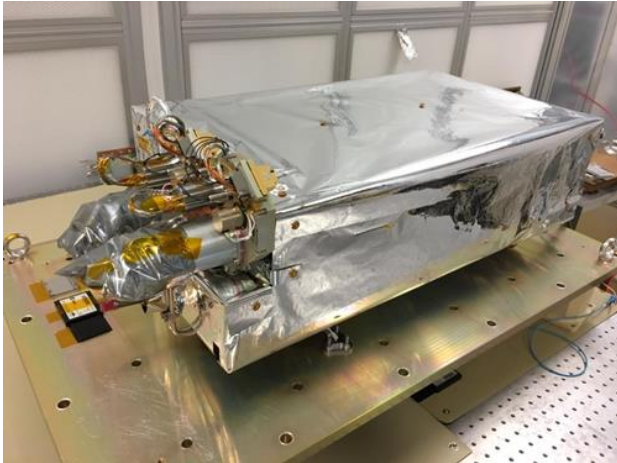


*Figure 33: The EUI telescopes just before delivery to Airbus (June 2017).*

The “Extreme Ultraviolet Imager” (EUI), one of the prime instruments on board Solar Orbiter, is a bundle of 3 telescopes for observations of the solar upper atmosphere, at unprecedented spatial resolution and with a large-angle view to see the full Sun, even from close by.

EUI will let us identify features on the Sun that are only 200 km apart, which is 5 times sharper than major contemporary missions such as NASA’s SDO mission. The large-angle view is needed to link structures and dynamic phenomena observed in high-resolution on the solar disk with the in-situ observations made by other instruments in the solar wind plasma surrounding the spacecraft.

Observing in extreme ultraviolet, EUI is perfectly placed to observe magnetic loops through which solar plasma is suspended far above the solar surface. These magnetic loops are very dynamic and can suddenly brighten and even burst. If these eruptions are directed towards Earth, they can have severe consequences on our technology such as GPS and radio communication, power grids, and pipelines.

Because of its close approach, EUI will be able to make exceptionally detailed images of our star. These will help scientists to unlock the secrets of the solar atmosphere: why is it so hot, what’s the nature of those magnetic loops and what puts them into motion? How do solar storms travel and evolve in space?

We are already looking forward to these exciting times!

### *The HOP334 solar observation campaign and the "lucky imaging" technique*

From 27 March 2017 till 4 April 2017, ROB took part in the international campaign "Joint observations of disk and off-disk structures between IRIS, HINODE, SUMER/SOHO and GBOs", also known as [HOP 334](#) (Hinode Operation Plan), which coordinated the solar observations of about twenty space-borne and ground-based observatories (resp. SBO and GBO). This campaign was primarily meant to support what is likely the last run of observations with the FUV-VUV spectrometer SUMER on board SOHO, one of the rare instruments capable of observing the Lyman  $\alpha$  spectral profile with high wavelength resolution.

The campaign had various targets: active regions (especially when they erupt), sunspots, filaments/prominences, spicules or coronal rain, observed over a wide range of wavelengths to cover different regimes of temperature and emission processes, for a comprehensive observation of the solar atmosphere from the photosphere to the extended corona.

ROB contributed with observations from space- and ground-based instruments. ROB's space-related data and imagery were provided by the PROBA2 spacecraft.

- The SWAP imager, observing the corona at 17.4 nm (EUV), performed off-pointing manoeuvres to follow erupting material further away than usual from the surface, and with an increased cadence;
- The LYRA radiometers observed with channels recording soft X-rays, EUV, Herzberg continuum and Lyman  $\alpha$ .

A number of ROB's ground-based telescopes also participated.

- The radio spectrographs of the Humain station (Callisto, ARCAS and HSRS) covered the range 45-1495 MHz to detect energetic electrons travelling through the corona and possibly into the interplanetary medium;
- Three USET telescopes in Uccle observed the Sun in  $H\alpha$ , Ca II k and broadband "white light" filters.

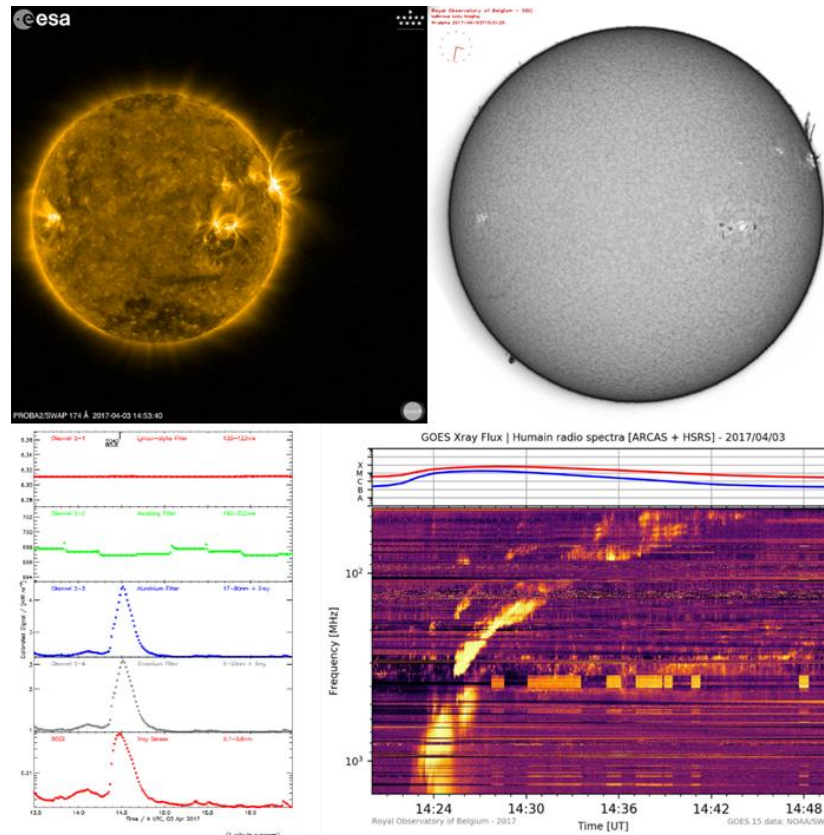


*Figure 34: Observations with ROB instruments during a solar eruption on 3 April 2017. From left to right and from top to bottom: PROBA2/SWAP off-pointed image; USET/ $H\alpha$  image; light curves in the 4 different channels of PROBA2/LYRA; radio observations at the Humain station, with the GOES X-ray light curves on top.*

During the campaign, about 10 noticeable radio events and 2 M-class flares were observed by the ROB instruments, one of the flares even producing a substantial signal in the Lyman  $\alpha$  channel of LYRA. This resulted in a unique data set associating space-borne instruments and ground-based observatories all over the world with complementary time coverage, "seeing" conditions and wavelength coverage, from the radio to X-ray wavelengths ranges.

The HOP 334 campaign offered a unique opportunity to test the "lucky imaging" technique on the  $H\alpha$  and Ca II k channels of the USET telescopes in Uccle. The idea of lucky imaging is to combine (parts of) the best images - recorded within a short time interval - into a single one, to reduce the distortion by the atmospheric turbulence and increase the signal-to-noise ratio. This allows us to see more and fainter details on the Sun. The camera software had been modified to record images at its maximum cadence of almost 4 images per second, and an optimal effective cadence of 10 seconds was chosen to match the cadence of other instruments taking part in the campaign. This 10-second cadence makes it possible to observe dynamic phenomena in the chromosphere, especially during eruptions.

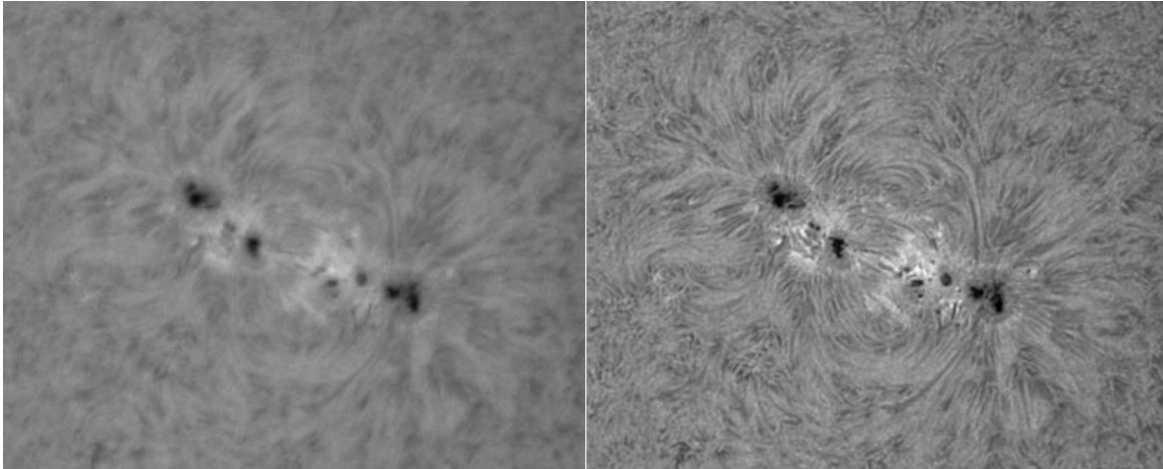


*Figure 35: On the left a close-up of active region (AR) NOAA 12645 imaged on 2 April 2017 at 08:00UTC with the USET H $\alpha$  - telescope. On the right the same region with much improved details as a result of the "lucky imaging" technique applied to 10 seconds worth of imagery.*

Because a full day of observations in these conditions produces hundreds of Gigabytes (8 TB in total for the complete campaign!), it was not possible to store them all on the acquisition computers of USET. A specific set-up was needed to cope with this large data flux, and the processing of the data -including calibration corrections- was also challenging. This campaign paved the way for more regular high-cadence observations of this type, to produce high-quality images with a high temporal resolution of dynamic events occurring in the solar chromosphere.

### *SOLAR-ISS, a new solar reference spectrum*

The accurate measurement of the solar spectral irradiance (SSI) outside the atmosphere, as well as its variability, is fundamental for solar physics, terrestrial atmospheric chemistry and Earth climate studies. The role of solar variability on climate change remains a topic of strong scientific and societal interest. An international scientific team including BIRA-IASB has accurately determined a new solar reference spectrum from measurements made by the SOLAR/SOLSPEC instrument onboard the International Space Station. This [study](#) was accepted for the journal *Astronomy and Astrophysics* in October 2017 and published in March 2018.

The Royal Belgian Institute for Space Aeronomy (BISA, BIRA-IASB) and the "Laboratoire Atmosphères, Milieux, Observations Spatiales" (LATMOS, formerly known as the "Service d'Aéronomie du CNRS") have been working on solar spectral irradiance and its variability since the 1970s. The design and development of the "SOLar SPECTrum" (SOLSPEC) instrument yields in a long, fruitful scientific and technical collaboration between the LATMOS (project manager) and BIRA-IASB, supported by the Belgian Science Policy (BELSPO). A former version of this instrument provided SSI measurements from several ESA and NASA space missions. SOLSPEC has acquired an undeniable international reputation, notably with the solar reference spectrum ATLAS-3. The recently published [study](#) allowed to go further using the new measurements obtained with SOLAR/SOLSPEC, the upgraded version of the instrument, part of the SOLAR payload onboard the COLUMBUS module of the International Space Station (Figure 36). The result is this new Solar Reference Spectrum (SOLAR-ISS).

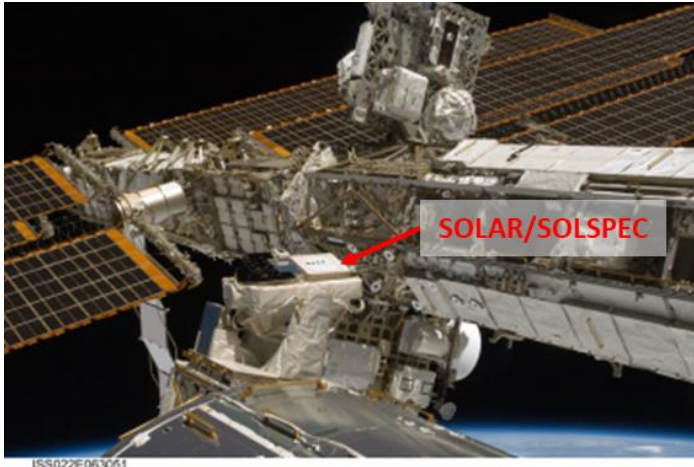


*Figure 36: The instrument SOLAR/SOLSPEC on board the International Space Station. SOLAR/SOLSPEC measured the solar spectrum from 5 April 2008 till 15 February 2017. Credits: NASA & ESA.*

Different fields of physics highlight the need for an absolute solar reference spectrum. For this, solar measurements have to be carried out from space to avoid atmospheric absorption. There is a need for robust instrumentation, resistant against the harsh space environment. It is of prime importance to design, characterise and calibrate the instrument before launch. For SOLAR/SOLSPEC, detailed studies took place at the BIRA-IASB laboratories for the development of the new optical, mechanical and electrical components and for the full radiometric characterisation performed after the refurbishment of the instrument.

SOLAR/SOLSPEC is designed for an absolute measurement of the spectral irradiance of the Sun (the solar radiant power received by a surface, per unit area, for each wavelength of the solar continuum). The required absolute calibration was carried out using a standard of spectral irradiance, the black body of the PTB (Physikalisch-Technische Bundesanstalt, Germany). Thanks to an internal lamp unit, it was possible during the mission to trace and correct any degradation via the SOLAR/SOLSPEC calibration coefficients. This traceability was essential for the determination of the new solar reference spectrum and the monitoring of the SSI variability during the mission (solar cycle 24). SOLAR-ISS is the result of a joint data processing by BIRA-IASB and LATMOS. This reference spectrum is the only one available over the extended wavelength range of 165 nm to 3000 nm. The accuracy is about 1%. The operations in orbit were carried out in perfect coordination with the B.USOC control center (Belgian User Support and Operations Center), also located at BIRA-IASB.

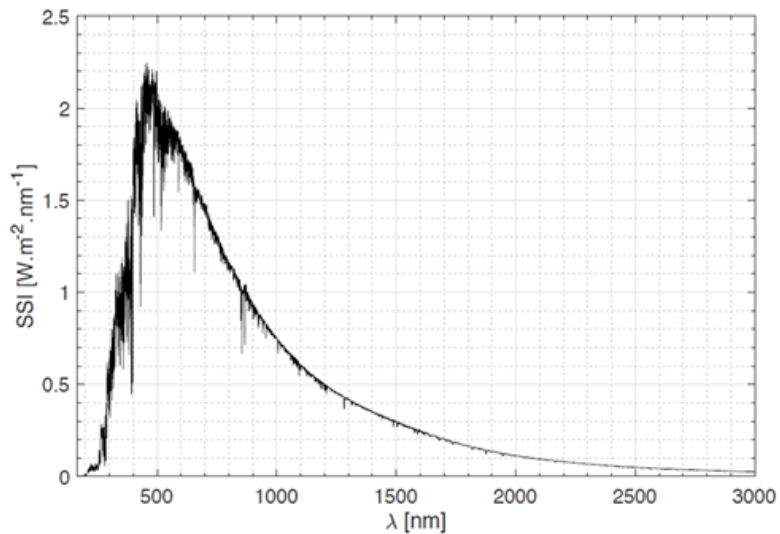


*Figure 37: SOLAR-ISS, the new reference solar spectrum. SOLAR-ISS is representative of the minimum of solar activity (April 2008).*

The SOLAR/SOLSPEC instrument data will also be used to track the spectral variability of solar irradiance over nearly a solar cycle (from 2008 to 2017). These are essential and valuable data for modeling the Earth's climate using climate chemistry models of the atmosphere. The spectral variations of solar irradiance are linked through complex mechanisms to the chemistry of the Earth's atmosphere and climate. During an 11-year solar cycle, the SSI variability in the UV is about 5-10%, while the variability of the total solar

irradiance is only 0.1%. This UV variability drives the ozone abundance and low stratosphere temperature inducing dynamic changes that may, according to recent research, influence circulation in the lower atmosphere. A reference solar spectrum and precise measurements of UV variability will contribute to further advances in this research area.



*Figure 38: No, a UFO has not landed next to the ROB's canteen. This is actually a radio telescope and part of the SPADE project (funded by BELSPO, through a BRAIN-BE grant). SPADE stands for Small Phased Array DEMonstrator and is aimed at observing the Sun. It will produce dynamic spectra of the Sun between 20 and 80 MHz with high sensitivity. An array consisting of eight of these low-cost radio telescopes will be deployed at the radio astronomy station of Humain, near Marche-en-Famenne (Belgium). But first of course, the instrument has to be tested, which is what the folks at the Royal Observatory of Belgium (ROB) were doing.*

## Applications, Modeling and Services

### SSA Space Weather Coordination Centre – User Support

Since the inauguration of the ESA Space Situational Awareness (SSA) Space Weather Coordination Centre (SSCC) in 2013, the Space Weather Group at the Royal Belgian Institute for Space Aeronomy is leading the SSCC in close collaboration with the Royal Observatory of Belgium. The SSCC serves as a central access point to a range of European space weather products and expertise to support users, including the general public. In 2017, the SSCC initiated the operation of space weather support campaigns for non-ESA users in the aviation and spacecraft operation domain. Gathering and tailoring information from the ESA SSA Space Weather Service Network, dedicated bulletins regarding actual and expected space weather conditions were delivered daily to test users in the form of textual (sms) and graphical (dashboard) presentation. The operational campaign was coordinated by a team of scientific SSCC operators. During and after the campaign feedback was collected from the test users, and used as input for further improving space weather services provided by the Network to fulfill the needs of the

users for mitigating the impacts of space weather on their operational systems.

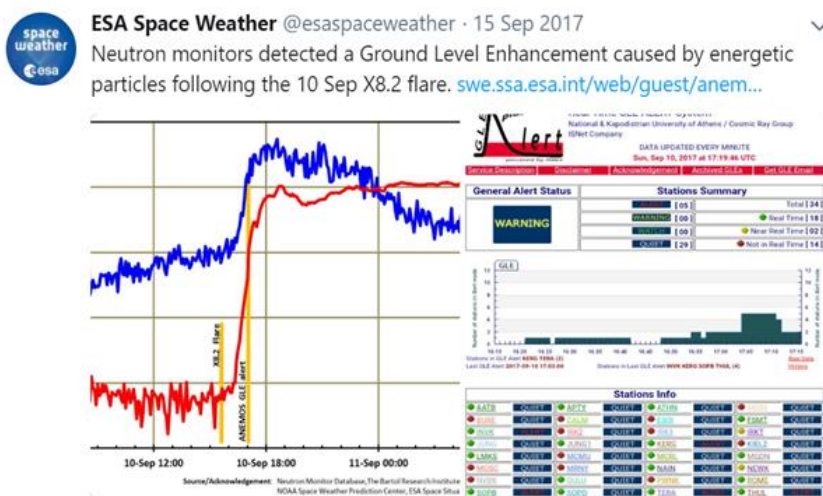


Figure 39: SSCC posted this Tweet concerning the Ground Level Enhancement (GLE) that took place on 10 September.

neutron monitors, an increase of 10 to 20% of radiation (compared to normal conditions) was estimated for flights over the poles at 12 km altitude. The SSCC was contacted by people whose relatives were flying over Northern Europe during the event, asking for more information. Fulfilling its role as first level user support, the SSCC provided a detailed evaluation of the impact of this period of increased solar activity in consultation with the SSA Expert Service Centre for Space Radiation. Observational information about the solar energetic particle storm was disseminated by the SSCC via the ESA Space Weather Twitter channel (@esaspaceweather).

## The reddish sun phenomenon on 16-17 October 2017

On 16-17 October 2017, a reddish sun was observed across a part of Western Europe. Many Europeans were impressed by the beauty and the rarity of this optical event that hit the headlines in the media. Various scientific institutes and newspapers have come up with a statement that the reddish sun was due to the remnants of Hurricane Ophelia dragging dust from the Sahara. At the same time, several flights in the UK, Sweden... were forced to land in emergency after reporting smoke in cockpit. There was a fair amount of confusion and misinformation being spread about the reddish sun phenomenon which resulted in unnecessary emergency landings. In reality, this optical phenomenon was caused by a smoke plume coming from wildfires located in Portugal and Spain. The misinterpretation given to this phenomenon clearly reveals its rarity at the European level where the last observation of this kind of events dates back to the end of September 1950 when a blue sun was observed caused by the smoke plume coming from the Chinchaga fire in North America. This blue sun was observed in France, in Switzerland, in Scotland, in Morocco... but not in Belgium due to a significant cloud cover.

The smoke plume coming from Portugal/Spain was observed by the Automatic-LIDAR-Ceilometers (ALC) that now offer the opportunity to monitor in real-time most aerosol plumes and especially their altitudes at high temporal (6s) and spatial scale (10m). The use of ALC network measurements in Belgium together with the operational dispersion model output from FLEXPART (short for FLEXPARTICLE dispersion model) made it possible to differentiate chronologically the passage of two aerosol plumes: the first one coming from the Sahara and the second one having its origin in Portugal/Spain and responsible for the reddish sun phenomenon. In this case, combining ceilometer measurements with the dispersion model FLEXPART made it possible to discriminate the sources rapidly.

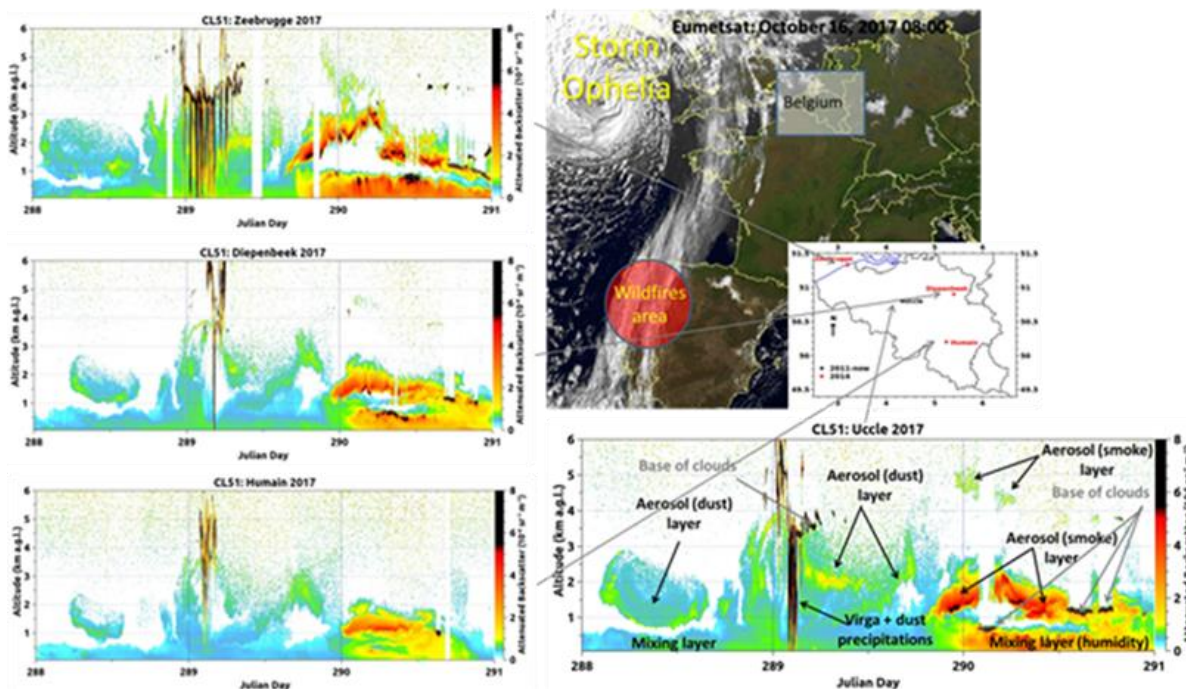


Figure 40: ALC measurements between 15 and 17 October 2017 in function of the altitude observed by the four ALC in Belgium with for Uccle, a description of each aerosol plumes validated by the dispersion model output.



*Figure 41: The reddish Sun on 17 October as photographed from the [RMI's roof](#). The phenomenon was a major news item on all main TV channels.*

Instrumental observation of smoke plumes in Europe is not uncommon. Over the last years, several smoke plumes not detectable to the naked eye have been observed by ALC in Europe. At the end of June 2013, an intercontinental smoke transport event was observed across Europe by satellite and ALC measurements. However, there were discussions on the region of origin of the smoke plume. Some scientists claimed that the observed plume originated from Colorado wildfires and others claimed that the smoke plume

came from Quebec wildfires – sources separated by more than 2000 km from each other! In this case, combining ceilometer measurements with the dispersion model FLEXPART made it again possible to discriminate the sources and highlighted that the main source contributing to the plume was coming from the Quebec wildfires.

The joint use of ALC measurements in Belgium together with the consultation of dispersion model output, removes uncertainties about the region of origin of the aerosol plumes for these events. This method ensures a better communication to authorities and the public, especially when the aerosol plume may generate a situation where quick decisions are required.

### *Ionospheric models used for calibration of GNSS timing stations.*

Atomic time scales based on a clock ensemble need as input the time differences between the clock readings. One technique used for remote clock comparison is based on GNSS data analysis. The reference time scale of a given GNSS constellation is then used as a common reference to which the ground clocks can be compared. This technique however needs an accurate calibration of the equipment in order to correct the time delay encountered by the signal inside the antenna, cable and receiver.

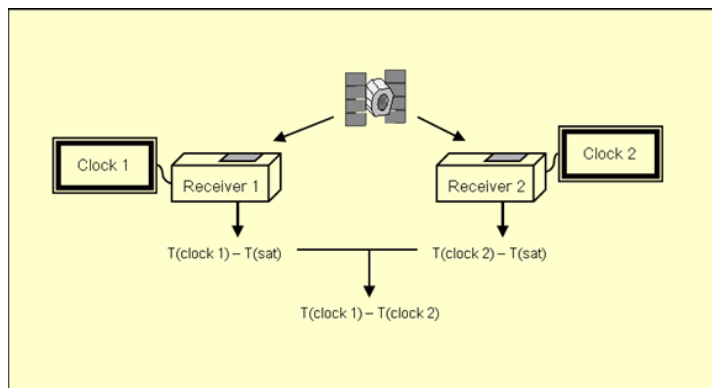


*Figure 42: Schematic view of GNSS time and frequency transfer. Using GNSS time transfer, the clocks of the [time laboratory of the ROB](#) are compared with other atomic clocks in the world and integrated to the computation of the Temps Atomique International (TAI) generated by the Bureau International des Poids et Mesures ([BIPM](#)) in Paris.*

Current calibration performances reach the nanosecond accuracy. However, the hardware delay is specific to a given signal frequency and modulation. In parallel, the delay induced by ionospheric refraction is also frequency dependent. Thus, the consistency of the calibration results among the different frequencies can theoretically be monitored using ionospheric models applied to the GNSS signal measurements of the calibrated stations. This study was carried out in 2017. An extensive analysis of the ionospheric models showed that the biases between these latter confer an uncertainty on the comparison estimated to 1.4 nanosecond (1 sigma) as shown in Figure 43.

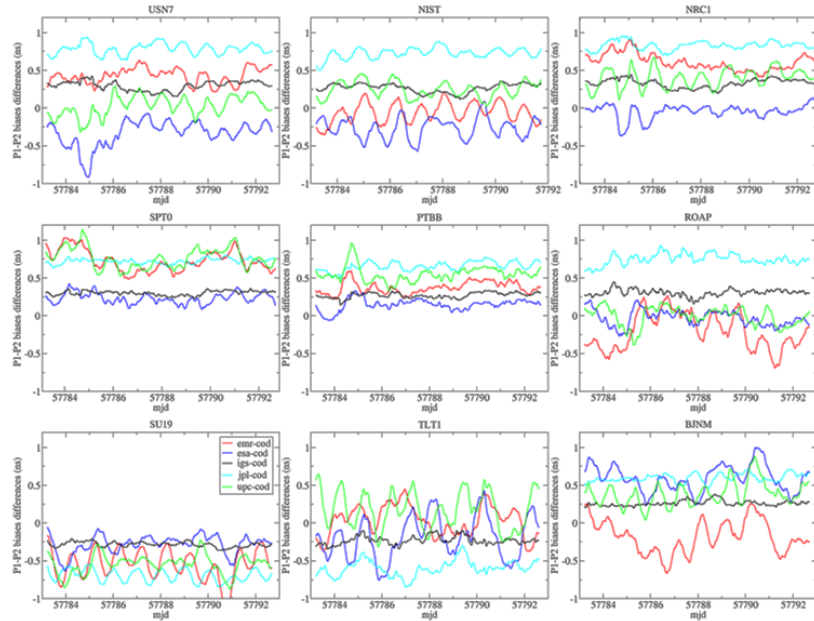


Figure 43: Differences (in nanoseconds; ns) between the inter-frequency delays computed using different ionospheric models, for stations in the US (top line), in Europe (middle line) and in Asia (bottom line).

Whenever a specific ionospheric model is chosen, the same technique can be used to study the long-term stability of the inter-signal hardware delays of the GNSS stations dedicated to remote clock comparisons. Due to the variations associated with the uncertainties in the ionospheric products, our results showed that only variations larger than 2 ns could be detected using a single station.

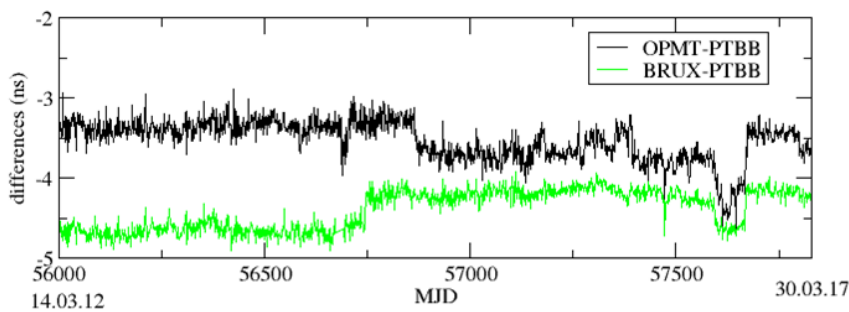
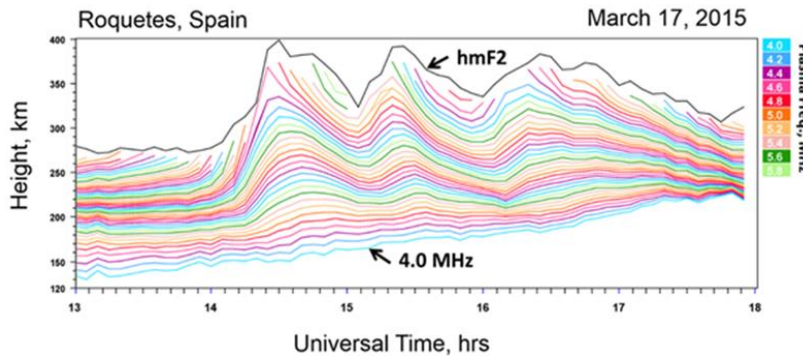


Figure 44: Differential hardware delays obtained for some timing stations, computed from the measured pseudo-ranges using the combined IGS ionospheric maps. (IGS: International GNSS Service)

However, as these ionosphere-induced variations are common to the stations of a same region, the difference between the solutions obtained for two stations separated by less than 2000 km can be analyzed more precisely to detect possible inter-signal delay variations. In the particular case shown in Figure 44, some jumps no larger than 400 picoseconds were detected in the difference of hardware delays of the two GPS codes for three European stations (OPMT in Paris, PTBB in Germany, and BRUX at ROB).

## Real-time monitoring of travelling ionospheric disturbances

The ionosphere is often being disturbed by various external factors such as solar radiation, geomagnetic field, gravity, etc. One specific kind of disturbances, the Travelling Ionospheric Disturbances (TIDs), is able to propagate over large distances, up to several thousands of kilometers, replicating similar variations in different places. When observed above a certain location over a period of time, the vertical distribution of the measured ionospheric electron density changes during the passage of a TID, exhibiting a wave-like pattern.



*Figure 45: Curves of equal electron density (isodensity contours) in the bottomside ionosphere, i.e. below the height (hmF2) of the peak ionospheric density. Each curve is identified by the corresponding plasma frequency (colour coded). Thus, each isodensity contour represents a certain electron density and how it varies over time. Note that there are many more measured frequencies than that there are colours, so the colour codes repeat themselves after several values of the frequencies, i.e. every 2 MHz. The plot clearly shows the effect of a TID passage, appearing as a wave between 14:00 and 17:00 UT. In this case, at 250 km altitude, the wave has an amplitude of about 25 km and a period of about 45 min.*

TIDs are attributed to atmospheric gravity waves that couple to the ionospheric plasma. As such, they contain information about the source that generates them which may be either natural or artificial. Natural sources include energy input from the Earth's auroral region, earthquakes, tsunamis, hurricanes, and others. Artificial sources can be ionospheric heating experiments, nuclear explosions and other



*Figure 46: The European network of digital ionospheric sounders used for identification and monitoring of TIDs. Each DPS4D sounder is referenced with its international code: Dourbes (DB049), Juliusruh (JR055), Pruhonice (PQ058), Ebro (EB040), and Athens (AT138). Lines represent existing links – solid lines indicate links that operate most frequently, arrows indicate direction of transmission.*

powerful blasts like industrial accidents and even rocket launches. TIDs contribute to the energy and momentum exchange between different regions of the ionosphere, especially during geomagnetic field disturbances.

It is very important to be able to identify and follow the development and movement of TIDs because they influence the modern-day services that rely on ionospheric radio wave propagation. For example, TIDs cause the high-frequency (HF) radio signals reflected by the ionosphere to deviate from their expected trajectories, thus causing errors in systems that are used to provide positioning and navigation services. TIDs also disturb HF radio communication systems.

In order to help the operators of technological systems affected by TIDs, the ionospheric

scientists in Europe -in cooperation with colleagues from the USA- developed a technique to measure the TID characteristics in real time. This new technique was developed based on the exploitation of the European network (see Figure 46) of [DPS4D](#) (Digisonde-Portable-Sounder-4D) advanced digital ionospheric sounders. The operation of these sounders can be synchronized to fulfill the operational specifications for the real-time identification of TIDs. The network topology includes both short-distance (less than 1000 km) and long-distance (more than 1000 km) links.

The technique was implemented for the first time to directly identify TIDs and specify the TID wave parameters based on measurements of the angle-of-arrival, Doppler frequency, and time-of-flight of

ionosphere-reflected HF radio pulses. In Figure 47, after examining the isodensity contours, TID signatures can clearly be seen between 18:00 UT and 22:00UT on 21 April 2017. Above the Ebro station (EB040), for example, the TID has an amplitude of about 25 km and a period of about 45 min observed at an altitude of 250 km. On this day, the TIDs are (most likely) triggered by the increase of the geomagnetic field activity in the auroral region, detected through geomagnetic measurements from that region.

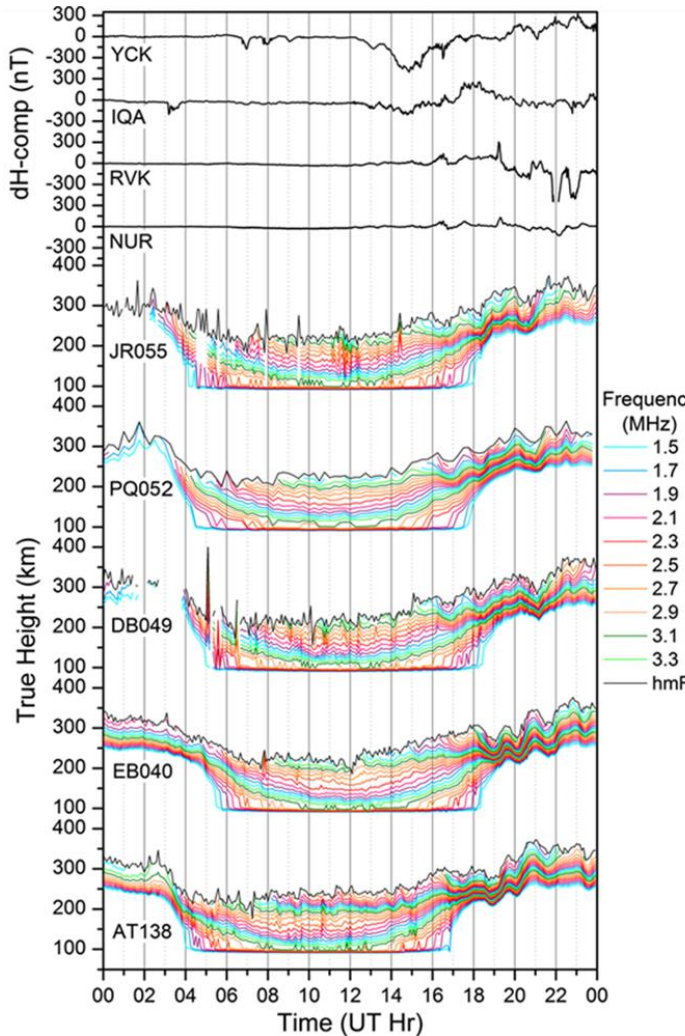


*Figure 47: Isodensity contours deduced from ionosonde measurements carried out on 21 April 2017 at the ionosonde stations JR055, PQ052, DB049, EB040, and AT138. For reference, the deviations of the horizontal component (H) of the geomagnetic field, as recorded at the auroral geomagnetic observatories of Yellowknife (YCK), Iqaluit (IQA), Rørvik (RVK), and Nurmijärvi (NUR), are shown at the top.*

The implementation of this technique for real-time operation based on the existing European digital ionosonde network was the objective of the recently completed international research project [Net-TIDE](#) (Pilot network for identification of Travelling Ionospheric Disturbances) which was funded by the NATO Science for Peace and Security ([SPS](#)) Programme. The project resulted in the successful operation of a first-of-this-kind (pilot) network for real-time detection of TIDs, including the development of a complex processing system for deriving the TID characteristics from measured signal parameters and for warning the users about ongoing strong TIDs (Figure 48). In addition, all identified TID events over Europe are stored in a database at the Global Ionospheric Radio Observatory (GIRO), allowing further research to obtain a better understanding of the

fundamental processes driving the formation and propagation of TIDs.

The importance and success of the Net-TIDE project led to attracting more partners (from France, Hungary, Cyprus, Bulgaria, and South Africa) and to widening the scope of our research and development activities related to TIDs and their effects. Thus, a larger consortium applied and received funding from the European Commission's Framework Programme for Research and Innovation, [HORIZON 2020](#), for a new international project, [Tech-TIDE](#): Warning and Mitigation Technologies for TIDs Effects.

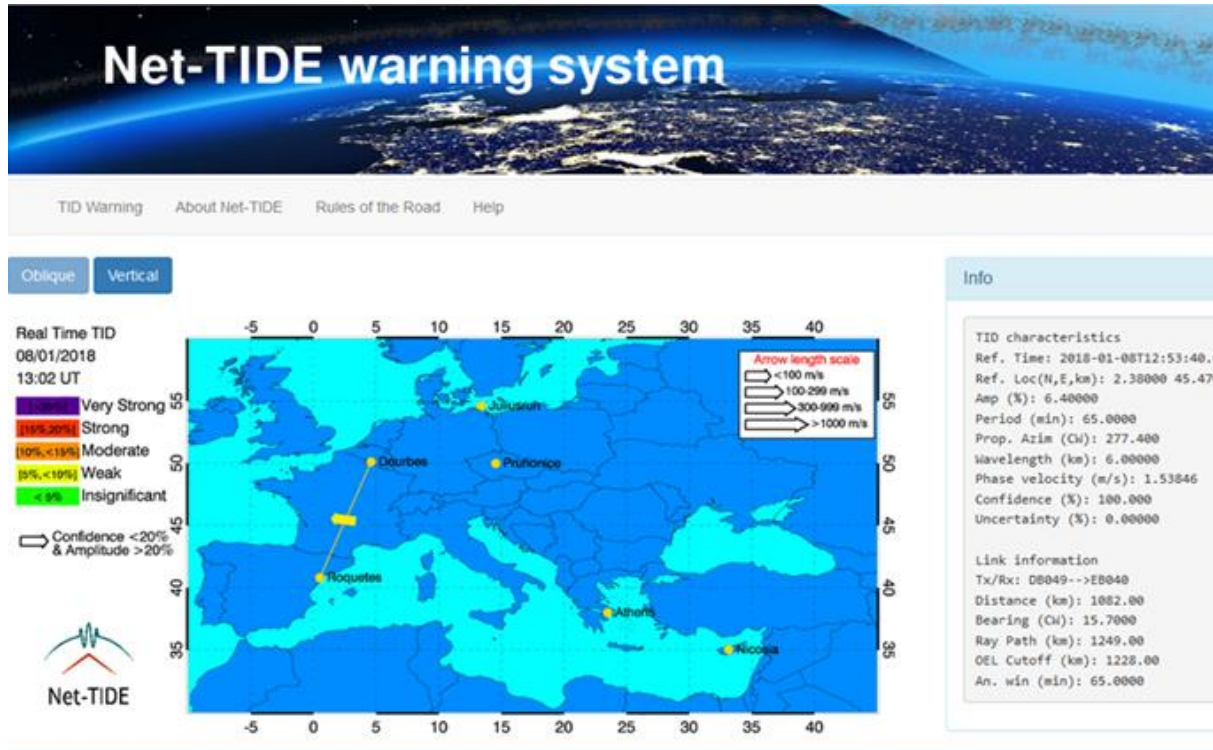


Figure 48: A screenshot of the real-time monitoring and warning system [webpage](#) developed during the international Net-TIDE project. In the above example, TID activity was encountered via the Dourbes-Roquetes link at 13:02UT on 8 January 2018. The estimated TID characteristics, such as amplitude, period, wavelength, phase velocity, etc., are readily provided for the user in the panel on the right side.

Because of the high occurrence frequency of TIDs (almost daily), and the variety of their characteristics regarding their velocity, propagation direction and amplitude, their identification and tracking is still very complicated and has not yet been achieved in continuous, fully operational service mode. Therefore, the overarching objective of the Tech-TIDE project is to design and test new viable TID impact mitigation strategies for the technologies affected and in close collaboration with operators of these technologies, to demonstrate the added value of the proposed mitigation techniques.

### *The ever-changing plasmasphere*

The upper layers of the Earth's atmosphere are (partially) ionised, thus forming the ionosphere. If they receive sufficient energy, the charged particles in the ionosphere can move upwards along the magnetic field lines. At equatorial latitudes, the field lines form closed loops arcing above the equator, so that

upflowing plasma remains trapped on those field lines: it fills the region of the inner magnetosphere commonly called the "plasmasphere".

The plasmasphere is very dynamic since it is affected by geomagnetic activity – geomagnetic activity tends to remove the plasmasphere's outer layers. The plasmasphere's size and structure are closely coupled to the degree of ionisation of the ionosphere. It also plays a role in the decay of the radiation belts. It therefore is of considerable importance for space weather monitoring to be able to model this component of the solar-terrestrial environment.

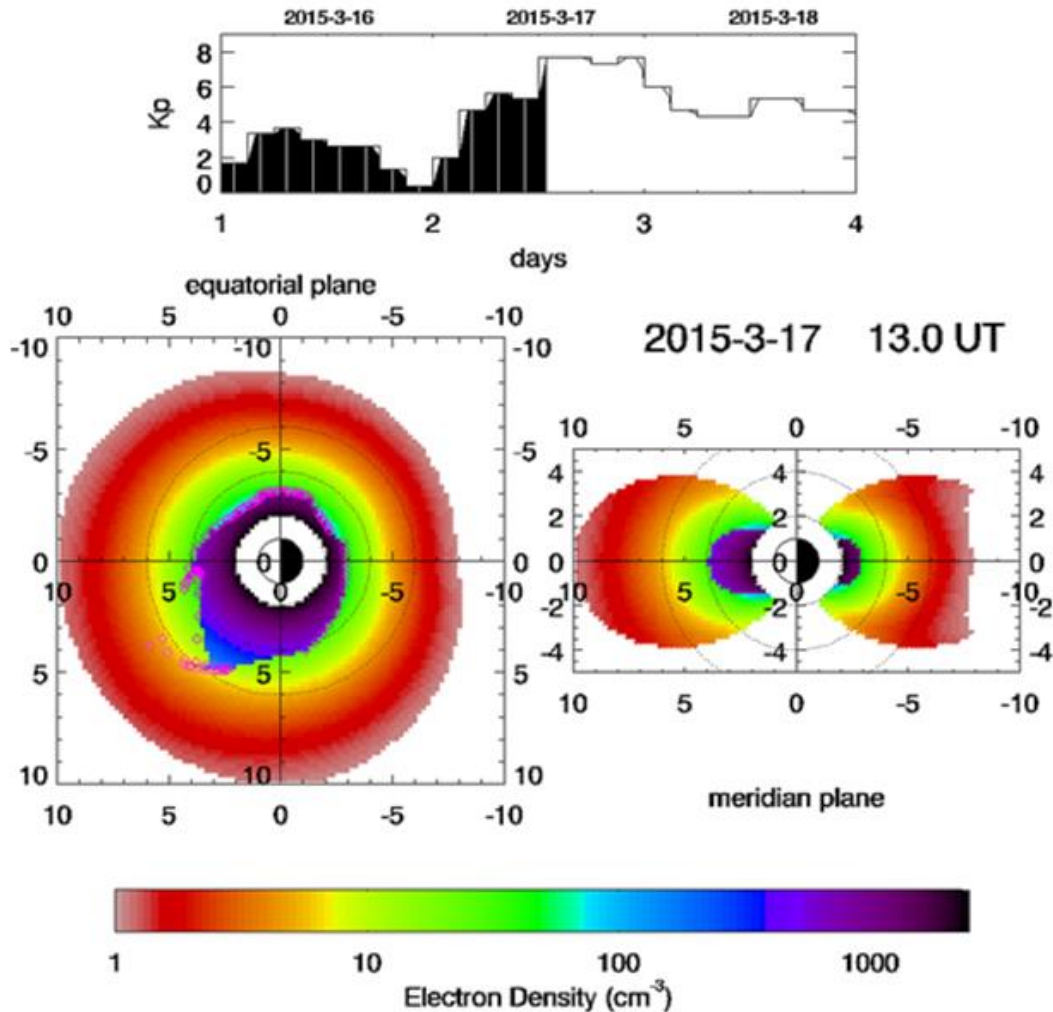


Figure 49: Top: Planetary geomagnetic activity index Bartels Kp observed from 16 to 18 March 2015. Bottom: Plasmasphere density (electron density) in the equatorial plane (left) and in the meridian plane (right) as obtained with the SPM plasmaspheric model (Pierrard and Voiculescu, 2011) for 17 March 2015 at 13:00 UT, during a geomagnetic storm. The plasmasphere corresponds to the dark region with higher density. Its outer boundary, the plasmopause, is indicated with diamonds. The plasma trough is the low density plasma region outside the plasmopause.

The three-dimensional dynamical plasmasphere model developed at IASB-BIRA has been used recently for comparison with satellite data. Measurements from THEMIS (Bandic et al., 2017) and PROBA-V for the radiation belts (López Rosson and Pierrard, 2017) have been used to study plasmasphere behaviour

during geomagnetic storms in detail. The plasmasphere model is coupled to an ionosphere model. Indeed, the ionosphere sets the boundary conditions that determine how the plasmasphere is refilled after a geomagnetic storm. The effects on the plasmasphere of a solar eclipse in March 2015 – which modified the ionospheric charge particle content - were also investigated ([Stankov et al., 2017](#)).

The model has been made available in real time and can be run for any chosen date on ESA's Space Situational Awareness [website](#). An example is shown in Figure 49.



*Figure 50: Amateur solar observers from Belgium and The Netherlands convened on 7 October for their [annual meeting](#) at the ROB. A talk on sunspots by Frédéric Clette and the visit of the USET solar telescopes belonged to the highlights.*

## Publications

This overview of publications consists of three lists: the peer-reviewed articles, the presentations and posters at conferences, and the public outreach talks and publications for the general public. It does not include non-refereed articles, press releases, the daily, weekly and monthly bulletins that are part of our public services,... These data are available at the [STCE-website](#) or upon request.

Authors belonging to the STCE have been highlighted in the list of peer reviewed articles.

### Peer reviewed articles

1. Bandic, M.; Verbanac, G.; **Pierrard, V.**; Cho, J.  
*Evidence of MLT propagation of the plasmopause inferred from THEMIS data*  
Journal of Atmospheric and Solar-Terrestrial Physics, 161, 55-63, 2017, DOI: 10.1016/j.jastp.2017.05.005
2. Bennett, G. V.; Johnson, H.R.; Weston, P.P.; Jones, J.; **Pottiaux, E.**  
*An assessment of ground-based GNSS Zenith Total Delay observation errors and their correlations using the Met Office UKV model*  
Quarterly Journal of the Royal Meteorological Society, 143, 707, 2436-2447, 2017, DOI: 10.1002/qj.3097
3. **Bolsée, D.; Pereira, N.; Gillotay, D.; Pandey, P.; Cessateur, G.**; Foujols, T.; Bekki, S.; Hauchecorne, A.; Meftah, M.; Damé, L.; Hersé, M.; **Michel, A.**; Jacobs, C.; Séla, A.  
*SOLAR/SOLSPEC mission on ISS: In-flight performance for SSI measurements in the UV*  
Astronomy & Astrophysics, 600, A21, 2017, DOI: 10.1051/0004-6361/201628234
4. Chu, X.; Bortnik, J.; Li, W.; Ma, Q.; Denton, R.; Yue, C.; Angelopoulos, V.; Thorne, R.M.; **Darrrouzet, F.**; Ozhogin, P.; Kletzing, C.A.; Wang, Y.; Menietti, J.  
*A neural network model of three-dimensional dynamic electron density in the inner magnetosphere*  
Journal of Geophysical Research: Space Physics, 122, 9183-9197, 2017, DOI: 10.1002/2017JA024464
5. **De Keyser, J.; Maes, L.; Maggiolo, R.**; Haaland, S.  
*Magnetopause thickness at the dawn and dusk flanks*  
Dawn-dusk asymmetries in planetary plasma environments (Eds. S. Haaland, A. Runov, C. Forsyth), AGU Monograph, 85-93, 2017, DOI: 10.1002/9781119216346.ch7
6. **De Wachter, E.; Kumps, N.; Vandaele, A.C.; Langerock, B.; De Mazière, M.**  
*Retrieval and validation of MetOp/IASI methane*  
Atmospheric Measurement Techniques, 10, 4623-4638, 2017, DOI: 10.5194/amt-10-4623-2017
7. **D'Huys, E.; Seaton, D.B.**; De Groof, A.; **Berghmans, D.**; Poedts, S.  
*Solar signatures and eruption mechanism of the August 14, 2010 coronal mass ejection (CME)*  
Journal of Space Weather and Space Climate, 7, A7, 2017, DOI: 10.1051/swsc/2017006
8. Drews, R.; Pattyn, F.; Hewitt, I.J.; Matsuoka, K.; Helm, V.; Berger, S.; **Bergeot, N.**; Favier, L.  
*Hydrological coupling between subglacial water conduit, esker, and ice-shelf channel across the grounding line of an Antarctic ice shelf*  
Nature Communications, 8, DOI: 10.1038/ncomms 15228
9. Dumbovic, M.; Srivastava, N.; Khodia, Y.; Vrsnak, B.; **Devos, A.; Rodriguez, L.**  
*Validation of the CME Geomagnetic forecast alerts under the COMESEP alert system*  
Solar Physics, 292, 96, 2017, DOI: 10.1007/s11207-017-1120-5
10. Gossart, A.; Souverijns, N.; Gorodetskaya, I.V.; Lhermitte, S.; Lenaerts, J.T.M.; Schween, J.H.; **Mangold, A.; Laffineur, Q.**; Van Lipzig, N.P.M.  
*Blowing snow detection from ground-based ceilometers: application to East Antarctica*  
The Cryosphere, 11, 6, 2755-2772, 2017, DOI: 10.5194/tc-11-2755-2017
11. Haaland, S.; Hasegawa, H.; **De Keyser, J.; Maes, L.**  
*Dawn-dusk asymmetries at the terrestrial magnetopause: Observations*  
Dawn-dusk asymmetries in planetary plasma environments (Eds. S. Haaland, A. Runov, C. Forsyth), AGU Monograph, 73-84, 2017, DOI: 10.1002/9781119216346.ch6
12. Haaland, S.; Lybekk, B.; **Maes, L.**; Laundal, K.M.; Pedersen, A.; Tenfjord, P.; Ohma, A.; Østgaard, N.; Reistad, J.P.; Snekvik, K.  
*North-south asymmetries in cold plasma density in the magnetotail lobes: Cluster observations*

- Journal of Geophysical Research: Space Physics, 122, 1, 136-149, 2017, DOI: 10.1002/2016JA023404
13. Kačmařík, M.; Douša, J.; Dick, G.; Zus, F.; **Brenot, H.**; Möller, G.; **Pottiaux, E.**; Kapłon, J.; Hordyniec, P.; Václavovic, P.; Morel, L.  
*Inter-technique validation of tropospheric slant total delays*  
Atmospheric Measurement Technique, 10, 2183-2208, 2017, DOI: 10.5194/amt-10-2183-2017
  14. **López Rosson, G.**; **Pierrard, V.**  
*Analysis of proton and electron spectra observed by EPT/PROBA-V in the South Atlantic Anomaly*  
Advances in Space Research, 60, 4, 796-805, 2017, DOI: 10.1016/j.asr.2017.03.022
  15. Lyubchik, O.; Kontar, E.P.; **Voitenko, Y.M.**; Bian, N.H.; Melrose, D.B.  
*Solar Plasma Radio Emission in the Presence of Imbalanced Turbulence of Kinetic-Scale Alfvén Waves*  
Solar Physics, 292, 9, 117, 2017, DOI: 10.1007/s11207-017-1140-1
  16. **Maes, L.**; **Maggiolo, R.**; **De Keyser, J.**; André, M.; Eriksson, A.; Haaland, S.; Li, K.; Poedts, S.  
*Solar illumination control of the polar wind*  
Journal of Geophysical Research: Space Physics, 122, 11468-11480, 2017, DOI: 10.1002/2017JA024615
  17. **Maggiolo, R.**; Hamrin, M.; **De Keyser, J.**; Pitkänen, T.; **Cessateur, G.**; **Gunell, H.**; **Maes, L.**  
*The delayed time response of geomagnetic activity to the solar wind*  
Journal of Geophysical Research: Space Physics, 122, 11109-11127, 2017, DOI: 10.1002/2016JA023793
  18. Meftah, M.; **Dominique, M.**; **BenMoussa, A.**; **Dammasch, I.E.**; **Bolsée, D.**; **Pereira, N.**; Damé, L.; Bekki, S.; Hauchecorne, A.  
*On-orbit degradation of recent space-based solar instruments and understanding of the degradation processes*  
Proceedings of the SPIE: Sensors and Systems for Space Applications X, 10196, 1019606, 2017, DOI: 10.1117/12.2250031
  19. Meftah, M.; Damé, L.; **Bolsée, D.**; **Pereira, N.**; **Sluse, D.**; **Cessateur, G.**; Irbah, A.; Sarkissian, A.; Hauchecorne, A.; Bekki, S.  
*A New Solar Spectrum from 656 to 3088 nm*  
Solar Physics, 292, 8, 101, 2017, DOI: 10.1007/s11207-017-1115-2
  20. Morosan, D.; ... ; **Magdaleníć, J.**; ... ; and 57 co-authors  
*The association of a J-burst with a solar jet*  
Astronomy & Astrophysics, 606, A81, 2017, DOI: 10.1051/0004-6361/201629996
  21. **Moschou, S.-P.**; **Pierrard, V.**; Keppens, R.; Pomoell, J.  
*Interfacing MHD and kinetic solar Wind Models and comparing their energetics*  
Solar Physics, 292, 139, 1-25, 2017, DOI: 10.1007/s11207-017-1164-6
  22. Möstl, C.; Isavnin, A.; Boakes, P.; Kilpua, E. K. J.; Davies, J.; Harrison, R.; Barnes, D.; Krupar, V.; Eastwood, J.; Good, S.; Forsyth, R.; Bothmer, V.; Reiss, M.; Amerstorfer, T.; Winslow, R.; Anderson, B.; Philpott, L.; **Rodriguez, L.**; Rouillard, A.; Gallagher, P.; Nieves-Chinchilla, T.; Zhang, T.  
*Modeling observations of solar coronal mass ejections with heliospheric imagers verified with the Heliophysics System Observatory*  
Space Weather, 15, 7, 955-970, 2017, DOI: 10.1002/2017SW001614
  23. Müller, D.; **Bogdan, N.**; Simon, F.; **Verstringe, F.**; **Bourgoignie, B.**; Csillaghy, A.; **Berghmans, D.**; Jiggins, P.; García-Ortiz, J.P.; Ireland, J.; Zahniy, S.; Fleck, B.  
*JHelioviewer - Time-dependent 3D visualization of solar and heliospheric data*  
Astronomy & Astrophysics, 606, A10, 2017, DOI: 10.1051/0004-6361/201730893
  24. Namaoui, H.; Kahlouche, S.; Belbachir, A.H.; **Van Malderen, R.**; **Brenot, H.**; **Pottiaux, E.**  
*GPS water vapour and its comparison with radiosondes and ERA-Interim data in Algeria*  
Advances in Atmospheric Sciences, 34, 5, 623-634, 2017, DOI: 10.1007/s00376-016-6111-1
  25. Paassilta, M.; Raukunen, O.; Vainio, R.; Valtonen, E.; Papaioannou, A.; Siipola, R.; Riihonen, E.; **Dierckxsens, M.**; **Crosby, N.B.**; Malandraki, O.; Heber, B.; Klein, K.-L.  
*Catalogue of 55-80 MeV solar proton events extending through solar cycles 23 and 24*  
Journal of Space Weather and Space Climate, 7, A14, 2017, DOI: 10.1051/swsc/2017013
  26. Patel, M.R.; ... ; **Drummond, R.**; **Thomas, I.R.**; **Depiesse, C.**; **Neefs, E.**; **Equeter, E.**; **Rsitic, B.**; **Berkenbosch, S.**; **Bolsée, D.**; **Willame, Y.**; **Vandaele, A.C.**; ... ; **Benmoussa, A.**; **Giordanengo, B.**; **Gissot, S.**; ... ; and 37 co-authors  
*NOMAD spectrometer on the ExoMars trace gas orbiter mission: part 2-design, manufacturing, and testing of the ultraviolet and visible channel*  
Applied Optics, 56, 10, 2771-2782, 2017, DOI: 10.1364/ao.56.002771
  27. **Pereira, N.**; **Bolsée, D.**; **Sluse, D.**; **Michel, A.**; Meftah, M.; Damé, L.; Irbah, A.  
*Design of an optical sun sensor for a space application: a reliable passive sun tracking device for the SOLAR/SOLSPEC instrument*  
Proceedings of the SPIE: Optical Sensors 2017 conference, 10231, 102311V, 2017, DOI: 10.1117/12.2265709

28. **Pierrard, V.**; Meyer-Vernet, N.  
*Electron Distributions in Space Plasmas*  
Kappa Distributions: Theory and Applications in Plasmas (Ed. G. Livadiotis), Elsevier, Chapter 11, 465-479, 2017, DOI: <https://doi.org/10.1016/B978-0-12-804638-8.00011-5>
29. Podladchikova, T.; **Van der Linden, R.**; Veronig, A.  
*Sunspot number second differences as precursor of the following 11-year sunspot cycle*  
The Astrophysical Journal, 850, 1, 81, 2017, DOI: [10.3847/1538-4357/aa93ef](https://doi.org/10.3847/1538-4357/aa93ef)
30. **Ranvier, S.**; **Anciaux, M.**; **Cardoen, P.**; **Gamby, E.**; **Bonnewijn, S.**; **De Keyser, J.**; **Pieroux, D.**; Lebreton, J.P.  
*Use of a Langmuir probe instrument on board a pico-satellite*  
IEEE Transactions on Plasma Science, 45, 8, 2007-2012, 2017, DOI: [10.1109/TPS.2017.2700211](https://doi.org/10.1109/TPS.2017.2700211)
31. Schmalwieser, A.W.; ...; **De Backer, H.**; **Bolsée, D.**; ...; and 46 co-authors  
*UV Index monitoring in Europe*  
Photochemical & Photobiological Sciences, 16, 9, 1349-1370, 2017, DOI: [10.1039/c7pp00178a](https://doi.org/10.1039/c7pp00178a)
32. Slapak, R.; **Gunell, H.**; Hamrin, M.  
*Observations of multiharmonic ion-cyclotron waves due to inverse ion-cyclotron damping in the northern magnetospheric cusp*  
Geophysical Research Letters, 44, 22-29, 2017, DOI: [10.1002/2016GL071680](https://doi.org/10.1002/2016GL071680)
33. **Stankov, S.M.**; **Bergeot, N.**; **Berghmans, D.**; **Bolsée, D.**; **Bruyninx, C.**; **Chevalier, J.-M.**; **Clette, F.**; **De Backer, H.**; **De Keyser, J.**; **D’Huys, E.**; **Dominique, M.**; **Lemaire, J.F.**; **Magdalenic, J.**; **Marqué, C.**; **Pereira, N.**; **Pierrard, V.**; **Sapundjiev, D.**; **Seaton, D.B.**; **Stegen, K.**; **Van der Linden, R.**; **Verhulst, T.G.W.**; **West, M.**  
*Multi-instrument observations of the solar eclipse on 20 March 2015 and its effects on the ionosphere over Belgium and Europe*  
Journal of Space Weather and Space Climate, 7, A19, 2017, DOI: [10.1051/swsc/2017017](https://doi.org/10.1051/swsc/2017017)
34. Temmer, M.; Dissauer, K.; Thalmann, J.K.; Veronig, A.M.; Tschernitz, J.; Hinterreiter, J.; **Rodriguez, L.**  
*On Flare-CME Characteristics from Sun to Earth Combining Remote-Sensing Image Data with In Situ Measurements Supported by Modeling*  
Solar Physics, 292, 7, 93, 2017, DOI: [10.1007/s11207-017-1112-5](https://doi.org/10.1007/s11207-017-1112-5)
35. Thiemann, E.; **Dominique, M.**; Pilinski, M.; Eparvier, F.  
*Vertical Thermospheric Density Profiles from EUV Solar Occultations made by PROBA2 LYRA for Solar Cycle 24*  
Space Weather, 15, 12, 1649-1660, 2017, DOI: [10.1002/2017SW001719](https://doi.org/10.1002/2017SW001719)
36. **Verhulst, T.G.W.**, **Stankov, S.M.**  
*Height-dependent sunrise and sunset: Effects and implications of the varying times of occurrence for local ionospheric processes and modelling*  
Advances in Space Research, 60, 8, 1797-1806, 2017, DOI: [10.1016/j.asr.2017.05.042](https://doi.org/10.1016/j.asr.2017.05.042)
37. **Verhulst, T.G.W.**; Altadill, D.; Mielich, J.; Reinisch, B.; Galkin, I.; Mouzakis, A.; Belehaki, A.; Buresova, D.; **Stankov, S.M.**; Blanch, E.; Kouba, D.  
*Vertical and oblique HF sounding with a network of synchronized ionosondes*  
Advances in Space Research, 60, 8, 1644-1656, 2017, DOI: [10.1016/j.asr.2017.06.033](https://doi.org/10.1016/j.asr.2017.06.033)
38. Zender, J.J.; Kariyappa, R.; Giono, G.; Bergmann, M.; **Delouille, V.**; Damé, L.; **Hochedez, J.-F.**; Kumara, S.T.  
*Segmentation of photospheric magnetic elements corresponding to coronal features to understand the EUV and UV irradiance variability*  
Astronomy & Astrophysics, 605, A41, 2017, DOI: [10.1051/0004-6361/201629924](https://doi.org/10.1051/0004-6361/201629924)

## Presentations and posters at conferences

1. Alfonsi, L.; Bergeot, N.  
*An international initiative for atmospheric research at the poles*  
URSI 2017 - General Assembly and Scientific Symposium, Montreal, Canada, 19-26 August 2017
2. Alfonsi, L.; Bergeot, N.; Correia, E.; Gulisano, A.; De Franceschi, G.  
*Radio Sciences Research on Antarctic Atmosphere - RESOURCE*  
IX Congreso Latinoamericano de Ciencia Antártica, Punta Arenas, Chile, 4-6 October 2017
3. Alfonsi, L.; Bergeot, N.; and 16 others  
*RESOURCE: An international initiative for atmospheric research at the poles*  
SCAR-GRAPE workshop (STCE), Brussels, Belgium, 4 December 2017
4. Altadill, D.; Blanch, E.; Paznukhov, V.; Zornoza, M.J.; Belehaki, A.; Verhulst, T.; Galkin, I.; Reinisch, B.; Buresova, D.; Mielich, J.; Parkinson, M.; Subirana, J.S.  
*Interferometry method to conventional ionosonde data in support of a pilot network for identification of travelling ionospheric disturbances*  
URSI 2017 - General Assembly and Scientific Symposium, Montreal, Canada, 19-26 August 2017
5. Balikhin, M.A.; Voitenko, Y.M.; Fedun, V.  
*Alfvénic Turbulence and Energy Release in Space Plasmas 2017 Workshop: Turbulence in Space and Laboratory Plasma and Impact on High Frequency (HF) Wave Propagation*, Arlington, Virginia, USA, 6-7 September 2017 (invited talk)
6. Barnes, D.; Davies, J.; Harrison, R.; Perry, C.; Möstl, C.; Rouillard, A.; Bothmer, V.; Rodriguez, L.; Eastwood, J.; Kilpua, E.; Gallagher, P.  
*A Catalogue of Coronal Mass Ejections Observed by the STEREO Heliospheric Imagers: Results from HELCATS*  
EGU General Assembly 2017, Vienna, Austria, 23-28 April 2017 (poster)
7. Berckmans, J.; Van Malderen, R.; Pottiaux, E.; Pacione, R.  
*Evaluation of the atmospheric water vapor content in the regional climate model ALARO-0 using GNSS observations from EPN Repro2*  
European Meteorological Society Annual Meeting 2017, Dublin, Ireland, 4-8 September 2017
8. Berckmans, J.; Van Malderen, R.; Pottiaux, E.; Pacione, R.  
*Evaluation of the atmospheric water vapor content in the regional climate model ALARO-0 using GNSS observations COST ES1206 - GNSS4SWEC Final Workshop*, Noordwijk, The Netherlands, 21-23 February 2017
9. Berckmans, J.; Van Malderen, R.; Pottiaux, E.; Pacione, R.  
*Evaluation of the atmospheric water vapor content in the regional climate model ALARO-0 using GNSS observations from EPN Repro2*  
EUREF Symposium, Wroclaw, Poland, 17-19 May 2017
10. Bergeot, N.; Chevalier, J.-M.; Darrouzet, F.; Rasson, J.; Lichtenberger, J.; Bruyninx, C.  
*Geospace environment monitoring at the Princess Elisabeth Antarctic (PEA) station: instrumentation and first results*  
URSI 2017 - General Assembly and Scientific Symposium, Montreal, Canada, 19-26 August 2017
11. Bergeot, N.; Chevalier, J.-M.  
*Climatological behaviour of the Ionospheric-Plasmaspheric Total Electron Content over Antarctica*  
SCAR-GRAPE workshop (STCE), Brussels, Belgium, 4 December 2017
12. Bergeot, N.; Chevalier, J.-M.  
*Climatological behaviour of the Total Electron Content at the South Pole*  
ESWW14, Oostende, Belgium, 27 November-1 December 2017 (poster)
13. Bolsée, D.; Pereira, N.; Sperfeld, P.; Pape, S.  
*Metrology of the Solar Spectral Irradiance at the Top Of Atmosphere in the Near Infrared using Ground Based Instruments. Final results of the PYR-ILIOS campaign (Mauna Loa Observatory, June-July 2016)*  
AGU Fall Meeting, New Orleans, Louisiana, USA, 11-15 December 2017 (poster)
14. Bourgoignie, B.; Nicula, B.; Verstringe, F.; Marqué, C.; Jiggins, P.; Müller, D.  
*JHelioviewer - Sneak Peek*  
ESWW14, Oostende, Belgium, 27 November-1 December 2017 (poster)
15. Brenot, H.; Rohm, W.; Kačmařík, M.; Möller, G.; Sá, A.; Tondás, D.; Rapant, L.; Biondi, R.; Manning, T.; Champollion, C.  
*Cross-validation of GNSS tomography models and methodological improvements using CORS network*  
EGU General Assembly 2017, Vienna, Austria, 23-28 April 2017 (poster)

16. Brenot, H.; Caumont, O.; Bosser, P.; Biondi, R.; Bock, O.; Ducrocq, V.; Van Roozendaal, M.  
*Interest of GNSS tomography for nowcasting in the frame of HyMeX*  
EGU General Assembly 2017, Vienna, Austria, 23-28 April 2017 (poster)
17. Bruyninx, C.; Pottiaux, E.  
*Monitoring of Real-time GNSS Broadcasters: Application to the EPN*  
EUREF Analysis Centres Workshop, Brussels, Belgium, 25-26 October 2017
18. Bruyninx, C.; Legrand, J.  
*Galileo-capability of the EUREF Permanent Network*  
EUREF Analysis Centres Workshop, Brussels, Belgium, 25-26 October 2017
19. Bruyninx, C.; Legrand, J.; Fabian, A.; Pottiaux, E.  
*Enhanced Assessment of EPN Station Performance*  
EUREF Symposium, Wroclaw, Poland, 17-19 May 2017
20. Bruyninx, C.; Legrand, J.; Fabian, A.  
*Improved Monitoring of GNSS Station Performance at the EPN Central Bureau*  
IGS Workshop 2017, Paris, France, 3-7 July 2017 (poster)
21. Calders, S.; Lamy, H.; Martínez Picar, A.; Tétard, C.; Verbeeck, C.; Gamby, E.  
*The Radio Meteor Zoo: involving Citizen Scientists in radio meteor research*  
International Meteor Conference, Petnica, Serbia, 21-24 September 2017
22. Caspi, A.; ... ; Zhukov, A.; West, M.; and 12 others  
*First results from the NASA WB-57 airborne observations of the Great American 2017 Total Solar Eclipse*  
AAS/SPD 48, Portland, Oregon, USA, 21-25 August 2017 (poster)
23. Caspi, A.; ... ; West, M.; ... ; Zhukov, A. and 22 others  
*Chasing the Great American 2017 Total Solar Eclipse: Coronal Results from NASA's WB-57F High-Altitude Research Aircraft*  
AGU Fall Meeting, New Orleans, Louisiana, USA, 11-15 December 2017 (invited talk)
24. Cessateur, G.; Bolsée, D.; Pereira, N.; Sperfeld, P.; Pape, S.  
*Metrology of the Solar Spectral Irradiance at the Top Of Atmosphere in the Near Infrared using Ground Based Instruments, Final results of the PYR-ILIOS campaign (Mauna Loa Observatory, June-July 2016)*  
AGU Fall Meeting, New Orleans, Louisiana, USA, 11-15 December 2017
25. Chatzinikos, M.; Pottiaux, E.; Bruyninx, C.; Legrand, J.  
*ROBER: A New Tool for Step-wise Analysis of the Quality of GNSS Network-based Processing*  
EUREF Symposium, Wroclaw, Poland, 17-19 May 2017 (poster)
26. Chatzinikos, M.; Pottiaux, E.; Bruyninx, C.; Legrand, J.  
*Enhancing the reliability of GNSS network solutions: Key Performance Indicators and decision models in the new tool "ROBER"*  
IGS Workshop 2017, Paris, France, 3-7 July 2017 (poster)
27. Chatzinikos, M.; Pottiaux, E.; Bruyninx, C.; Legrand, J.  
*ROBER: Progress Towards a New Tool for the Day-to-Day Management of a GNSS Analysis Centre*  
EUREF Analysis Centres Workshop, Brussels, Belgium, 25-26 October 2017
28. Chevalier, J.-M.; Bergeot, N.  
*Near real-time monitoring of the solar activity impact on European region from the EPN data*  
EUREF Analysis Centres Workshop, Brussels, Belgium, 25-26 October 2017
29. Chevalier, J.-M.; Bergeot, N.  
*Real-Time Alert System for GNSS Signal Degradation Caused by Solar Radio Bursts*  
ESWW14, Oostende, Belgium, 27 November-1 December 2017 (poster)
30. Chevalier, J.-M. ; Bergeot, N. ; Marqué, C. ; Bruyninx, C.  
*Warning System for GNSS Signal Degradation Caused by Solar Radio Bursts*  
URSI 2017 - General Assembly and Scientific Symposium, Montreal, Canada, 19-26 August 2017
31. Crapolicchio, R.; Casella, D.; Marqué, C.  
*Radio observations of recent solar flares from ESA Soil Moisture and Ocean Salinity (SMOS) Mission*  
ESWW14, Oostende, Belgium, 27 November-1 December 2017 (poster)
32. Crosby, N.B.; Dierckxsens, M.; Kruglanski, M.; De Donder, E.; Calders, S.; Messios, N.; Glover, A.  
*ESA SSA Space Radiation Expert Service Centre: The Importance of Community Feedback*  
EGU General Assembly 2017, Vienna, Austria, 23-28 April 2017 (poster)
33. Damé, L.; Meftah, M.; Bolsée, D.; Pereira, N.; Hauchecorne, A. ; Bekki, S.; Irbah, A.; Cessateur, G.; Sluse, D.  
*A new solar reference spectrum from 165 to 3088 nm*  
EGU General Assembly 2017, Vienna, Austria, 23-28 April 2017 (poster)
34. Dammasch, I.; Dominique, M.; Katsiyannis, A.C.; Wauters, L.

*LYRA status update*

ESWW14, PROBA2 SWT meeting, Oostende, Belgium, 27 November-1 December 2017

35. Darrouzet, F.; Lichtenberger, J. De Keyser, J.; Pierrard, V.; Koroncay, D.

*Plasmaspheric study with VLF antennas installed in Antarctica and in Belgium and with an empirical plasmaspheric model*

SCAR-GRAPE workshop (STCE), Brussels, Belgium, 4 December 2017

36. Dasso, S.; Masías-Meza, J.-J.; Demoulin, P.; Rodríguez, L.; Janvier, M.

*Magnetic clouds and their driven shocks/sheaths near Earth: geoeffective properties studied with a superposed epoch technique*

ESWW14, Oostende, Belgium, 27 November-1 December 2017 (poster)

37. Dasso, S.; Masías-Meza, J.-J.; Demoulin, P.; Rodríguez, L.; Janvier, M.

*Superposed Epoch Study of Magnetic Clouds and their Driven Shocks/Sheaths Near Earth*

IAU Symposia 335: Space Weather of the Heliosphere: Processes and Forecasts, Exeter, UK, 17-21 July 2017 (poster)

38. Decraemer, B.; Zhukov, A.; Van Doorselaere, T.

*HELMet streamers In the solar corona and their Oscillations (HELIOS)*

Culham Plasma Physics Summer School, Abingdon, UK, 17-28 July 2017 (poster)

39. Decraemer, B.; Zhukov, A.; Van Doorselaere, T.

*Three-dimensional structure of coronal streamers observed by SOHO/LASCO and STEREO/COR2*

ESPM-15, Budapest, Hungary, 4-8 September 2017 (poster)

40. De Donder, E.; Crosby, N.B.; Messios, N.; Calders, S.; Dierckxsens, M.; Chabanski, S.

*Space Weather Services for Human Space Flight Missions Symposium "25 years of Belgians in space", SCK-CEN, Mol, Belgium, 6 October 2017 (poster)*

41. Defraigne, P.; Huang, W.

*Calibration of DCBs in timing GNSS stations*

IGS Workshop 2017, Paris, France, 3-7 July 2017

42. Defraigne, P.; Bertrand, B.; Huang, W.; Rovera, D.

*Validation of the Inter-Frequency Calibration of Timing GNSS Receivers*

European Frequency and Time Forum 2017, Besançon, France, 10-13 July 2017

43. de Franceschi, G.; Bergeot, N.

*GNSS Research and Application for Polar Environment*

SCAR-GRAPE workshop (STCE), Brussels, Belgium, 4 December 2017

44. De Keyser, J.; Ranvier, S.; Anciaux, M.; Gamby, E.; Lamy, H.

*Piggybacking a small Langmuir probe instrument on Altius 1<sup>st</sup> International Altius Symposium, Brussels, Belgium, 2-3 May 2017 (poster)*

45. De Keyser, J.; Anciaux, M.; Bonnewijn, S.; Cardoen, P.; Demoulin, Ph.; Fussen, D.; Gamby, E.; Pieroux, D.; Ranvier, S.; Van Ransbeeck, E.

*PICASSO: Pico-Satellite for Atmospheric and Space Science Observations*

ESWW14, Tutorial, Oostende, Belgium, 27 November-1 December 2017

46. Delouille, V.; Moon, Kevin; Hero, Alfred O.; Hofmeister, S.; Reiss, M.; Veronig, A.

*Supervised and non-supervised classification in solar physics using advanced techniques*

Space Weather: a Multi-Disciplinary Approach, Leiden, The Netherlands, 25-29 September 2017 (invited talk)

47. D'Huys, E.; Berghmans, D.; and the SWAP team

*SWAP Status Update*

ESWW14, PROBA2 SWT meeting, Oostende, Belgium, 27 November-1 December 2017 (invited talk)

48. D'Huys, E.; Seaton, D.B.; De Groof, A.; Berghmans, D.; Poedts, S.

*Solar signatures and eruption mechanism of the August 14, 2010 coronal mass ejection*

ESWW14, Oostende, Belgium, 27 November-1 December 2017 (poster)

49. Dierckxsens, M.; Crosby, N.B.

*The SEP Forecast Tool within the COMESEP Alert System*

IAU Symposia 335: Space Weather of the Heliosphere: Processes and Forecasts, Exeter, UK, 17-21 July 2017 (poster)

50. Dierckxsens, M.; Marsh, M.; Richardson, I.G.; Quinn, P.; Mays, M.L.; Kuznetsova, M.M.; and the SEP Working Team and Scoreboard members

*Assessing Space Weather Applications and Understanding: SEP Working Team and SEP Scoreboard*

IAU Symposia 335: Space Weather of the Heliosphere: Processes and Forecasts, Exeter, UK, 17-21 July 2017 (poster)

51. Dierckxsens, M.; Marsh, M.; Mays, L.

*SEP Scoreboard: Real-time Forecasting validation*

HESPERIA Workshop, Paris, France, 27 February-2 March 2017

52. Dolla, L.; Kraaikamp, E.; Marqué, C.; D'Huys, E.; West, M.; Dammasch, I.; Berghmans, D.

*An overview of the contribution of the Royal Observatory of Belgium to the SUMER/IRIS/GBOs/Hinode HOP 334 campaign*

STCE annual meeting, Uccle, Belgium, 8 June 2017

53. Dolla, L.; Kraaikamp, E.; Marqué, C.; West, M.; Dammasch, I.; Berghmans, D.

*An overview of the contribution of the Royal Observatory of Belgium to the SUMER/IRIS/GBOs/Hinode HOP 334 campaign*

19<sup>th</sup> EUI consortium meeting, Uccle, Belgium, 30 May-1 June 2017

54. Dolla, L.; Zhukov, A.; Rodriguez, L.; Verdini, A.

*The role of Alfvénic turbulence in the acceleration of the fast solar wind: present "linkage" observations*

Solar Orbiter Workshop 7, Granada, Spain 3-7 April 2017

55. Dolla, L.; Zhukov, A.; Rodriguez, L.

*A simulation of PROBA-3/ASPIICS operations during CME-Watch observations*

Proba-3 SWT meeting #6, Wroclaw, Poland, 4-6 December 2017

56. Dolla, L.

*An update on the PROBA-3/ASPIICS spectral sensitivity with the new wideband filter*

Proba-3 SWT meeting #6, Wroclaw, Poland, 4-6 December 2017

57. Dominique, M.

*The biggest flare of solar cycle 24 observed by PROBA2*

ESWW14, Oostende, Belgium, 27 November-1 December 2017 (poster)

58. Dominique, M.; Zhukov, A.; Dolla, L.; Inglis, A.; Lapenta, G.

*Multi-instrument observation of subminute quasi-periodic pulsations in solar flares*

AAS/SPD 48, Portland, Oregon, USA, 21-25 August 2017

59. Dominique, M.; Zhukov, A.; Dolla, L.; Lapenta, G.; Ryan, D.; Hayes, L.

*Update on quasi-periodic pulsations in solar flares*

CHARM meeting, Brussels, Belgium, 10 March 2017

60. Dominique, M.; Zhukov, A.; Dolla, L.; Inglis, A.; Lapenta, G.

*Multi-instrument observations of sub-minute quasi-periodic pulsations (QPPs) in solar flares*

ESPM-15, Budapest, Hungary, 4-8 September 2017 (poster)

61. Dominique, M.; Thiemann, E.

*Retrieval of O and N2 distributions from PROBA2/LYRA occultation data*

1<sup>st</sup> International Altiis Symposium, Brussels, Belgium, 2-3 May 2017 (poster)

62. Douša, J.; ... ; Pottiaux, E.; ... ; Brenot, H.; and 15 others

*Working Group 1 "Advanced GNSS Processing Techniques" of the COST Action GNSS4SWEC: Overview of main achievements*

EGU General Assembly 2017, Vienna, Austria, 23-28 April 2017

63. Drews, R.; ... ; Bergeot, N.; and 12 others

*Fun at Antarctic grounding lines: Ice-shelf channels and sediment transport*

EGU General Assembly 2017, Vienna, Austria, 23-28 April 2017

64. Dumbovic, M.; Srivastava, N.; Khodia, Y.; Vrsnak, B.; Devos, A.; Rodriguez, L.

*Validation of the CME Geomagnetic forecast alerts under COMESEP alert system*

EGU General Assembly 2017, Vienna, Austria, 23-28 April 2017 (poster)

65. Eastwood, J.; Krupar, V.; Magdalenic, J.; Bisi, M.; Gopalswamy, N.; Davies, J.; Harrison, R.; Barnes, D.

*Cataloguing radio emission associated with coronal mass ejections: results from the HELCATS project*

EGU General Assembly 2017, Vienna, Austria, 23-28 April 2017 (poster)

66. Fabian, A.; Bruyninx, C.; Legrand, J.

*A new GNSS station Metadata Management and dissemination system in support of multiple networks*

EUREF Symposium, Wroclaw, Poland, 17-19 May 2017

67. Fabian, A.; Bruyninx, C.; Legrand, J.

*Management and dissemination of GNSS site log metadata using the new GeodesyML standard*

EUREF Analysis Centres Workshop, Brussels, Belgium, 25-26 October 2017

68. García-Rigo, A.; ... ; Bergeot, N.; and 24 others

*St. Patrick's Day 2015 geomagnetic storm analysis based on Real Time Ionosphere Monitoring*

EGU General Assembly 2017, Vienna, Austria, 23-28 April 2017 (poster)

69. Gustavsson, B.; Gunell, H.; Lamy, H.

*Observations of Ionospheric Langmuir-waves Enhanced by Electron Precipitation*

EGU General Assembly 2017, Vienna, Austria, 23-28 April 2017

70. Harrison, R.; Davies, J.; Perry, C.; Möstl, C.; Rouillard, A.; Bothmer, V.; Rodriguez, L.; Eastwood, J.; Kilpua, E.; Gallagher, P.; Odstrcil, D.

*Overview of the HELCATS project*

EGU General Assembly 2017, Vienna, Austria, 23-28 April 2017 (invited talk)

71. Hofmeister, S.; Reiss, M.; Veronig, A.; Temmer, M.; Delouille, V.; Vennerstrom, S.  
*The reasons for false alarms at the prediction of high-speed solar wind streams near Earth, and consequences for the prediction at other planets*  
ESWW14, Oostende, Belgium, 27 November-1 December 2017
72. Janssens, J.  
*Status Manuscripts SWSC Journal*  
ESWW14, Oostende, Belgium, 27 November-1 December 2017
73. Janssens, J.; Ishii, M.  
*Live Space Weather Forecast*  
ESWW14, Oostende, Belgium, 27 November-1 December 2017
74. Janssens, J.; Cid, C.  
*Live Space Weather Forecast*  
ESWW14, Oostende, Belgium, 27 November-1 December 2017
75. Jones, J.; Guerova, G.; Dousa, J.; Dick, G.; De Haan, S.; Pottiaux, E.; Bock, O.; Pacione, R.  
*COST Action ES1206: Advanced GNSS Tropospheric Products for Monitoring Severe Weather Events and Climate (GNSS4SWEC)*  
EGU General Assembly 2017, Vienna, Austria, 23-28 April 2017 (poster)
76. Jones, J.; Guerova, G.; Dousa, J.; Dick, G.; De Haan, S.; Pottiaux, E.; Bock, O.; Pacione, R.  
*The Current Status and Future of GNSS-Meteorology in Europe*  
AGU Fall Meeting, New Orleans, Louisiana, USA, 11-15 December 2017 (poster)
77. Jones, J.; Guerova, G.; Dousa, J.; Dick, G.; De Haan, S.; Pottiaux, E.; Bock, O.; Pacione, R.  
*COST Action ES1206: Advanced GNSS Tropospheric Products for Monitoring Severe Weather Events and Climate (GNSS4SWEC)*  
European Meteorological Society Annual Meeting 2017, Dublin, Ireland, 4-8 September 2017
78. Katsiyannis, A.C.; Dominique, M.; Pierrard, V.; López Rosson, G.; De Keyser, J.; Berghmans, D.; Kruglanski, M.; Dammasch, I.; De Donder, E.  
*LYRA/EPT Perturbations Project*  
ESWW14, Oostende, Belgium, 27 November-1 December 2017 (poster)
79. Katsiyannis, A.C.; Dominique, M.; Pierrard, V.; López Rosson, G.; De Keyser, J.; Berghmans, D.; Kruglanski, M.; Dammasch, I.; De Donder, E.  
*The detection of ultra-relativistic electrons in low Earth orbit*  
ESWW14, Oostende, Belgium, 27 November-1 December 2017
80. Kačmařík, M.; Dousa, J.; Dick, G.; Zus, F.; Brenot, H.; Pottiaux, E.; Möller, G.; Kaplon, J.; Vaclavovic, P.; Morel, L.; Hordyniec, P.  
*Inter-technique validation of tropospheric slant total delays*  
COST ES1206 - GNSS4SWEC Final Workshop, Noordwijk, The Netherlands, 21-23 February 2017
81. Klos, A.; Pottiaux, E.; Van Malderen, R.; Bock, O.; Bogusz, J.  
*Study on homogenization of synthetic GNSS-retrieved IWW time series and its impact on trend estimates with autoregressive noise*  
EGU General Assembly 2017, Vienna, Austria, 23-28 April 2017 (poster)
82. Klos, A.; Pottiaux, E.; Van Malderen, R.; Bock, O.; Bogusz, J.  
*Synthetic benchmark datasets for homogenization of IWW time series retrieved by GPS*  
COST ES1206 - GNSS4SWEC Final Workshop, Noordwijk, The Netherlands, 21-23 February 2017
83. Klos, A.; Pottiaux, E.; Van Malderen, R.; Bock, O.; Bogusz, J.  
*A homogenisation of Integrated Water Vapour Time Series Retrieved from GPS and ERA-Interim: Building Synthetic Benchmark Datasets*  
COST ES1206 sub-Working Group "Data Homogenisation" - 2<sup>nd</sup> Workshop, Warsaw, Poland, 23-25 January 2017
84. Klos, A.; Pottiaux, E.; Van Malderen, R.; Bogusz, J.; Gruszczynska, M.; Bock, O.; Chimani, B.; Elias, M.; Guijarro, J.A.; Ning, T.  
*Homogenisation of synthetic dataset: First results of contribution delivered with various statistical approaches*  
COST ES1206 sub-Working Group "Data Homogenisation" - 2<sup>nd</sup> Workshop, Warsaw, Poland, 23-25 January 2017
85. Klos, A.; Van Malderen, R.; Pottiaux, E.; Bock, O.; Bogusz, J.; Chimani, B.; Domonkos, P.; Elias, M.; Gruszczynska, M.; Guijarro, J.A.; Zengin, S.; Ning, T.  
*A set of synthetic Integrated Water Vapour time series: a way to benchmark the homogenisation algorithms*  
IAG Workshop: Satellite Geodesy for Climate Studies, 19-21 September 2017, Bonn, Germany
86. Kraaikamp, E.; Dolla, L.  
*A Lucky Imaging contribution to the SUMER/IRIS/GBOs/Hinode HOP 334 campaign*  
ESPM-15, Budapest, Hungary, 4-8 September 2017 (poster)
87. Kraaikamp, E.; Verbeeck, C.

*Solar Demon flare and dimming statistics from AIA observations 2010-2017*  
ESWW14, Oostende, Belgium, 27 November-1 December 2017 (poster)

88. Kraaikamp, E.; Dolla, L.  
*Ludicrous imaging at USET - High cadence ground based H- $\alpha$  and Ca-II K observations*  
STCE annual meeting, Uccle, Belgium, 8 June 2017

89. Kraaikamp, E.; Dolla, L.; Marqué, C.; West, M.; Dammasch, I.; Berghmans, D.  
*Ludicrous imaging at USET - High cadence ground based H- $\alpha$  and Ca-II K observations for SUMER/IRIS/GBOs/Hinode HOP 0334 campaign*  
19<sup>th</sup> EUI consortium meeting, Uccle, Belgium, 30 May-1 June 2017

90. Kronberg, E.A.; ... ; Pierrard, V.; Borremans, K.; and 10 others  
*On usage of electron observations from Cluster/RAPID/IES instrument in Earth's radiation belts and ring current*  
EGU General Assembly 2017, Vienna, Austria, 23-28 April 2017

91. Kruglanski, M.; Devos, A.; Calders, S.; De Donder, E.; Berghmans, D.; Andries, J.; Crosby, N.; Dierckx, M.; Glover, A.  
*Provision of space weather bulletins in support to ESA missions*  
EGU General Assembly 2017, Vienna, Austria, 23-28 April 2017 (poster)

92. Krupar, V.; Magdalenic, J.; West, M.; D'Huys, E.; Prech, L.; Kruparova, O.  
*An analysis of solar eruptive processes using combined EUV and radio measurements*  
Second VarSITI General Symposium, Irkutsk, Russia, 10-15 July 2017 (poster)

93. Laffineur, Q.; Haeffelin, M.; Bravo-Aranda, J.-A.; Drouin, M.-A.; Lhuisset, A.; Dupont, J.-C.; De Backer, H.  
*ALC profiling: valuable information to support the radiation fog forecasting in the airports*  
European Meteorological Society Annual Meeting 2017, Dublin, Ireland, 4-8 September 2017

94. Laffineur, Q.; Haeffelin, M.; Bravo-Aranda, J.-A.; Drouin, M.-A.; Lhuisset, A.; Dupont, J.-C.; De Backer, H.  
*PARAFOG: a new decision support system for the airports to monitor and to predict radiation fog based on automatic LIDAR-ceilometer measurements*  
WMO Aeronautical Meteorology Scientific Conference, Toulouse, France, 6-10 November 2017

95. Laffineur, Q.; Haeffelin, M.; Bravo-Aranda, J.-A.; Drouin, M.-A.; Casquero-Vera, J.-A.; Dupont, J.-C.; De Backer, H.

*Forecasting of radiation fog with a new decision support system based on automatic LIDAR-ceilometer measurements*  
EGU General Assembly 2017, Vienna, Austria, 23-28 April 2017 (poster)

96. Lamy, H.; Echim, M.; Cessateur, G.; Simon Wedlund, C.; Gustavsson, B.; Maggiolo, R.; Gunell, H.; Darrouzet, F.; De Keyser, J.  
*From discrete auroral arcs to the magnetospheric generator: numerical model and case study*  
AGU Fall Meeting, New Orleans, Louisiana, USA, 11-15 December 2017

97. Lamy, H.; Tétard, C.; Anciaux, M.; Ranvier, S.; Martínez Picar, A.; Calders, S.; Verbeeck, C.  
*First observations with the BRAMS radio interferometer*  
International Meteor Conference, Petnica, Serbia, 21-24 September 2017

98. Lamy, H.; Calders, S.; Tétard, C.; Verbeeck, C.; Martínez Picar, A.; Gamby, E.  
*The Radio Meteor Zoo: searching for meteors in BRAMS radio observations*  
European Planetary Science Congress 2017, Riga, Latvia, 17-22 September 2017

99. Lazar, M.; Fichtner, H.; Pierrard, V.; Poedts, S.; Yoon, P.  
*Suprathermal populations: from observations to realistic interpretation*  
EGU General Assembly 2017, Vienna, Austria, 23-28 April 2017 (poster)

100. Lefèvre, L.; Clette, F.  
*Sunspot number: The ongoing modernization of a long-term reference*  
Second VarSITI General Symposium, Irkutsk, Russia, 10-15 July 2017 (invited talk)

101. Lefèvre, L.  
*How to best (better) concatenate sunspot series?*  
SSN workshop, Reading, UK, 9 February 2017

102. Lyubchik, O.; Kontar, E.P.; Voitenko, Y.M.; Bian, N.H.; Melrose, D.B.  
*Solar plasma radio emission in the presence of imbalanced turbulence of kinetic-scale Alfvén waves*  
4<sup>th</sup> UK-Ukraine-Spain Meeting on Solar and Space Physics, Kyiv, Ukraine, 28 August-1 September 2017

103. Magdalenic, J.; Temmer, M.; Krupar, V.; Marqué, C.; Veronig, A.; Eastwood, J.  
*The February 15, 2011 CME-CME interaction and possibly associated radio emission*  
EGU General Assembly 2017, Vienna, Austria, 23-28 April 2017 (poster)

104. Magdaleníć, J.; Harra, L.; Matthews, S.; Berghmans, D.; Krupar, V.; Verbeeck, C.; Mueller, D.  
*Active region jets: can we predict what we will see with Solar Orbiter?*  
Solar Orbiter Workshop 7, Granada, Spain 3-7 April 2017 (poster)
105. Magdaleníć, J.; Fallows, R.; Marqué, C.; Mann, G.; LOFAR and Solar KSP members  
*Extraordinary fine structures of type III radio bursts observed by LOFAR*  
Annual Meeting of the KSP "Solar Physics and Space Weather with LOFAR", Cardiff, UK, 8 December 2017
106. Magdaleníć, J.; Marqué, C.; Fallows, R.; Mann, G.  
*Fine structures of type II radio burst observed by LOFAR*  
International Workshop on Solar, Heliospheric and Magnetospheric Radioastronomy: The legacy of Jean-Louis Steinberg (1922-2016), Meudon, France, 6-10 November 2017
107. Magdaleníć, J.  
*Constraining CMEs and Shocks by Observations and Modelling throughout the inner heliosphere*  
ESPM-15, Budapest, Hungary, 4-8 September 2017 (invited talk)
108. Magdaleníć, J.  
*Radio Observations and Space Weather*  
URSI 2017 - General Assembly and Scientific Symposium, Montreal, Canada, 19-26 August 2017 (invited talk)
109. Maggiolo, R.; Hamrin, M.; Cessateur, G.; De Keyser, J.; Gunell, H.; Maes, L.; Pitkänen, T.  
*The time response of the plasmashet  $O^+$  density to the solar wind*  
IAPSO/IAMAS/IAGA Joint Assembly, Cape Town, South Africa, 27 August-1 September 2017
110. Magin, T.; ... ; De Keyser, J.; Lamy, H.; and 10 others  
*Investigation of the meteor phenomenon: Plasmatron wind-tunnel experiments and ground observations*  
61<sup>st</sup> Course of the International School of Quantum Electronics ("Hypersonic Meteoroid Entry Physics"), Erice, Italy, 3-7 October 2017
111. Malisse, V.; Verbeeck, C.  
*STAFF: more than just a website, a powerful tool for space weather forecasters and researchers*  
ESWW14, Fair, Oostende, Belgium, 27 November-1 December 2017 (poster)
112. Marqué, C.; Klein, K.-L.; Monstein, C.; Opgenoorth, H.; Pulkkinen, A.; Buchert, S.; Krucker, S.; Van Hoof, R.; Thulesen, P.  
*Impact of the November 04<sup>th</sup> 2015 solar radio burst on air traffic operations*  
ESWW14, Oostende, Belgium, 27 November-1 December 2017 (poster)
113. Marqué, C.; Klein, K.-L.; Monstein, C.; Opgenoorth, H.; Pulkkinen, A.; Buchert, S.; Krucker, S.; Van Hoof, R.; Thulesen, P.  
*Impact of the November 04<sup>th</sup> 2015 solar radio burst on air traffic operations*  
International Workshop on Solar, Heliospheric and Magnetospheric Radioastronomy: The legacy of Jean-Louis Steinberg (1922-2016), Meudon, France, 6-10 November 2017 (poster)
114. Martínez Picar, A.; Marqué, C.; Magdaleníć, J.  
*Building SPADE - Status Update*  
International Workshop on Solar, Heliospheric and Magnetospheric Radioastronomy: The legacy of Jean-Louis Steinberg (1922-2016), Meudon, France, 6-10 November 2017 (poster)
115. Martínez Picar, A.; Marqué, C.  
*Using a small phased array for meteor observations*  
International Meteor Conference, Petnica, Serbia, 21-24 September 2017
116. Mierla, M.; Scolini, C.; Mays, L.; Pomoell, J.; Rodriguez, L.  
*Study of September 4, 2010 CME using ENLIL and EUHFORIA*  
International CCMC-LWS Working Meeting: Assessing Space Weather Understanding and Applications, Cape Canaveral, Florida, USA, 3-7 April 2017
117. Mierla, M.; Inhester, B.; Zhukov, A.  
*Error estimates for polarization angles from SECCHI/COR1 Proba-3 SWT meeting #6, Wroclaw, Poland, 4-6 December 2017*
118. Mierla, M.  
*Propagation of coronal mass ejections from low corona to interplanetary space*  
Rocks&Stars II conference, Göttingen, Germany, 13-16 September 2017
119. Mierla, M.; Scolini, C.; Mays, L.; Pomoell, J.; Rodriguez, L.  
*Study of September 4, 2010 CME using ENLIL and EUHFORIA*  
CHARM meeting, Brussels, Belgium, 10 March 2017
120. Mierla, M.  
*Coronal Mass Ejections and Geomagnetic Storms*  
STCE workshop on "Geomagnetic storms and solar eruptions: from Sun to Earth", Brussels, Belgium, 31 January 2017
121. Mierla, M.  
*Coronal Mass Ejections and Geomagnetic Storms*

SOLARNET IV meeting on “The Physics of the Sun from the Interior to the Outer Atmosphere”, Lanzarote, Spain, 16-20 January 2017 (invited talk)

122. Mierla, M.; Scolini, C.; Mays, L.; Pomoell, J.; Rodriguez, L.  
Comparison between EUHFORIA and ENLIL: CME on September 4, 2010  
ESWW14, Oostende, Belgium, 27 November-1 December 2017 (poster)

123. Mierla, M.; Scolini, C.; Mays, L.; Pomoell, J.; Rodriguez, L.  
Comparison between EUHFORIA and ENLIL: CME on September 4, 2010  
ESPM-15, Budapest, Hungary, 4-8 September 2017 (poster)

124. Möstl, C.; ... ; Rodriguez, L.; and 19 others  
*Modeling observations of solar coronal mass ejections with heliospheric imagers verified with the Heliophysics System Observatory*  
ESWW14, Oostende, Belgium, 27 November-1 December 2017 (poster)

125. Möstl, C.; ... ; Rodriguez, L.; and 10 others  
*Modeling of coronal mass ejections with the STEREO heliospheric imagers verified with in situ observations by the Heliophysics System Observatory*  
EGU General Assembly 2017, Vienna, Austria, 23-28 April 2017 (poster)

126. Moon, K.; Delouille, V.; Hero, A.O.  
*Image Patch Analysis of Sunspots and Active Regions*  
AGU Fall Meeting, New Orleans, Louisiana, USA, 11-15 December 2017 (poster)

127. Nicula, B.; Verstringe, F.; Bourgoignie, B.; Berghmans, D.; Felix, S.; von Stachelski, S.; Serquet, M.; Csillaghy, A.; Jiggins, P.; Mueller, D.  
*JHelioviewer for Solar Orbiter*  
Solar Orbiter Modelling and Data analysis Working Group (MADAWG), Madrid, Spain, 10 July 2017

128. Nogherotto, R.; Biondi, R.; Leclair de Bellevue, J.; Brenot, H.  
*Characterization of tropical cyclones in the South Indian Ocean by using GNSS observations*  
EGU General Assembly 2017, Vienna, Austria, 23-28 April 2017 (poster)

129. Pacione, R.; Bruyninx, C.; Brockmann, E.; Söhne, W.  
*EPN data and products in support of atmospheric monitoring*  
COST ES1206 - GNSS4SWEC Final Workshop, Noordwijk, Netherlands, 21-23 February 2017

130. Pacione, R.; Pottiaux, E.

*IAG JWG 4.3.8: GNSS tropospheric products for Climate: Objectives and Future Plans*  
EGU General Assembly 2017, Vienna, Austria, 23-28 April 2017 (poster)

131. Pacione, R.; Pottiaux, E.; Van Malderen, R.; Ning, T.  
*Long-Term Ground-Based GNSS Tropospheric Products for Climate*  
IAG Workshop: Satellite Geodesy for Climate Studies, Bonn, Germany, 19-21 September 2017

132. Palmerio, E.; Kilpua, E.K.J.; Mierla, M.; Rodriguez, L.; Isavnin, A.  
*Quantifying the evolution and propagation of solar flux ropes in the corona*  
ESPM-15, Budapest, Hungary, 4-8 September 2017

133. Pierrard, V.  
*Characteristics of electron velocity distributions in space plasmas*  
Statistical Physics conference, Corfu, Greece, 10-14 July 2017 (invited talk)

134. Pierrard, V.  
*Plasmapause and plasmasphere simulations*  
URSI 2017 - General Assembly and Scientific Symposium, Montreal, Canada, 19-26 August 2017

135. Pierrard, V.; Lazar, M.  
*Cluster velocity distribution functions at 1 AU compared with solar corona and solar wind characteristics at other distances*  
27<sup>th</sup> Cluster workshop, Bled, Slovenia, 11-15 September 2017

136. Pierrard, V.  
*From kinetic models to predictive tools: solar wind and plasmasphere*  
ESWW14, Oostende, Belgium, 27 November-1 December 2017 (poster)

137. Pierrard, V.; López Rosson, G.; Cyamukungu, M.; Benck, S.; Borisov, S.  
*4 years of EPT/PROBA-V: Observations of the Dynamics of the Radiation Belts*  
ESWW14, Oostende, Belgium, 27 November-1 December 2017 (poster)

138. Pierrard, V.; Lazar, M.; Moschou, S.P.  
*Kinetic features observed in electron distributions and their consequences in solar wind modelling*  
EGU General Assembly 2017, Vienna, Austria, 23-28 April 2017 (poster)

139. Plotnikov, I.; ... ; Rodriguez, L.; and 13 others  
*Long-Term Tracking of Corotating Density Structures Using Heliospheric Imaging (catalogue of CIRs during 2007-2014)*

EGU General Assembly 2017, Vienna, Austria, 23-28 April 2017

140. Podladchikova, O.; D'Huys, E.; Mierla, M.; and the SWAP Team  
*Particle acceleration event observed in the extended solar corona by SWAP telescope during off-pointing campaign on 01 April 2017*  
ESWW14, PROBA2 SWT meeting, Oostende, Belgium, 27 November-1 December 2017, (invited talk)

141. Poedts, S.; ... ; Rodriguez, L.; Mierla, M.; Magdalenic, J.; and 10 others  
*EUHFORIA: a solar wind & CME evolution model*  
ESWW14, Oostende, Belgium, 27 November-1 December 2017

142. Pottiaux, E.; Van Malderen, R.; Berckmans, J.; Mangold, A.; Bruyninx, C.  
*Atmospheric Water Vapour Observations at ROB and RMI for Weather and Climate Monitoring*  
SCAR-GRAPE workshop (STCE), Brussels, Belgium, 4 December 2017

143. Pottiaux, E. ; De Haan, S. ; Halloran, G. ; Jones, J. ; Rohm, W.  
COST Action ES1206 Working Group 2: Status and summary of Achievements  
COST ES1206 - GNSS4SWEC Final Workshop, Noordwijk, The Netherlands, 21-23 February 2017

144. Pottiaux, E.; Klos, A.; Van Malderen, R.; Elias, M.; Guijarro, J.A.; Ning, T.; Chimani, B.; Zengin, S.  
*Deriving Error Metrics for the Homogenization of Integrated Water Vapour (IWV) Time Series: The Case of the Synthetic Benchmark Datasets*  
COST ES1206 - GNSS4SWEC Final Workshop, Noordwijk, The Netherlands, 21-23 February 2017

145. Pottiaux, E.; Van Malderen, R.; Brenot, H.; Berckmans, J.  
*National Report of Belgium, 2017*  
COST ES1206 - GNSS4SWEC Final Workshop, Noordwijk, The Netherlands, 21-23 February 2017

146. Pottiaux, E.; Van Malderen, R.; Klos, A.; Elias, M.; Ning, T.; Guijarro, J.A.; Chimani, B.  
*Deriving Error Metrics for the Homogenization of Integrated Water Vapour (IWV) Time Series: The Case of the Synthetic Benchmark Datasets*  
COST ES1206 sub-Working Group "Data Homogenisation" - 2<sup>nd</sup> Workshop, Warsaw, Poland, 23-25 January 2017

147. Ranvier, S.; Waets, A.; Cipriani, F.; Anciaux, M.; Gamby, E.; Cardoen, P.; Bonnewijn, S.; De Keyser, J.; Pieroux, D.; Lebreton, J.-P.  
*SLP: a Langmuir Probe Instrument on board a CubeSat*

14<sup>th</sup> International Planetary Probe Workshop, The Hague, The Netherlands, 12-16 June 2017 (poster)

148. Ranvier, S.; Demoulin, P.; Pieroux, D.; Fussen, D.; De Keyser, J.; Anciaux, M.; Gamby, E.; Cardoen, P.; Bonnewijn, S.  
*Status of the PICASSO mission*  
9<sup>th</sup> European CubeSat Symposium, Oostende, Belgium, 29 November-1 December 2017

149. Ranvier, S.; Waets, A.; Cipriani, F.; Anciaux, M.; Gamby, E.; Cardoen, P.; Bonnewijn, S.; De Keyser, J.; Pieroux, D.; Lebreton, J.-P.  
*SLP: a Langmuir Probe Instrument for Space Weather Investigations*  
9<sup>th</sup> European CubeSat Symposium, Oostende, Belgium, 29 November-1 December 2017

150. Reinisch, B.; ... ; Verhulst, T.; Stankov, S.; and 14 others  
*NetTIDE - Pilot Ionosonde Network for Identification of Travelling Ionospheric Disturbances*  
URSI 2017 - General Assembly and Scientific Symposium, Montreal, Canada, 19-26 August 2017

151. Ritter, B.; Karatekin, Ö.; Gerbal, N.; Carrasco, J.A.; Ranvier, S.; De Keyser, J.  
*LUCE: a small spacecraft for near lunar environment exploration*  
EGU General Assembly 2017, Vienna, Austria, 23-28 April 2017 (poster)

152. Ritter, B.; Karatekin, Ö.; Gerbal, N.; Van Hove, B.; Carrasco, J.; Ranvier, S.; De Keyser, J.  
*SOLVE: a small spacecraft for near lunar environment exploration*  
European Planetary Science Congress 2017, Riga, Latvia, 17-22 September 2017 (poster)

153. Rodriguez, L.; Crosby, N.; Veronig, A.; Vrsnak, B.; Vennerstrom, S.; Malandraki, O.; Dalla, S.; Srivastava, N.  
*The COMESEP Space Weather Alert System*  
Space Weather: a Multi-Disciplinary Approach, Leiden, The Netherlands, 25-29 September 2017 (poster)

154. Rodriguez, L.; Scolini, C.; Mierla, M.; Zhukov, A.N.; West, M.  
*Space weather monitor at the L5 point: a case study of a CME observed with STEREO B*  
ESPM-15, Budapest, Hungary, 4-8 September 2017 (poster)

155. Rodriguez, L.; Willems, S.; Pant, V.; Mierla, M.; Devos, A.; Hosteaux, S.  
*Automatic detection of CMEs in STEREO-HI data for the FP7 HELCATs project*  
EGU General Assembly 2017, Vienna, Austria, 23-28 April 2017 (poster)

156. Rodriguez, L.; Zhukov, A.N.; Dolla, L.  
*Operating ASPIICS during the time of high solar activity*  
Proba-3 SWT meeting #6, Wroclaw, Poland, 4-6 December 2017
157. Sapundjiev, D.; Verhulst, T.; Stankov, S.; Jodogne, J.C.  
*The Belgian space weather observatory in Dourbes*  
IAU Symposia 335: Space Weather of the Heliosphere: Processes and Forecasts, Exeter, UK, 17-21 July 2017
158. Sapundjiev, D.; Stankov, S.; Jodogne, J.C.  
*Past, present and future of the cosmic ray observatory in Dourbes, Belgium*  
NMDB Workshop – 10 Years Neutron Monitor Database, Athens, Greece, 20-23 March 2017
159. Scolini, C.; Mierla, M.; Verbeke, C.; Poedts, S.; Rodriguez, L.; Pomoell, J.  
*Study of the September 4, 2010 Coronal Mass Ejection: Comparison of the EUHFORIA and ENLIL Predictive Capabilities*  
IAU Symposia 335: Space Weather of the Heliosphere: Processes and Forecasts, Exeter, UK, 17-21 July 2017 (poster)
160. Scolini, C.; Verbeke, C.; Poedts, S.; Chané, E.; Pomoell, J.; Zuccarello, F.P.  
*Modelling Coronal Mass Ejections with EUHFORIA: Testing the Effect of Different Shapes on Predictions at 1 AU*  
ESWW14, Oostende, Belgium, 27 November-1 December 2017 (poster)
161. Scolini, C.; Verbeke, C.; Poedts, S.; Rodriguez, L.; Pomoell, J.; Cramer, W.D.; Raeder, J.; Gopalswamy, N.; Zuccarello, F.P.  
*Sun-To-Earth Simulations Of Geoeffective Coronal Mass Ejections With EUHFORIA: A Heliospheric-Magnetospheric Model Chain Approach*  
AGU Fall Meeting, New Orleans, Louisiana, USA, 11-15 December 2017 (poster)
162. Scolini, C.; Verbeke, C.; Poedts, S.; Rodriguez, L.; Pomoell, J.; Cramer, W.D.; Raeder, J.; Gopalswamy, N.  
*Sun-To-Earth Simulations Of Geoeffective Coronal Mass Ejections With EUHFORIA: A Heliospheric-Magnetospheric Model Chain Approach*  
ESWW14, Oostende, Belgium, 27 November-1 December 2017 (poster)
163. Scolini, C.; Poedts, S.; Chané, E.; Cramer, W. D.; Raeder, J.; Pomoell, J.; Janhunen, P.  
*Study of the July 12, 2012 CME and its impact at Earth with EUHFORIA: a heliospheric-magnetospheric model chain approach*  
13<sup>th</sup> International Conference on Substorms, Portsmouth, New Hampshire, USA, 25-29 September 2017 (poster)
164. Scolini, C.; Verbeke, C.; Poedts, S.; Pomoell, J.  
*Modelling Coronal Mass Ejections with EUHFORIA: Testing the Effect of Different Shapes on Predictions at 1 AU*  
ICNSP 2017, Leuven, Belgium, 18-20 September 2017 (poster)
165. Simeonov, T.; Vey, S.; Alshawaf, F.; Dick, G.; Guérova, G.; Güntner, A.; Hohmann, C.; Lopez, E.; Pottiaux, E.; Trost, B.; Wickert, J.  
*Monitoring of water cycle elements using GNSS geodetic receivers in North-East Germany at sub-daily resolution*  
European Meteorological Society Annual Meeting 2017, Dublin, Ireland, 4-8 September 2017 (poster)
166. Stankov, S.; Verhulst, T.  
*On the importance of solar eclipse geometry in the interpretation of ionospheric observations*  
AGU Fall Meeting, New Orleans, Louisiana, USA, 11-15 December 2017
167. Stankov, S.; Verhulst, T.  
*Nowcast of the BeNeLux regional magnetic activity for use in space weather applications*  
IAPSO/IAMAS/IAGA Joint Assembly, Cape Town, South Africa, 27 August-1 September 2017
168. Talpeanu, D.-C.; Zuccarello, F.; Chane, E.; Poedts, S.; D'Huys, E.; Hosteaux, S.; Mierla, M.  
*Numerical Modelling of Stealth Solar Eruptions; Initiation and Signatures at 1AU*  
ESWW14, Oostende, Belgium, 27 November-1 December 2017 (poster)
169. Talpeanu, D.-C.; Zuccarello, F.; Chane, E.; Poedts, S.; D'Huys, E.; Hosteaux, S.; Mierla, M.  
*Numerical Modelling of Stealth Solar Eruptions*  
ICNSP 2017, Leuven, Belgium, 18-20 September 2017 (poster)
170. Talpeanu, D.-C.; Rachmeler, L.; Mierla, M.  
*Observational Analysis of Coronal Fans*  
ESPM-15, Budapest, Hungary, 4-8 September 2017 (poster)
171. Talpeanu, D.-C.; Zuccarello, F.; Chane, E.; Poedts, S.; D'Huys, E.; Hosteaux, S.; Mierla, M.  
*Numerical Modelling of Stealth Solar Eruptions*  
Numerical Techniques in MHD Simulations, Cologne, Germany, 16-18 August 2017
172. Talpeanu, D.-C.; Rachmeler, L.; Mierla, M.  
*Observational Analysis of Coronal Fans*  
ESWW14, PROBA2 SWT meeting, Oostende, Belgium, 27 November-1 December 2017 (invited talk)
173. Temmer, M.; Thalmann, J.; Dissauer, K.; Veronig, A.; Tschernitz, J.; Hinterreiter, J.; Rodriguez, L.

*Flare-CME characteristics from Sun to Earth combining observations and modeling*  
EGU General Assembly 2017, Vienna, Austria, 23-28 April 2017 (poster)

174. Savani, N.; Riley, N.; West, M.  
*Assessing Space Weather Applications and Understanding: IMF Bz at L1*  
AGU Fall Meeting, New Orleans, Louisiana, USA, 11-15 December 2017 (poster)

175. Thiemann, E.; Dominique, M.  
*Retrieval of O and N2 distributions from PROBA2/LYRA occultation data*  
ESWW14, Oostende, Belgium, 27 November-1 December 2017 (poster)

176. Thiemann, E.; Eparvier, F.; Andersson, L.; Pilinski, M.; Chamberlin, P.; Fowler, C.; Dominique, M.; Bougher, S.; Gröller, H.; Girazian, Z.; Lillis, R.  
*New Measurements of Mars Thermospheric Variability from MAVEN EUVM Solar Occultations*  
AGU Fall Meeting, New Orleans, Louisiana, USA, 11-15 December 2017

177. Thiemann, E.; Eparvier, F.; Andersson, L.; Dominique, M.; Pilinski, M.; Girazian, Z.; Gröller, H.; Elrod, M.; Bougher, S.; Lillis, R.  
*MAVEN EUVM Solar Occultation Measurements of Mars Thermospheric CO2*  
International Conference on Mars Aeronomy 2017, Boulder, Colorado, 15-19 May 2017

178. Vandenbussche, S.; Kumps, N.; De Mazière, M.  
*Use of satellite data for source detection and monitoring of dust aerosol*  
EUMETSAT Meteorological Satellite Conference 2017, Rome, Italy, 2-6 October 2017

179. Vandenbussche, S.; Kumps, N.; De Mazière, M.  
*A new insight in mineral dust aerosol sources using 10 years of three-dimensional dust distribution from IASI measurement*  
International Conference on Aerosol Cycle (ICAC) : Source - Aging - Sinks – Impacts, Lille, France, 21-23 March 2017

180. Van Malderen, R.; Pottiaux, E.; Klos, A.; Bock, O.; Bogusz, J.; Chimani, B.; Elias, M.; Gruszczynska, M.; Guijarro, J.A.; Zengin, S.; Ning, T.  
*The homogenisation of GPS Integrated Water Vapour time series: methodology and benchmarking the algorithms on synthetic datasets*  
European Meteorological Society Annual Meeting 2017, Dublin, Ireland, 4-8 September 2017

181. Van Malderen, R.; Pottiaux, E.; Stankunavicius, G.; Beirle, S.; Legrand, J.; Brenot, H.; Wagner, T.; De Backer, H.; Bruyninx, C.

*A world-wide analysis of the time variability of Integrated Water Vapour, based on ground-based GNSS and GOMESCIA satellite retrievals, and with reanalyses as auxiliary tools*  
European Meteorological Society Annual Meeting 2017, Dublin, Ireland, 4-8 September 2017

182. Van Malderen, R.; Pottiaux, E.  
*Robust, non-parametric techniques for the identification of change-points in the mean*  
COST ES1206 sub-Working Group “Data Homogenisation” - 2<sup>nd</sup> Workshop, Warsaw, Poland, 23-25 January 2017

183. Van Malderen, R.; Pottiaux, E.  
*Overview and goals of the sub-WG activity on homogenization in COST action GNSS4SWEC*  
COST ES1206 sub-Working Group “Data Homogenisation” - 2<sup>nd</sup> Workshop, Warsaw, Poland, 23-25 January 2017

184. Van Malderen, R.; Pottiaux, E.  
*Identified break points by iterative use of non-parametric rank-sum tests: The ‘IGS repro 1’ dataset*  
COST ES1206 sub-Working Group “Data Homogenisation” - 2<sup>nd</sup> Workshop, Warsaw, Poland, 23-25 January 2017

185. Van Malderen, R.; Pottiaux, E.  
*Identified break points by iterative use of non-parametric rank-sum tests: Case-Study of the Synthetic Dataset*  
COST ES1206 sub-Working Group “Data Homogenisation” - 2<sup>nd</sup> Workshop, Warsaw, Poland, 23-25 January 2017

186. Van Malderen, R.; Pottiaux, E.  
*Future plans and outcome of our activities*  
COST ES1206 sub-Working Group “Data Homogenisation” - 2<sup>nd</sup> Workshop, Warsaw, Poland, 23-25 January 2017

187. Van Malderen, R.; Pottiaux, E.  
*Future Activities of the sub-Working Group on Data Homogenization*  
COST ES1206 - GNSS4SWEC Final Workshop, Noordwijk, The Netherlands, 21-23 February 2017

188. Van Malderen, R.; Pottiaux, E.  
*Activities of the sub-working group on data homogenization*  
COST ES1206 - GNSS4SWEC Final Workshop, Noordwijk, The Netherlands, 21-23 February 2017

189. Van Malderen, R.; Pottiaux, E.; Klos, A.; Bock, O.; Bogusz, J.; Chimani, B.; Elias, M.; Gruszczynska, M.; Guijarro, J.A.; Zengin, S.; Ning, T.  
*Results of the homogenization tools on the synthetic benchmark IWV datasets*  
COST ES1206 - GNSS4SWEC Final Workshop, Noordwijk, The Netherlands, 21-23 February 2017

190. Van Malderen, R.; Pottiaux, E.; Legrand, J.; Brenot, H.; Beirle, S.; Wagner, T.; De Backer, H.; Bruyninx, C.

*A world-wide analysis of the time variability of Integrated Water Vapour, based on ground-based GNSS and GOMESCIA satellite retrievals, and with reanalyses as auxiliary tools*

COST ES1206 - GNSS4SWEC Final Workshop, Noordwijk, The Netherlands, 21-23 February 2017

191. Van Malderen, R.; Pottiaux, E.; Klos, A.; Bock, O.; Bogusz, J.; Chimani, B.; Elias, M.; Gruszczynska, M.; Guijarro, J.A.; Zengin, S.; Ning, T.

*The homogenization of GPS Integrated Water Vapour time series: methodology and benchmarking the algorithms on synthetic datasets*

Homogenization and Interpolation Conference, Budapest, Hungary, 3-7 April 2017

192. Van Schaeybroeck, B.; Termonia, P.; De Ridder, K.; Fettweis, X.; Gobin, A.; Luyten, P.; Marbaix, P.; Pottiaux, E.; Stavrakou, T.; Van Lipzig, N.; Van Ypersele, J.-P.; Willems, P.

*The foundation for climate services in Belgium: CORDEX.be*  
EGU General Assembly 2017, Vienna, Austria, 23-28 April 2017

193. Van Schaeybroeck, B.; Termonia, P.; De Ridder, K.; Fettweis, X.; Gobin, A.; Luyten, P.; Marbaix, P.; Pottiaux, E.; Stavrakou, T.; Van Lipzig, N.; Van Ypersele, J.-P.; Willems, P.; and the URSI team

*The foundations for climate services in Belgium: CORDEX.be*

European Meteorological Society Annual Meeting 2017, Dublin, Ireland, 4-8 September 2017 (poster)

194. Vansintjan, R.; Mampaey, B.; Delouille, V.; Berghmans, D.

*The SOLARNET Solar Virtual Observatory prototype*

SOLARNET IV meeting on "The Physics of the Sun from the Interior to the Outer Atmosphere", Lanzarote, Spain, 16-20 January 2017

195. Verbeeck, C.; Lamy, H.; Calders, S.; Tetard, C.; Martinez Picar, A.

*Overview of major shower observations 2016-2017 by the BRAMS network*

International Meteor Conference, Petnica, Serbia, 21-24 September 2017

196. Verbeeck, C.

*Revisiting the EUI commissioning and cruise phase*

19<sup>th</sup> EUI Consortium Meeting, Brussels, Belgium, 30 May – 1 June 2017

197. Verbeeck, C.

*Commissioning Phase revisited*

20<sup>th</sup> EUI Consortium Meeting, Guildford, UK, 13-15 September 2017

198. Verbeeck, C.; Stegen, K.

*What can EUI do for you? Onboard science programs*  
20<sup>th</sup> EUI Consortium Meeting, Guildford, UK, 13-15 September 2017

199. Verbeke, C.; Scolini, C.; Pomoell, J.; Poedts, S.; Asvestari, E.; Kilpua, E.

*Modeling Coronal Mass Ejections with EUHFORIA: a Parameter Study of a Flux Rope Model*

ESWW14, Oostende, Belgium, 27 November-1 December 2017

200. Verbeke, C.; Scolini, C.; Pomoell, J.; Poedts, S.; Asvestari, E.; Kilpua, E.

*Modeling Coronal Mass Ejections with EUHFORIA: a Parameter Study of a Flux Rope Model*

AGU Fall Meeting, New Orleans, Louisiana, USA, 11-15 December 2017

201. Verhulst, T.; Stankov, S.

*Effect of altitude-dependent times of sunrise and sunset in ionospheric modelling*

URSI 2017 - General Assembly and Scientific Symposium, Montreal, Canada, 19-26 August 2017

202. Verhulst, T.

*Sanity checking of the Frequency-Angular-Sounding (FAS) results*

Net-TIDE Project Final Meeting, Heraklion, Crete, 4-6 October 2017

203. Verhulst, T.

*Digisonde-to-Digisonde (D2D) network operations*

Net-TIDE Project Final Meeting, Heraklion, Crete, 4-6 October 2017

204. Verhulst, T.

*Pilot Network for Identification of Travelling Ionospheric Disturbances in Europe*

RMI Conference on Ionosphere and Space Weather, Brussels, Belgium, 8 March 2017

205. Voitenko, Y.

*Turbulence and spectral transport from MHD to kinetic scales: plasma heating and particles acceleration*

Solar Terrestrial and Experimental Plasma Physics Synergy: STEPPS, Leiden, The Netherlands, 10-13 April 2017 (invited talk)

206. Voitenko, Y.; De Keyser, J.; Pierrard, V.; Gogoberidze, G.

*MHD-kinetic transformation of Alfvénic turbulence and future space missions*

4<sup>th</sup> UK-Ukraine-Spain Meeting on Solar and Space Physics, Kyiv, Ukraine, 28 August-1 September 2017 (invited talk)

207. Voitenko, Y.; Pierrard, V.; Melnik, V.; Brazhenko, A.; Frantsuzenko, A.

*Solar Coronal Radio Bursts at 1.5-3 Solar Radii Above Active Regions*

URSI 2017 - General Assembly and Scientific Symposium, Montreal, Canada, 19-26 August 2017 (poster)

208. Wauters, L.; Dominique, M.; Dammasch, I.; Kretzschmar, M.

*Eruptive phenomena observed in LYRA lyman-alpha*  
AAS/SPD 48, Portland, Oregon, USA, 21-25 August 2017

209. West, M.; Seaton, D.B.; Dennis, B.; Feng, L.; Palmerio, E.

*Further Exploration Of Post-Flare Giant Arches*  
ESPM-15, Budapest, Hungary, 4-8 September 2017  
(poster)

210. West, M.; Seaton, D.B.; Dennis, B.; Feng, L.; Palmerio, E.

*Further Exploration Of Post-Flare Giant Arches*  
IAU Symposia 335: Space Weather of the Heliosphere: Processes and Forecasts, Exeter, UK, 17-21 July 2017  
(poster)

211. West, M.; Seaton, D.B.; Dennis, B.; Feng, L.

*Further Exploration of Post-Flare Giant Arches*  
AAS/SPD 48, Portland, Oregon, USA, 21-25 August 2017  
(poster)

212. West, M.; Seaton, D.B.; Dennis, B.; Feng, L.; Palmerio, E.; Savage, S.

*Post-Flare Giant Arches - Unanswered Questions*

AGU Fall Meeting, New Orleans, Louisiana, USA, 11-15 December 2017

213. Zucca, P.; Morosan, D.; Gallagher, P.; Fallows, R.; Rouillard, A.; Magdalenic, J.; Vocks, C.; Marqué, C.; Klein, K.-L.; Mann, G.

*Kinematics and shock locations of a spatial resolved solar type II radio burst with LOFAR*  
EGU General Assembly 2017, Vienna, Austria, 23-28 April 2017 (poster)

214. Zucca, P.; Morosan, D.; Fallows, R.; Rouillard, A.; Magdalenic, J.; Klein, K.-L.; LOFAR and Solar KSP members  
*Shock location and CME 3D reconstruction of the first spatial resolved solar type II radio burst with LOFAR*  
International Workshop on Solar, Heliospheric and Magnetospheric Radioastronomy: The legacy of Jean-Louis Steinberg (1922-2016), Meudon, France, 6-10 November 2017

215. Zucca, P.; Morosan, D.; Fallows, R.; Rouillard, A.; Magdalenic, J.; Klein, K.-L.; LOFAR and Solar KSP members  
*Study of the signature of a coronal shock with LOFAR and multi-viewpoint observations, space weather implications*  
ESWW14, Oostende, Belgium, 27 November-1 December 2017 (invited talk)

## Public Outreach: Talks and publications for the general public

1. Bergeot, N.  
*On se fait un petit détour par l'Antarctique?*  
Clés pour l'Univers ASBL, Prison Berkendael, 25 April 2017
2. Bergeot, N.; Chevalier J.-M.  
*Ionospheric products from ROB*  
ASTRON visit at ROB, Brussels, Belgium, 14 September 2017
3. Bergeot, N.; Podladchikova, O.; and the SWAP team  
*PROBA2 satellite & ESA Science: Space Research at the Royal Observatory of Belgium and BELSPO*  
Science Forum South Africa, Pretoria, Republic of South Africa, 7-8 December 2017
4. Delouille, V. ; Vanlommel, P.  
*La Météo Spatiale*  
Jeunesse Scientifique , 31 Oct 2017
5. D'Huys, E.; and the SWAP, LYRA, and PROBA2 teams  
*PROBA2 Running Presentation at ESWW14 Fair*  
ESWW14, Fair, Oostende, Belgium, 29 November 2017
6. Janssens, J.  
*Stormachtig ruimteweer tijdens de 24<sup>ste</sup> zonnecyclus*  
VVS Algemene Vergadering, Heysel, Brussels, 22 April 2017
7. Janssens, J.  
*De kunst van het zonnewaarnemen*  
Volkssterrenwacht MIRA, Grimbergen, 3 May 2017
8. Janssens, J.  
*Drivers of Space Weather (Part 2)*  
SWIC, ROB, 8 May 2017
9. Janssens, J.  
*Space Weather Effects*  
SWIC, ROB, 9 May 2017
10. Janssens, J.  
*SIDC/RWC & URSIgram + exercises*  
SWIC, ROB, 23 May 2017
11. Janssens, J.; Marqué, C.  
*Sensors*  
SWIC, ROB, 23 May 2017
12. Janssens, J.  
*Een zonnecyclus H-alfa waarnemingen*  
VVS/KNVWS - Annual meeting BE & NL Solar Sections, ROB, 7 October 2017
13. Lamy, H.  
*Properties of meteoroids from forward scatter radio observations*  
61<sup>st</sup> Course of the International School of Quantum Electronics ("Hypersonic Meteoroid Entry Physics"), Erice, Italy, 3-7 October 2017
14. Vanlommel, P.; Janssens, J.  
*STCE Newsletter*  
Weekly newsletter, <http://www.stce.be> , 2017
15. Vanlommel, P.  
*Drivers of Space Weather (Part 1)*  
SWIC, ROB, 8 May 2017
16. Vanlommel, P.  
*Space weather data exercise*  
SWIC, ROB, 23 May 2017
17. Vanlommel, P.; and the SILSO team  
*Zonnevlekken - een eeuwenoude schat van informatie*  
Zonnekijkdag, Cosmodrome Genk, 2 July 2017
18. Vanlommel, P.; and the PROBA2 team  
*PROBA2, een micro-satelliet*  
Zonnekijkdag, Cosmodrome Genk, 2 July 2017
19. Vanlommel, P.  
*Krachtige zonnestorm op komst - kijken naar de Zon*  
Zonnekijkdagen, Cosmodrome Genk, 2 July 2017
20. Vanlommel, P.  
*Watch out, a powerful solar storm is on its way!*  
Talk Cosmic to me, 21 August 2017
21. Vanlommel, P.  
*De Zon*  
VVS, Summer School Astronomy, 28 August 2017
22. Vanlommel, P.  
*Ontdekkingsreis naar de Zon*  
Volkssterrenwacht Urania, Hove, 10 October 2017
23. Vanlommel, P.  
*Krachtige zonnestorm op komst*  
Elcker-Ik, Antwerpen, 14 November 2017
24. Verbeeck, C.  
*Zonnewetenschappen en Ruimteweer op de Koninklijke Sterrenwacht*  
Observatiestage studenten secundaire school, ROB, 20 February 2017

25. Verbeeck, C.  
*Radiometeorwaarnemingen*  
Volkssterrenwacht Urania, Hove, 8 December 2017

26. Voitenko, Y.  
*Kinetic waves and instabilities*  
The International School of Space Science (ISSS) Course  
Complexity and Turbulence in Space Plasmas L'Aquila,  
Italy, 17-22 September 2017 (two invited lectures)

## List of abbreviations

~	About, proportional to	BRAIN-be	Belgian Research Action through Interdisciplinary Networks (BELSPO)
2D	Two dimensional		
3D	Three dimensional		
A	Article	BRAMS	Belgian Radio Meteor Stations
AAS	American Astronomical Society	B.USOC	Belgian User Support and Operation Centre
ACE	Advanced Composition Explorer	Bz	Component of the IMF perpendicular to the ecliptic (“north-south” component)
AFFECTS	Advanced Forecast For Ensuring Communications Through Space	C-class flare	Common x-ray flare
AGU	American Geophysical Union	C/N <sub>0</sub>	Carrier-to-Noise density
AIA	Atmospheric Imaging Assembly (SDO)	Ca II H	A blue line in the solar spectrum at 396.85 nm
ALC	Automatic LIDAR Ceilometer	Ca II K	A blue line in the solar spectrum at 393.37 nm
ALTIUS	Atmospheric Limb Tracker for Investigation of the Upcoming Stratosphere	CACTus	Computer Aided CME Tracking software
AMRVAC	Adaptive Mesh Refinement – Versatile Advection Code	CALLISTO	Compound Astronomical Low frequency Low cost Instrument for Spectroscopy and Transportable Observatory
AR	Active Region	CAS	Chinese Academy of Sciences
ARCAS	Augmented Resolution Callisto Spectrometer	CB	Central Bureau (EPN)
ASGARD	An educational space programme for schools (no acronym)	CCMC	Community Coordinated Modeling Center
ASPIICS	Association of Spacecraft for Polarimetric and Imaging Investigation of the Corona of the Sun (PROBA-3)	CESRA	Community of European Solar Radio Astronomers
ASTRON	Netherlands Institute for Radio Astronomy - Stichting Astronomisch Onderzoek in Nederland	CH	Coronal Hole
ATLAS	Atmospheric Laboratory for Applications & Science	CHARM	Contemporary physical challenges in Heliospheric and AstRophysical Models
AU	Astronomical Unit; about 150 million km	CIR	Co-rotating Interaction Region
BE	Belgium	Cluster	ESA/NASA mission to study the Earth’s magnetosphere (no acronym)
BELSPO	Belgian Science Policy Office	CME	Coronal Mass Ejection
BeNELux	Belgium, The Netherlands, and Luxembourg	CNES	Centre national d’études spatiales (France)
BIPM	Bureau International des Poids et Mesures	CNRS	Centre national de la recherche scientifique (France)
BIRA	Koninklijk Belgisch Instituut voor Ruimte-Aëronomie	CO <sub>2</sub>	Carbon Dioxide
BISA	Royal Belgian Institute for Space Aeronomy	COMESSEP	COronal Mass Ejections and Solar Energetic Particles
		COPUOS	COmmittee on the Peaceful Uses of Outer Space (UN)
		COR (1/2)	Coronagraph (Inner/Outer) onboard STEREO

CORDEX	COordinated Regional Climate Downscaling Experiment	ESERO	European Space Education Resource Office
CORS	Continuously Operating Reference Stations (GNSS)	ESOC	European Space Operations Centre
COSPAR	COMmittee on SPACe Research	ESP	EUV SpectroPhotometer (SDO)
COST	(European) COoperation in Science & Technology	ESPM	European Solar Physics Meeting
COTS	Commercial off-the-shelf	ESTEC	European Space Research and Technology Centre
CSL	Centre Spatial de Liège	ESWW	European Space Weather Week
CubeSat	A small satellite measuring 10cm x 10cm x 10cm	EU	European Union
Δ	Delta (difference)	EUHFORIA	European Heliospheric Forecasting Information Asset
D2D	Digisonde-to-Digisonde	EUI	Extreme-Ultraviolet Imager (Solar Orbiter)
dB-Hz	decibel-Hertz (bandwidth relative to 1 Hz)	EUMETSAT	European Organisation for the Exploitation of Meteorological Satellites
DCBs	Differential Code Biases	EUREF	EUropean Reference Frame
Digisonde	Digitally Integrating Goniometric IonoSONDE	EUV	Extreme Ultraviolet
DOI	Digital Object Identifier	EUVI	Extreme Ultraviolet Imager (STEREO/SECCHI)
DPS4D	Digisonde-Portable-Sounder-4D	EUVM	EUV Monitor (MAVEN)
DSCOVER	Deep Space Climate Observatory	EVE	Extreme ultraviolet Variability Experiment (SDO)
Dst	Disturbance Storm Time index (geomagnetic)	ExoMars	Exobiology on Mars (ESA, Roscosmos)
E	East	F <sub>10.7 cm</sub>	Solar radio flux at 10.7 cm wavelength
EC	European Commission	F <sub>2</sub>	Main ionospheric layer
ECMWF	European Centre for Medium-range Weather Forecasts	FAS	Frequency-Angular-Sounding
ECS	European CubeSat Symposium	FLEXPART	FLEXible PARTicle dispersion model
Eds.	Editors	FN	False Negative
EGU	European Geosciences Union	foF2	Critical frequency F2-layer
EISCAT	European Incoherent SCATter scientific association	FOV	Field-Of-View
EIT	Extreme ultraviolet Imaging Telescope (SOHO)	FP	False Positive
ENLIL	Sumerian god of wind and storms (NOT an acronym)	FP7	Framework Programme 7 (EU)
ENVISAT	Environmental Satellite (ESA)	FUV	Far Ultraviolet
EPN	EUREF Permanent Network	Galileo	European GNSS
EPT	Energetic Particle Telescope (PROBA-V)	GeodesyML	Geodesy Markup Language
ERA	ECMWF re-analysis	GB	Gigabyte (10 <sup>9</sup> bytes)
ERAI	ERA-Interim	GBO	Ground-Based Observatory
ES	Earth System (Science and Environmental Management (COST))	GeV	Giga electronvolt (10 <sup>9</sup> . 1.6 . 10 <sup>-19</sup> Joule)
ESA	European Space Agency	GFZ	Deutsches GeoForschungsZentrum (German Research Centre for Geosciences)
ESAC	European Space Astronomy Centre		
ESC	Expert Service Centre		

GHz	Gigahertz ( $10^9$ Hz)	HXR	Hard x-rays
GIRO	Global Ionospheric Radio Observatory	HyMeX	HYdrological cycle in the Mediterranean EXperiment
GLE	Ground Level Enhancement	Hz	Hertz (per second)
GLONASS	GLObal NAVigation Satellite System (Russia)	IAG	International Association of Geodesy
GNSS	Global Navigation Satellite System	IAGA	International Association of Geomagnetism and Aeronomy
GNSS4SWEC	Advanced GNSS tropospheric products for the monitoring of Severe Weather Events and Climate	IAMAS	International Association of Meteorology and Atmospheric Sciences
GOES	Geostationary Operational Environmental Satellite	IAPSO	International Association for the Physical Sciences of the Oceans
GOME	Global Ozone Monitoring experiment (SCIAMACHY)	IAS(B)	Institut royal d'Aéronomie Spatiale de Belgique
GOMESCIA	GOME/SCIAMACHY/GOME-2	IASI	Infrared Atmospheric Sounding Interferometer (MetOp)
GPS	Global Positioning System (USA)	IAU	International Astronomical Union
GRAPE	GNSS Research and Application for Polar Environment	ICAC	International Conference on Aerosol Cycle
GSFC	Goddard Space Flight Center	ICME	Interplanetary CME
h	Planck's constant ( $6.62607004 \times 10^{-34}$ m <sup>2</sup> kg / s)	ICNSP	International Conference on Numerical Simulation of Plasmas
H	Hydrogen	ICT	Information and Communication Technologies
H-alpha ( $H\alpha$ )	A red visible spectral line at 656.28 nm created by Hydrogen	IEEE	Institute of Electrical and Electronics Engineers
HELCATS	HELiospheric Cataloguing, Analysis and Techniques Service	IES	Imaging Electron Spectrometer (Cluster)
HELIOS	HELMet streamers In the solar corona and their Oscillations	IGS	International GNSS Service
HESPERIA	High Energy Solar Particle Events forecasting and Analysis project	IMC	International Meteor Conference
HF	High Frequency	IMF	Interplanetary Magnetic Field
HI	Heliospheric Imager (STEREO)	INGV	Istituto nazionale di geofisica e vulcanologia
$h_m F_2$	peak density height of $F_2$ -layer	IR	Infrared
HMI	Heliospheric and Magnetic Imager (SDO)	IRI	International Reference Ionosphere
HOME	Advances in Homogenisation Methods of Climate Series: An Integrated Approach (COST)	IRIS	Interface Region Imaging Spectrograph
HOP	Hinode Operation Plan	IRM	Institut Royal Météorologique
HSRS	Humain Solar Radio Spectrograph	ISBN	International Standard Book Number
HSS	High Speed Stream	ISS	International Space Station
HuRAS	Humain Radio Astronomy Station	ISSN	International Standard Serial Number
		ISSS	International School of Space Science

IT	Information Technology	LDE	Long Duration Event
IWV	Integrated Water Vapour	LEO	Low Earth Orbit
jHV	jHelioViewer	LIDAR	Light Detection And Radar
JSWSC	Journal of Space Weather and Space Climate	LIEDR	Local Ionospheric Electron Density profile Reconstruction
JWG	Joint Working Group	LMSAL	Lockheed Martin Solar and Astrophysics Laboratory
K	(1) Local K-index: A 3-hour geomagnetic index, ranging from 0 (quiet) to 9 (extremely severe storm) ; (2) degrees Kelvin	LOC	Local Organising Committee
K*	Local 1-minute resolution K index	LOFAR	Low-Frequency Array
KAW	Kinetic Alfvén Waves	LT	Local Time
keV	kilo electronvolt ( $10^3 \cdot 1.6 \cdot 10^{-19}$ Joule)	LUCE	LUNar CubeSats for Exploration
kHz	kilo Hertz ( $10^3$ /second)	Ly- $\alpha$	Lyman-alpha, a spectral line in the VUV at 121.6 nm
km	kilometer	LYRA	Large Yield Radiometer, formerly called Lyman Alpha Radiometer (PROBA2)
KMI	Koninklijk Meteorologisch Instituut	LWS	Living With a Star
KNMI	Koninklijk Nederlands Meteorologisch Instituut	$\mu\text{m}$	micrometer ( $10^{-6}$ meter)
KNVWS	Koninklijke Nederlandse Vereniging voor Weer- en Sterrenkunde	M-class	Medium class satellite
K <sub>p</sub>	A geomagnetic index, ranging from 0 (quiet) to 9 (extremely severe storm)	M-class flare	Medium x-ray flare
KSB	Koninklijke Sterrenwacht van België	MADAWG	Modelling and Data analysis Working Group (Solar Orbiter)
KSP	Key Science Project	MAVEN	Mars Atmosphere and Volatile EvolutionN (NASA)
KUL	Katholieke Universiteit Leuven	MB	Megabyte ( $10^6$ bytes)
kV	kiloVolt ( $10^3$ Volt)	MetOp	Meteorological Operational satellite (ESA)
$\lambda$	wavelength	MeV	Mega electronvolt ( $10^6 \cdot 1.6 \cdot 10^{-19}$ Joule)
l/m <sup>2</sup>	Liter per square meter	MHD	Magnetohydrodynamics
L	Letter (manuscript)	MHz	Megahertz ( $10^6$ /s)
L*	Set of Earth's magnetic field lines which cross the Earth's magnetic equator at * earth radii from the centre of the Earth (e.g. L = 2)	MIT	Massachusetts Institute of Technology
L1	First Lagrangian point	MJD	Modified Julian Day
L1, L2	GPS frequencies: L1 = 1575.42 MHz, L2 = 1227.60 MHz	MLT	Magnetic Local Time
LASCO	Large Angle Spectrometric Coronagraph (SOHO); small (C2) and wide (C3) field of view	ms	millisecond ( $10^{-3}$ meter)
LATMOS	Laboratoire ATmosphères, Milieux, Observations Spatiales (France)	v	Frequency
		N	North
		N-S	North-South
		N <sub>2</sub>	Nitrogen
		NASA	National Aeronautics and Space Administration
		NATO	North Atlantic Treaty Organization
		NeQuick	Electron density Quick calculation model (ionospheric model)
		Net-TIDE	Pilot Network for Identification of Travelling

	Ionospheric Disturbances in Europe	RAPID	Research with Adaptive Particle Imaging Detector (Cluster)
NIR	Near IR		
NL	The Netherlands	RAS	Royal Astronomical Society
NM	Neutron Monitor	ReSource	Radio Sciences Research on Antarctic Atmosphere
nm	nanometer ( $10^{-9}$ meter)		
NMDB	Neutron Monitor DataBase	RHESSI	Reuven Ramaty High Energy Solar Spectroscopic Imager
$N_m F_2$	peak density of $F_2$ -layer		
NOAA	National Oceanic and Atmospheric Administration	RMI(B)	Royal Meteorological Institute (of Belgium)
NOMAD	Nadir and Occultation for Mars Discovery (ExoMars)	ROB	Royal Observatory of Belgium
ns	nanosecond ( $10^{-9}$ second)	$R_{sun}$	Solar radius (~ 696.000 km)
nT	nano-Tesla ( $10^{-9}$ Tesla)	RWC	Regional Warning Center
O	Oxygen	s	second
O <sub>3</sub>	Ozone	S	South
ORB	Observatoire Royal de Belgique	SBO	Space-Based Observatory
		SC24	Solar Cycle 24
		SCAR	Scientific Committee on Antarctic Research
ORFEES	Observation Radio Fréquences pour l'Etude des Eruptions Solaires	SCIAMACHY	SCanning Imaging Absorption spectrometer for Atmospheric CHartographY (ENVISAT)
P2SC	PROBA2 Science Center		
PARAFOG	Predictive Alert of Radiation FOG	SCK-CEN	Studiecentrum voor Kernenergie – Centre d'Etude de l'Energie Nucléaire
PEA	Princess Elisabeth Antarctic	SDO	Solar Dynamics Observatory
PFSS	Potential Field Source Surface	SECCHI	Sun Earth Connection Coronal and Heliospheric Investigation (STEREO)
pfu	particle (proton) flux unit: the number of particles registered per second, per square cm, and per steradian	SEP	Solar Energetic Particle
PhD	Doctor of Philosophy	SFU, sfu	Solar Flux Unit ( $10^{-22}$ W m <sup>-2</sup> Hz <sup>-1</sup> )
PI	Principal Investigator		
PICASSO	PICo-satellite for Atmospheric and Space Science Observations	SIDC	Solar Influences Data analysis Center
POLENET	POLar Earth observing Network	SILSO	Sunspot Index and Long-term Solar Observations
PROBA	PRoject for OnBoard Autonomy	SIMBA	Sun-earth IMBALance radiometer
PRODEX	PROgramme for the Development of scientific Experiments	SLP	Sweeping / Segmented / Single / Split / Spherical Langmuir Probe
ps	picosecond ( $10^{-12}$ second)	SLT	Solar Local Time
PTB	Physikalisch-Technische Bundesanstalt (Germany)	SMOS	Soil Moisture and Ocean Salinity (ESA)
Q&A	Questions and Answers	sms	short message service
QPP	Quasi-periodic pulsation	SN	Sunspot Number
$\rho_i$	ion gyroradius	SN	Space weather and Near-earth objects
R&D	Research and Development	SOC	Science Operations Centre
R-ESC	Space Radiation ESC	SOHO	Solar & Heliospheric Observatory

SOLAR-ISS	Name of the new Solar Reference Spectrum	SWIC	Space Weather Introductory Course
Solo	Solar Orbiter	SWIFF	Space Weather Integrated Forecasting Framework
SOLSPEC	SOLar SPECtrum	SWPC	Space Weather Prediction Center (USA)
SOLVE	Small spacecraft fOr near Lunar enViroment Exploration	SWSC	Space Weather and Space Climate journal
SORCE	Solar Radiation and Climate Experiment	SWT	Science Working Team
SPADE	Small Phased Array DEmonstrator	SWx	Space weather
SPD	Solar Physics Division (AAS)	SXR	Soft x-rays
SPENVIS (-NG)	SPace ENVironment Information System (- Next Generation)	TAI	Temps Atomique International
SPIE	The International Society for Optical Engineering	TB	Terabyte ( $10^{12}$ bytes)
SPM	SWIFF Plasmasphere Model	TEC	Total Electron Content
SPS	Science for Peace and Security (NATO)	Tech-TIDE	Warning and Mitigation Technologies for TIDs Effects
sr	steradian	TECu	TEC unit ( $10^{16}e\cdot m^{-2}$ )
SRB	Solar Radio Burst	THEMIS	Time History of Events and Macroscale Interactions during Substorms (NASA mission)
SREM	Standard Radiation Environment Monitor (Integral, Rosetta)	TID	Travelling Ionospheric Disturbance
SSA	Space Situational Awareness	TN	True Negative
SSCC	SSA Space Weather Coordination Centre	TP	True Positive
SSI	Solar Spectral Irradiance	TSI	Total Solar Irradiance
SSN	SunSpot Number	UCL	Université Catholique de Louvain
STAFF	Solar Timelines viewer for AFFECTS	UFO	Unidentified Flying Object
STCE	Solar-Terrestrial Centre of Excellence	UHF	Ultra High Frequency
STCL	Space Technology & Calibration Laboratories	UK	United Kingdom
STEPs	Solar Terrestrial and Experimental Plasma Physics Synergy	ULB	Université libre de Bruxelles
STEREO	Solar-TErrestrial RELations Observatory	UNCOPUOS	United Nations Committee on the Peaceful Use of Outer Space
SUMER	Solar Ultraviolet Measurements of Emitted Radiation (SOHO)	URSI	International Union of Radio Science – Union Radio-Scientifique Internationale
SUVI	Solar Ultraviolet Imager (GOES)	US(A)	United States (of America)
SWAP	Sun Watcher using APS detector and image Processing (PROBA2)	USET	Uccle Solar Equatorial Table (Coordinated) Universal Time
SWAVES	STEREO WAVES	UT(C)	(Coordinated) Universal Time
SWE	Space Weather	UV	Ultraviolet
		UVIS	Ultraviolet and Visible
		v	Velocity (speed)
		V	Volt
		VarSITI	Variability of the Sun and Its Terrestrial Impact
		VHF	Very High Frequency
		VKI	Von Karman Institute
		VLF	Very Low Frequency

VSWMC	Virtual Space Weather Modelling Centre	WG	Working Group
VUB	Vrije Universiteit Brussel	WMO	World Meteorological Organization
VUV	Vacuum ultraviolet	WP	Work Package
VVS	Vereniging Voor Sterrenkunde	WRC	World Radiation Center
W	(1) Watt; (2) West	WS	Workshop
W/m <sup>2</sup>	Watt per square meter	WSA	Weddell Sea Anomaly
WAVES	Radio and plasma wave investigation (WIND, STEREO)	X-class flare	Extreme x-ray flare
WDC	World Data Center		